การเพิ่มความเสถียรภาพของออล-ทรานส์เรทินิลแอซีเทตด้วยนาโนเอ็นแคปซูเลชัน

นางสาว สุนัดดา อารซูเกียรติ์

STABILITY ENHANCEMENT OF ALL-*TRANS* RETINYL ACETATE THROUGH
NANOENCAPSULATION

Miss Sunatda Arayachukeat

A Thesis Submitted in Partial Fulfillment of the Requirements

for the Degree of Master of Science Program in Petrochemistry and Polymer Science

Faculty of Science

Chulalongkorn University

Academic Year 2009

Thesis title   STABILITY ENHANCEMENT OF ALL-*TRANS* RETINYL

                    ACETATE THROUGH NANOENCAPSULATION

By   Miss Sunatda Arayachukeat

Field of Study   Petrochemistry and Polymer Science

Thesis Advisor   Associate Professor Supason Wanichwaecharungruang,

Ph.D.

Accepted by the Faculty of Science, Chulalongkorn University in Partail Fulfillment of the Requirements for the Master's Degree

………………………………….Dean of the Faculty of Science

(Professor Supot Hannongbua, Dr.rer.nat.)

THESIS COMMITEE

....Chairman

(Associate Professor Supawan Tantayanon, Ph.D.)

....Thesis Advisor

(Associate Professor Supason Wanichwaecharungruang, Ph.D.)

…………………………………….Examiner

(Assistant Professor Voravee Hoven, Ph.D.)

……………………………………….External examiner

(Thammarat Panyathanmaporn, Ph.D.)

สุนัดดา อารยชูเกียรติ์: การเพิ่มเสถียรภาพของออล-ทรานส์เรทินิลแอซีเทตด้วยนาโนเอ็น
แคปซูเลชัน (STABILITY ENHANCEMENT OF ALL-TRANS RETINYL ACETATE
THROUGH NANOENCAPSULATION) อ. ที่ปรึกษาวิทยานิพนธ์หลัก: รศ.ดร.ศุภศร
วนิชเวชารุ่งเรือง

ในงานวิจัยนี้ได้กักเก็บออล-ทรานส์เรทินิลแอซีเทต (ATRA) ลงในอนุภาคขนาดนาโนที่
เตรียมจากพอลิเมอร์ที่เหมาะสม พบว่าการกักเก็บ ATRA ด้วย พอลิเอทิลลีนไกลคอลเอมเพก-4-
เมทอกซีซินนาโมอิลฟทาโลอิลไคโตซาน (PCPLC) ได้อนุภาคที่มีขนาด 113.2 ± 27.1 นาโนเมตร
ซึ่งมีประสิทธิภาพการกักเก็บ 80.03 ± 0.5 % มีความสามารถในการบรรจุ 21.06 ± 0.1 % ใน
สภาวะที่ไม่มีแสงและมีแสงอัลตร้าไวโอเลตเอฉายในระดับ 45.9 จูลต่อตารางเซนติเมตร ATRA ที่
ถูกกักเก็บมีความเสถียรสูงกว่า ATRA อิสระถึง 40% และ 36% ตามลำดับ นอกจากนี้การศึกษา
การซึมผ่านหนังลูกหนูของ ATRA ที่ถูกกักเก็บในอนุภาค PCPLC ด้วยฟรานซ์ดิฟฟิวชันเซลล์
พบว่าอนุภาคที่กักเก็บ ATRA ไม่สามารถซึมผ่านหนังลูกหนูได้ จากนั้นทำการติดตามตำแหน่ง
ของอนุภาค PCPLC และ ATRA ในหนังลูกหนู ด้วยกล้องจุลทรรศน์ที่ใช้ลำแสงเลเซอร์ช่วยในการ
มองภาพตัวอย่างในลักษณะ 3 มิติ พบว่ารูขุมขนเป็นเส้นทางที่อนุภาคเข้าสู่ชั้นผิวหนัง นอกจากนี้
ยังพบว่า ATRA สามารถถูกปลดปล่อยออกจากอนุภาคเข้าสู่เนื้อเยื่อบริเวณรอบรูขุมขน

สาขาวิชา..ปิโตรเคมีและวิทยาศาสตร์พอลิเมอร์..ลายมือชื่อนิสิต……………………………………..
ปีการศึกษา………..2552………………………….ลายมือชื่อ อ.ที่ปรึกษาวิทยานิพนธ์หลัก…………………

KEYWORDS: NANOENCAPSULATION/ ALL-*TRANS* RETINYL ACETATE/ ETHYL CELLULOSE/ CHITOSAN DERIVATIVE

SUNATDA ARAYACHUKEAT: STABILITY ENHANCEMENT OF ALL-TRANS RETINYL ACETATE THROUGH NANOENCAPSULATION. THESIS ADVISOR: ASSOC. PROF. SUPASON WANICHWEACHARUNGRUANG, Ph.D.

In this work, encapsulation of all-*trans* retinyl acetate was investigated using appropriate polymer. The result showed that ATRA-encapsulated poly(ethylene glycol)-4-methoxycinnamoylphthaloylchitosan (PCPLC) nanoparticles gave the particle size of 113.2 ± 27.1 nm. The encapsulation efficiency was $77.9 \pm 2.5\%$ at ATRA loading of $21.06 \pm 0.1\%$. The stability study under light-proof condition and when exposed to 45.9 J/cm^2 of UVA radiation indicated ~40% and ~36% higher stability of the encapsulated ATRA over free ATRA, respectively. Penetration study with Franz diffusion cell revealed that the encapsulated particles could not transdermally penetrate across the baby mouse skin. Further investigation using confocal fluorescent laser scanning microscope indicated that hair follicle was the skin penetrating route of the particles. In addition, the accumulated particles at the hair follicles released ATRA out into the surrounding tissue.

Field of Study :.Petrochemistry and Polymer Science..Student's Signature……………

Academic Year :……………..2009............................Advisor's Signature………......

ACKNOWLEDGEMENTS

CONTENTS

List of Tables

List of Figures

List of Schemes

List of Abbreviations

ATRA	all-*trans* retinyl acetate
cm^{-1}	per centimeter (s)
CLSM	confocal laser scanning microscope
DS	degree of substitution
DMSO	dimethyl sulfoxide
DLS	dynamic light scattering
EC	ethyl cellulose
h	hour
Hz	hertz
J	joule
MWCO	molecular weight cut-off
mJ	millijoule
mW	milliwatt
mV	millivoltage
mL	milliliter (s)
μg	microgram (s)
nm	nanometer (s)
%	percent
ppm	parts per million
PCPLC	mPEG-4-methoxycinnamoylphthaloylchitosan
PPLC	mPEG-phthaloylchitosan
PVA-C1	Poly (vinylalcohol-co-vinyl-cinnamate) degree substitution of 0.30
PVA-C2	Poly (vinylalcohol-co-vinyl-cinnamate) degree substitution of 0.44
SEM	Scanning electron microscope
TEM	Transmission electron microscope
UV	ultraviolet
v	volume
w	weight

λ	wavelength
ζ	zeta

CHAPTER I
INTRODUCTION

1.1 Retinoids

Vitamin A and its derivatives, both natural and synthetic, are recognized as the high-potential substances for prevention and treatment of photoaging. They have been commonly used for the treatment of severe acne and skin inflammation [1], increased autolysis of keratinocytes, increased glycogen deposition, increased synthesis of collagen and elastin [2, 3] and treatment of inflammatory skin diseases. However, despite these interesting features, its utility is strongly limited by several disadvantages, such as skin irritation, very low water solubility, and high instability in the presence of air, light, water, heat and ultraviolet radiation. UVA and UVB radiation reduce the vitamin A content of the human epidermis [4] Side effects of vitamin A were skin irritation, erythema, peeling and burning [5, 6, 7, 8]. The following topical retinoids are recognized as being useful:

Natural retinoids
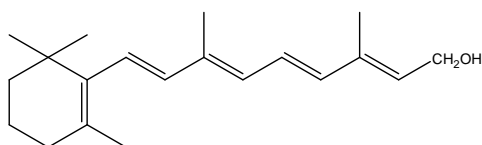
Retinol (vitamin A alcohol)
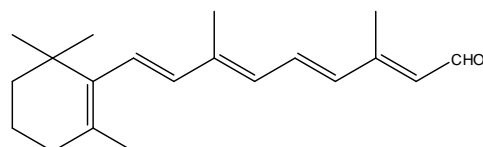
Retinaldehyde (vitamin A aldehyde)
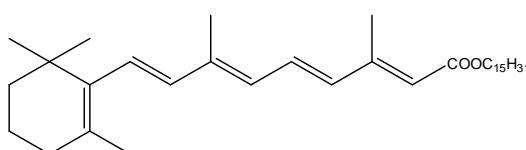
Retinyl-palmitate (vitamin A ester)
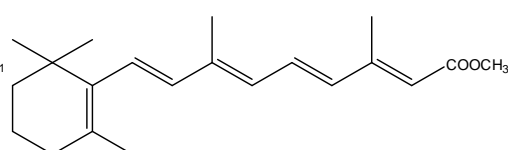
Retinyl-acetate (vitamin A ester)
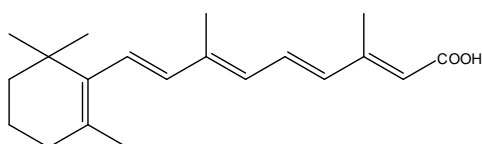
Tretinoin (all-trans retinoic acid,
 vitamin A acid)
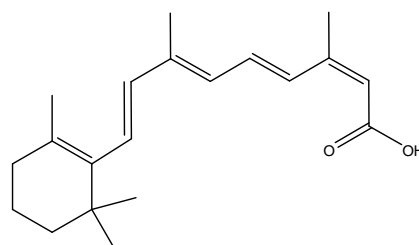
Isotretinoin (13-cis retinoic acid)
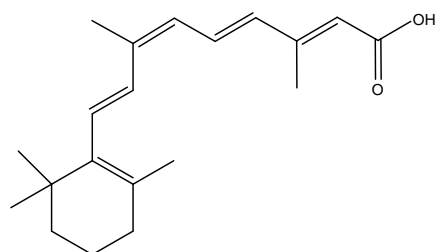
Alitretinoin (9-cis retinoic acid)

Synthetic retinoids
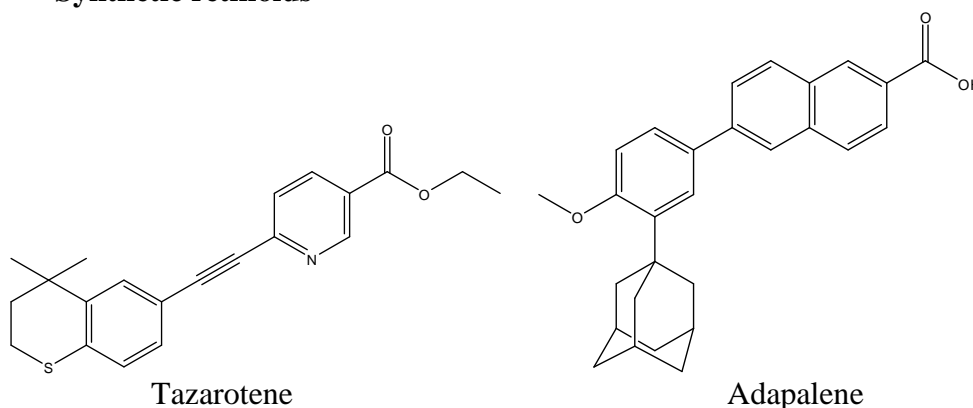
Tazarotene   Adapalene

Figure1.1. Structure of vitamin A derivatives.

Tretinoin, isotretinoin, alitretinoin, tazarotene and adapalene are registered as drugs; the others are cosmeceuticals (medicinally active cosmetics) [2]. All-*trans* retinyl acetate (ATRA), a retinyl ester, is frequently used in cosmeceuticals because they are very stable. Upon entering the cell, ATRA first need to be converted to retinol and retinaldehyde by cleavage of the ester bond, and then oxidized into retinoic acid. Retinyl eaters have been shown to increase the epidermal thickness in human skin [2, 3, 9].

1.2 Metabolism of retinoids

In the skin, vitamin A is known to influence a wide range of biological processes, including sebaceous gland activity, cell-mediated immune responses and epidermal cell growth, differentiation and maintenance [10]. It has been found that vitamin A and its derivatives can increase epidermal thickness, elastin and collagen in the skin [2, 3, 11]. Vitamin A homeostasis, the process by which the body reacts to changes in order to keep conditions inside the body, in the skin requires that the levels of retinol, retinyl ester, and metabolites of retinol be tightly controlled. An important step in maintaining adequate retinol levels in the skin is retrieval of retinyl esters from their

storage sites in the skin followed by hydrolysis to retinol. It should be noted that the intracellular site for storage of retinyl esters in the skin is not known. In some tissues, such as retinal pigment epithelium, where retinoids serve a unique physiological function, retinyl esters are stored in specialized lipid bodies known as retinosome or retinyl ester-storage particles. Retinosomes bud off of the endoplasmic reticulum and are ultimately found near the plasma membrane. It is also possible that retinyl esters are stored in cytoplasmic neutral lipid droplets rather than in specialized structures. Intracellular retinyl esters can be mobilized from their storage sites by retinyl ester hydrolases. It is noteworthy that intracellular retinyl esters may be the preferred source of retinol used for subsequent formation of powerfully bioactive metabolites such as retinoic acid [12]. Retinyl esters must be enzymatically converted in the skin first to retinol by cleavage of the ester bond. As mentioned earlier that the retinol must be converted by a two-step oxidative process into the active tretinoin, follow with oxidation of retinol to retinaldehyde and retinaldehyde to retinoic acid [10]. The limitations on enzymatic and oxidative processes in the skin explain the decreased effectiveness of both retinyl esters and retinol compared with retinoic acid.

1.3 Aging
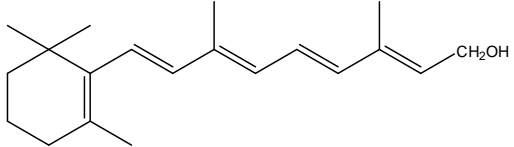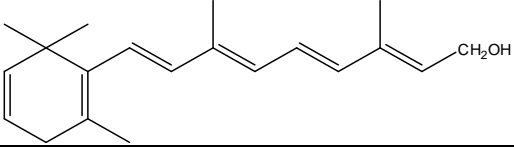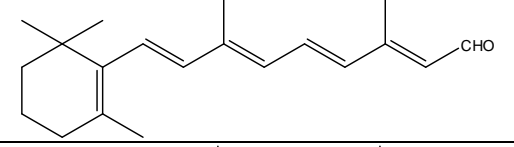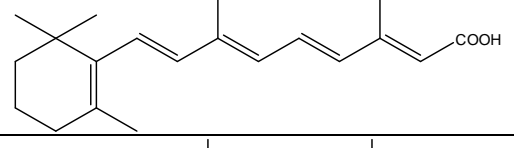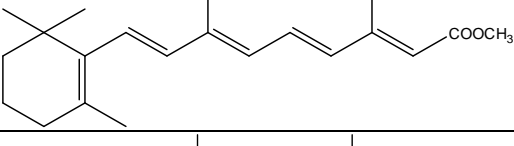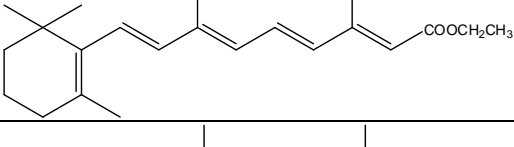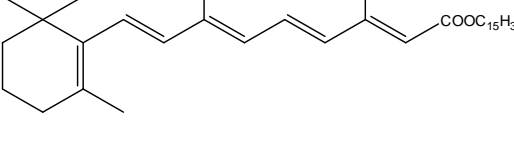
The effects of vitamin A on aging skin are an area of great interest. Aging is associated with changes throughout the skin; however, many of the most dramatic effects due to aging occur in the dermis. An age-related reduction in the number of interstitial dermal fibroblasts has been observed in human skin [13, 14]. Reduced synthesis of collagen is observed in aged skin, especially after the seventh decade [15]. In addition, enhanced degradation of dermal collagen and elastin is observed in aging skin [16, 17, 18, 19]. These changes in the dermis are thought to be largely responsible for the thin, fragile, and finely wrinkled properties of naturally aged skin. Topical application of vitamin A can moderate many of these biochemical changes in aged skin. Cellular and histological markers for age-related changes were measured, and included: collagen synthesis/collagen gene expression, dermal matrix metalloproteinase (MMP) levels, and fibroblast growth [20]. A progressive decrease in numbers of dermal fibroblasts was noted with increasing age as well as thinning

and increased disorganization of collagen bundles dermis. In addition, retinoids have also been shown to have similar effects on photo aged skin [20, 21].

1.4 Degradation of retinoids

The different chemical classes of vitamin A (Table 1.1) show slightly different chemical properties. The alcohol form is very sensitive when exposed to air but is stable in an oil solution. The aldehyde and acid forms are slightly less sensitive to air oxidation. The ester form is most stable to oxidation. This oxidation stability can be expressed by: Retinol< Retinal< Retinoic acid< Retinyl ester.

Table1.1. Chemical properties of retinoids

Retinoid Name (Alternate Name)	Chemical Formula	Molecular Weight	Chemical Stability	Structure
Vitamin A$_1$ alcohol (Retinol)	C$_{19}$H$_{29}$COH	286.44	Very oxidative	
Vitamin A$_2$ alcohol (Retinol$_2$)	C$_{19}$H$_{27}$COH	284.42	Very oxidative	
Vitamin A aldehyde (Retinal)	C$_{19}$H$_{27}$CHO	284.42	Oxidative	
Vitamin A acid (Retinoic acid)	C$_{19}$H$_{27}$COOH	300.42	Less oxidative	
Vitamin A acetate (Retinyl acetate)	C$_{19}$H$_{29}$COOCH$_3$	328.50	Stable	
Vitamin A propionate (Retinyl propionate)	C$_{19}$H$_{29}$COOC$_2$H$_5$	342.52	Stable	
Vitamin A palmitate (Retinyl palmitate)	C$_{19}$H$_{29}$COOC$_{15}$H$_{31}$	524.88	Most stable	

Retinyl acetate, retinyl propionate and retinyl palmitate are the popular ester derivatives. Retinyl acetate has the smallest molecular weight among all retinyl esters. Retinyl acetate, therefore, most likely penetrates the skin better than retinyl propionate and retinyl palmitate [22].

The instability of vitamin A to oxidation when exposed to air, sunlight and UV light [23, 24, 25] are well recognized. Even the most stable derivative, ester form, still degrades quickly. Photo-oxidation of retinyl acetate with UV light gives five compounds (Scheme 1.1), dihydroactinidiolide (a), β-ionone (b), 2-hydroxy-2,6,6-trimethylcyclohexanone (c), geronic acid (d) and desoxyxanthoxin (e) [26, 27].

(a) dihydroactinidiolide   (b) β-ionone

(c)   (d) geronic acid   (e)

desoxyxanthoxin

2-hydroxy-2, 6, 6-trimethylcyclohexanone
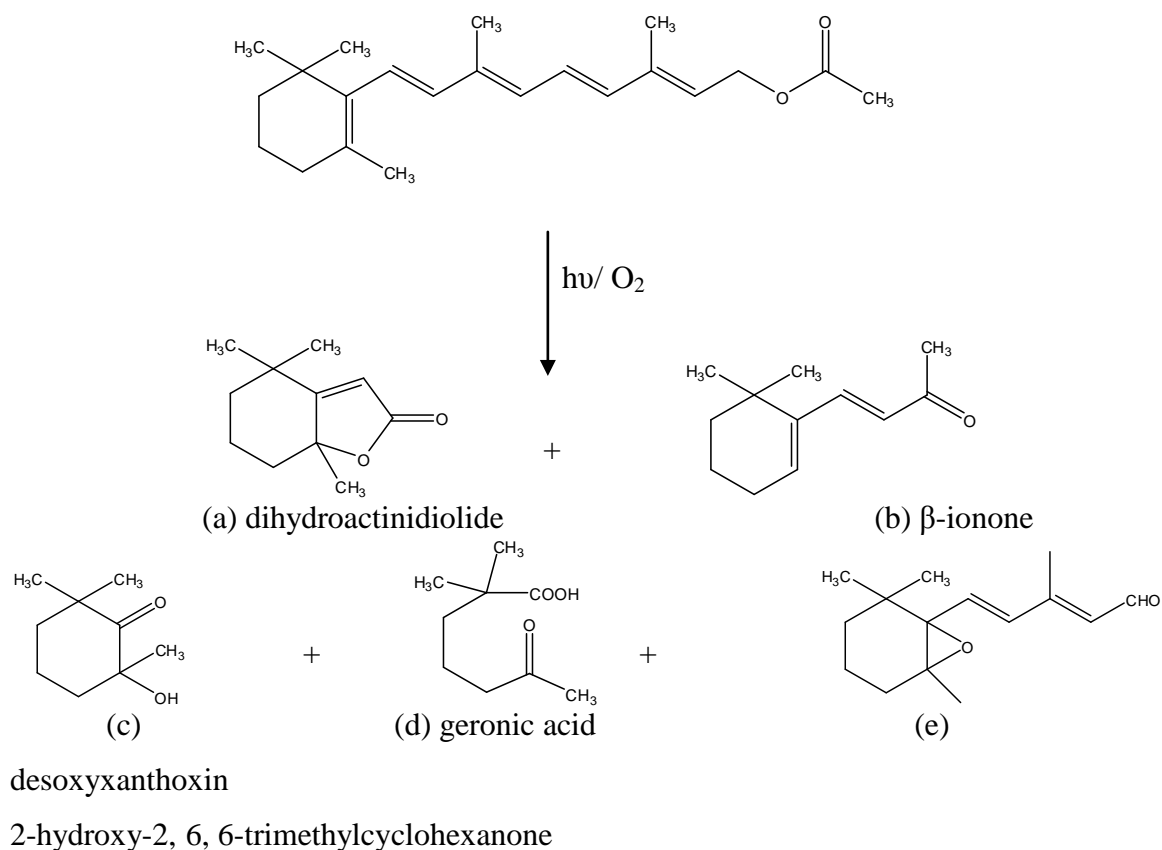
Scheme1.1. Photo-oxidation of retinyl acetate with UV light

Study on the instability of retinyl acetate in a polar solvent have suggested a possible intermediacy of the highly polarized singlet excited state of which its efficiency interaction with polar solvent has leaded to the formation of degradation products (Scheme 1.2) [28].
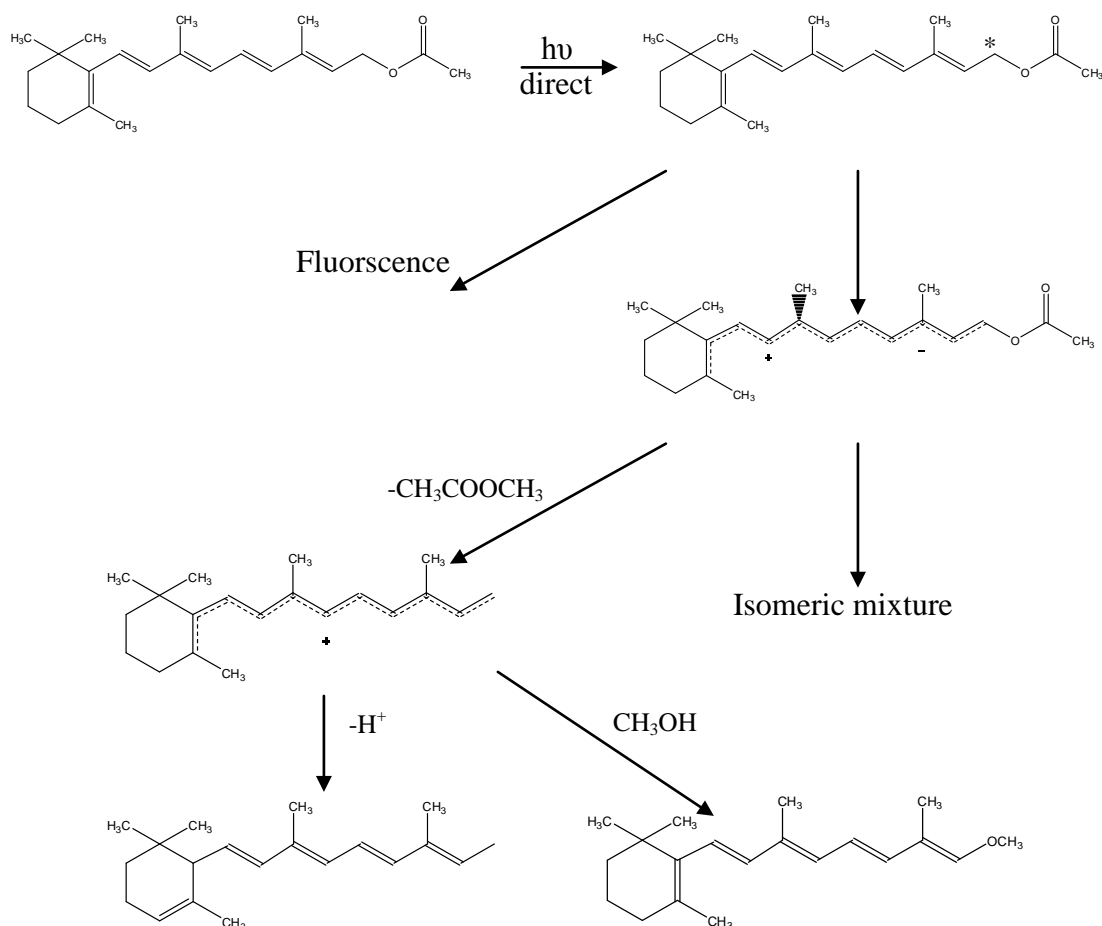
Scheme1.2. Ionic photodissociation of retinyl acetate

1.5 Drug delivery system for vitamin A

Many efforts have been made over the past decades to overcome insoluble property of vitamin A. the formulation is one of the chief areas of drug delivery where nanotechnology promises to improve safety and efficacy. The encapsulation of vitamin A derivative with different kinds of delivery systems such as liposome [29, 30], niosome [31], solid lipid nanoparticle [1, 6, 32, 33], emulsion [24, 35] and polymeric nanoparticles [4, 35] have been proposed as method to help improving its stability, solubility, safety and efficiency. Interestingly, close examination of the above reports has prompted us to realize that their loading capacities were only < 0.1- 0.5% (w/w) for most liposomes, 3.39- 6.70% (w/w) for most emulsion systems, 0.10- 4.89 % (w/w) for most solid lipid nanoparticles and 4.76-17.35% (w/w) for polymeric

nanoparticles. In addition, most studies either did not cover the stability assessment or showed only insignificant improvement of all-*trans* retinyl acetate stability upon encapsulation. Thus, a more efficient loading system which can improve stability of vitamin A and its derivatives is still required. Over the past 15 years, polymeric nanoparticles and nanospheres have been extensively studied as drug carriers in the pharmaceutical field such as poly-ε-caprolactone [35], chitosan [4], N-Phthaloylchitosan-g-mPEG [36, 37] and polylactic-co-glycolic acid (PLGA) [38]

Amphiphilic polymers have gained increasing interest as drug and cosmetic carriers because of their ability to entrap biologically active molecules. Their loading capacity and controlled release properties depend on the type of drug and the type of polymer used. In this research, ethyl cellulose, chitosan derivatives and poly (vinyl alcohol-co-vinyl-cinnamate) derivatives (PVA-C) were chosen for ATRA encapsulation. Chitosan derivatives and poly (vinyl alcohol-co-vinyl-cinnamate) derivatives with UV absorptive functionality substitution were developed and prepared into carrier systems.

1.6 Ethyl cellulose
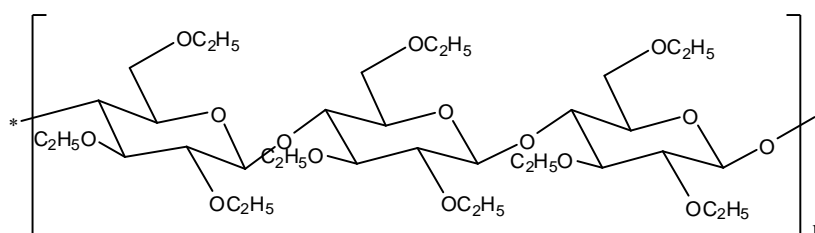
Figure1.2. Structure of ethyl cellulose

Ethyl cellulose (EC) is a derivative of cellulose in which some of the hydroxyl groups on the repeating glucose units are converted into ethyl ether groups. The number of ethyl groups can vary depending on the manufacture. It is mainly used in drug delivery systems, a thin-film coating material and a food additive as an emulsifier. Although many polymers are used in the pharmaceutical industry, the most widely used are the cellulose derivatives: methylcellulose, hydroxypropyl methylcellulose, hydroxypropyl cellulose, ethylcellulose, cellulose acetate phthalate and

hydroxypropyl methylcellulose phthalate. All are derived from, and hence possess, the polymeric bacebone of cellulose, which contains a basic repeating structure of β-anhydroglucose units; each unit having three replaceable hydroxyl groups (Table 1.2). Ethyl cellulose is the most stable of the cellulose derivatives. It is resistant to alkalis; both dilute and concentrate, but sensitive to acids. Ethyl cellulose takes up little water from moist air or during immersion, and this evaporates readily leaving ethyl cellulose unchanged. Light, visible or ultraviolet radiation, has no discoloring action on ethyl cellulose. Effect of heat up to its softening point has little effect on ethyl cellulose. The high thermal softening points or glass-transition temperatures of hydroxypropyl cellulose, Ethyl cellulose and hydroxypropyl methylcellulose were 120, 140 and 180°C, respectively. Ethyl cellulose formulations, if not stabilized are subject to oxidative degradation in the presence of sunlight or ultraviolet light and at made higher temperatures [39]. Ethyl cellulose is a water-insoluble polymer used in controlled-release dosage forms. In the absence of polymer swelling ability, Ethyl cellulose compactibility becomes a key factor in such systems, because release kinetics would depend on the porosity of the hydrophobic compact. Although Ethyl cellulose is considered insoluble, it can take up water [40]. This is because of its hydrogen bonding capability with water owing to the polarity difference between the oxygen atom and the ethyl group of the polymer [41].
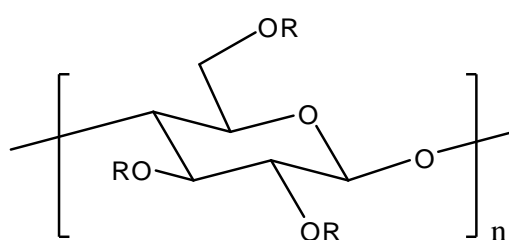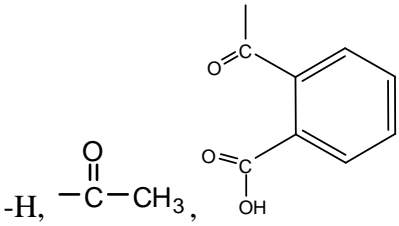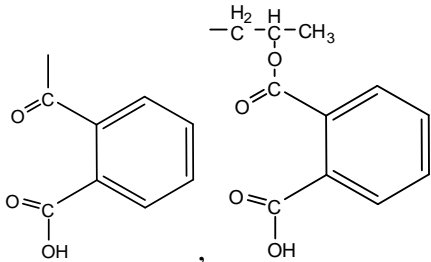
Table1.2. Structure of cellulose derivatives.

Polymer	Substituent group [R]
Methylcellulose	-H, -CH$_3$
Hydroxypropyl methylcellulose	-H, -CH$_3$, -CH$_2$-CH-CH$_3$ | OH
Hydroxypropyl cellulose	-H, -CH$_2$-CH-CH$_3$ | OH
Ethyl cellulose	-H, -CH$_2$CH$_3$
Cellulose acetate phthalate	
Hydroxypropyl methylcellulose phthalate	-H, -CH$_3$, -CH$_2$-CH-CH$_3$, | OH

1.7 Chitosan
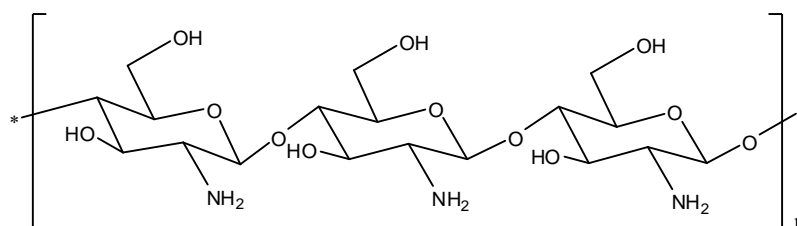
Figure1.3. Structure of chitosan

Chitosan is a derivative of chitin, a natural polysaccharide found in the shells of crustaceans such as crabs and shrimps. Some consider chitin as a derivative of cellulose because both polymers share strikingly similar molecular structures, except that cellulose contains hydroxyl groups and chitosan contains amides group at the C2 position of the monomers. The chemical structure of chitosan exhibits high crystallinity through inter- and intramolecular hydrogen bond network. Combining with the high molecular weight developed naturally, chitosan has poor solubility property. Chitosan exhibits a variety of physicochemical and biological properties, such as good biocompatibility, biodegradability, bioactivity, and lack of toxicity and allergenicity. It is a very attractive substance for use in biomaterials and pharmaceutical science.

In 2008, Anumansirikul et al. [42] prepared chitosan derivative, poly (ethylene glycol)-phthaloylchitosan (PPLC) and poly(ethylene glycol)-4-methoxycinnamoylphthaloylchitosan (PCPLC) and encapsulated 2-ethylhexyl-4-methoxycinnamate (EHMC) into chitosan derivative by dialysis method. The nanospheres gave the encapsulation efficiency higher than 99% and loading of 67 %. These two spheres were quite interesting since they possessed UV absorption property.
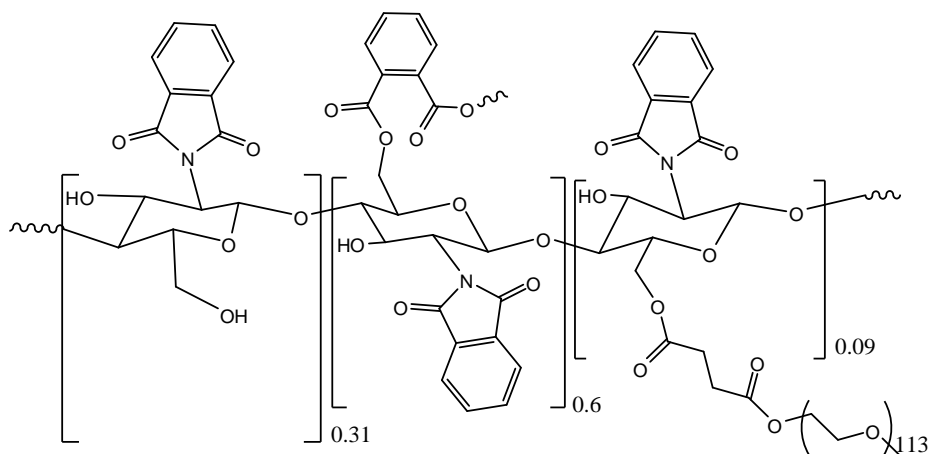
Figure1.4. Structure of poly(ethylene glycol)-phthaloylchitosan (PPLC)
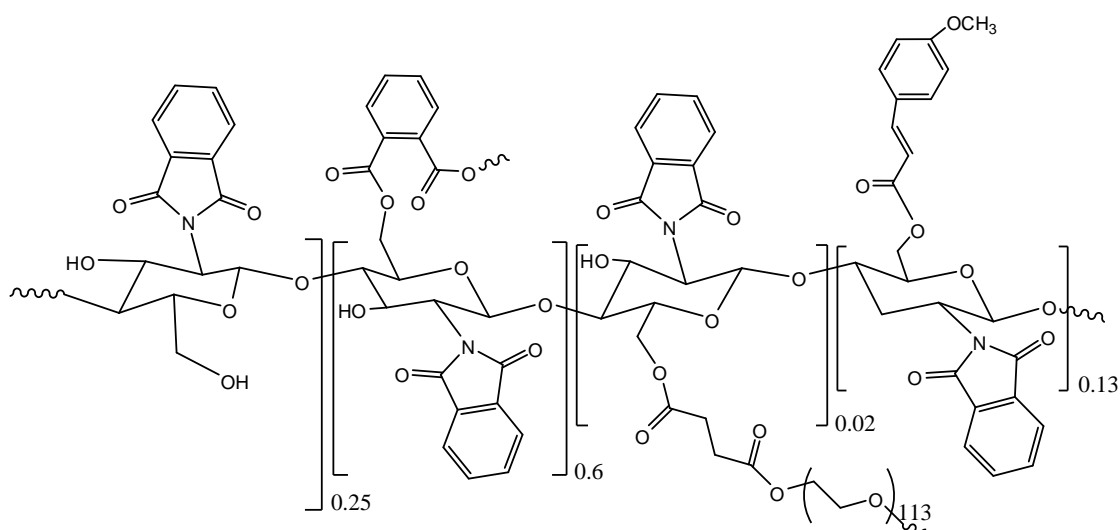
Figure1.5. Structure of poly(ethylene glycol)-4-methoxycinnamoylphthaloylchitosan (PCPLC)

1.8 Poly(vinyl acohol)
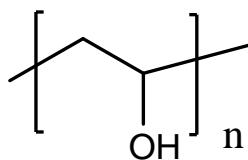
Figure1.6. Structure of poly (vinyl alcohol)

Poly(vinyl acohol) is highly hydrophilic synthetic polymers used since the early 1930s. Poly(vinyl alcohol) was first prepared by Hermann and Haehnel in 1924 by hydrolyzing polyvinyl acetate in ethanol with potassium hydroxide. Poly(vinyl

alcohol) is produced commercially from polyvinyl acetate, usually by a continuous process. The acetate groups are hydrolyzed by ester interchange with methanol in the presence of anhydrous sodium methylate or aqueous sodium hydroxide. The physical characteristics and its specific functional uses depend on the degree of polymerization and the degree of hydrolysis. Poly(vinyl alcohol) is classified into two classes namely: partially hydrolyzed and fully hydrolyzed. Poly(vinyl alcohol) derivatives was selected in this work due to its biocompatibility, biodegradability, non-toxicity, non-carcinogenicity and water-soluble polymer. This polymer is also accepted pharmaceutically safe polymer to both human and environment.

1.9 Literature reviews of EC carrier

In 2005, Santhi et al. [43] prepared betamethazone nanospheres from ethyl cellulose by a modified method of desolvation and crosslinking. These researches focused on the preparation at various drug: polymer ratios and *in vitro* release of the drug-encapsulated spheres in the cream. The betamethazone loadings were found 23.9±1.8%, 36.9±1.1%, 62.4±2.0%, 74.0±0.2% and 20.9±1.4%, respectively for betamethazone concentration in polymer (mg/mg) 6.25, 12.5, 18.8, 25 and 50. The percentage of release from the drug-loaded nanospheres was in the range from 74 to 96%. The release of betamethazone from the conventional cream was faster than that from the nanospheres bound cream. The cumulative release of drug from conventional cream at the 6 h was 57%, while it was only 28% for the nanospheres bound cream.

In 2008, Choy et al. [44] prepared piroxicam-loaded ethyl cellulose and rhodamine-loaded ethyl cellulose by precision particle fabrication (PPF) technique. The encapsulation efficiency of piroxicam-loaded ethyl cellulose and rhodamine-loaded ethyl cellulose were 6.4-51 and 63-80%, respectively. The polymer viscosity showed no significant effect on the release of piroxicam but significantly affected the release of rhodamine.

In 2009, Ravikumara et al. [45] arranged nimesulide-loaded into ethyl cellulose (EC) and methylcellulose (MC) nanoparticles *via* desolvation method. The particles size was in an averaged range of 244 to 1056 nm and 1065 to 1710 nm for EC and MC nanoparticles, respectively. The size of particles increased when the

concentration of polymer increased. The encapsulation efficiency of nimesulide-loaded EC and MC nanoparticles varied between 32.8% and 64.9%, respectively and nimesulide loading ranged from 1.41% to 6.12%.

In 2009, Valot et al. [46] prepared ibuprofen-loaded ethyl cellulose microcapsules by water in oil emulsion-solvent evaporation method. The encapsulation yield of ibuprofen was close to 100% and the particles size was around 20-60 µm.
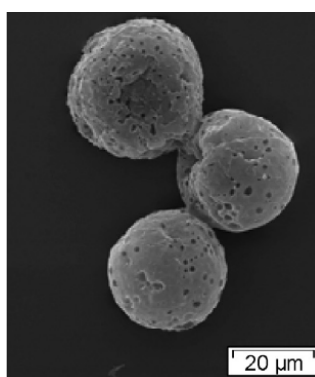
Figure1.7. SEM photograph of ibuprofen-loaded ethyl cellulose microcapsules

In 2010, Sansukcharearnpon et al. [47] prepared fragrance-loaded nanospheres from polymer-blend of ethylcellulose (EC), hydroxypropyl methylcellulose (HPMC) and poly(vinyl alcohol) (PV(OH)) using solvent displacement method. Six fragrances including camphor, citronellal, eucalyptol, limonene, menthol and 4-tert-butylcyclohexyl acetate, were studied. The process presented encapsulation efficiency higher than 80% and gave fragrance loading capacity higher than 40% at fragrance: polymer weight ratio of 1:1. The particles size of fragrance-encapsulated spheres showed hydrodynamic diameters of less than 450 nm.

1.10 Literature reviews of chitosan derivatives

In 2006, Opanasopit et al. [36] synthesized N-phthaloylchitosan-grafted poly (ethylene glycol) methyl ether (mPEG) (PLC-g-mPEG) and formed a core-shell micelles of camptothecin (CPT) encapsulated via dialysis method. *In vitro* release studied on CPT-loaded PLC-g-mPEG micelles compared with unprotected CPT in

phosphate-buffer saline (PBS) pH 7.4 showed that CPT-loaded PLC-g-mPEG micelles could prevent the hydrolysis of the lactone group of the drug.

In 2006, Yuan et al. [48] synthesized cholesterol-modified chitosan (CS-CH) at substitution degrees of 1.7-4.7 % cholesterol group by an EDC-mediated coupling reaction. The cholesterol-modified chitosan could be used to formulate nanoparticles by self-aggregated with diafiltrarion method. Cyclosporine A (Cy A) as the model drug was loaded into the spheres using dialysis method. The particles size diameter was less than 230 nm and the encapsulation efficiency at 6.2% of drug loading was 41.8%.

a) b)
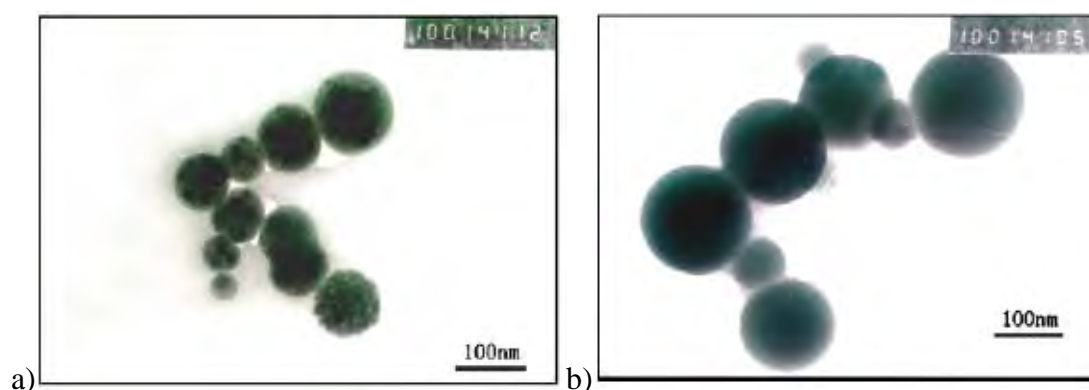
Figure1.8. TEM photograph of (a) CS-CH nanoparticles at 4.7% degree of substitution, (b) CS-CH nanoparticles at 1.7% degree of substitution

In 2007, Opanasopit et al. [37] prepared all-*trans* retinoic acid loaded into N-Phthaloylchitosan-grafted poly(ethylene glycol) methyl ether (PLC-g-mPEG) by dialysis method. The particle size was about 80-160 nm and was affected by initial drug-loading and % degrees of deacetylation (DD) of the starting chitosan. The incorporation efficiency decreased (Fig.1.9), ranging from 98 to 1.5% with an increase in the initial all-*trans* retinoic acid loading and the %DD. The all-*trans* retinoic acid loading was 4.7to10.7 %.
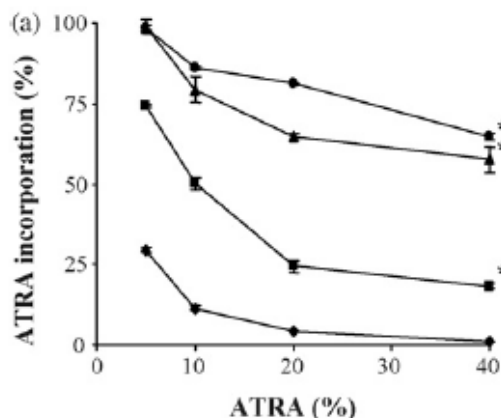
Figure1.9. Effect of percent degree of deacetylation (DD) of chitosan and all-*trans* retinoic acid concentration on all-*trans* retinoic acid incorporation efficiency in polymeric micelles. (◆) 80%DD; (■) 85%DD; (▲) 90%DD; (●) 95%DD

In 2009, Ngawhirunpat et al. [49] loaded camptothecin into cholic acid chitosan-grafted poly(ethylene glycol) methyl ether (CS-mPEG-CA) micelles through various physical encapsulation methods e.g., dialysis, emulsion and evaporation methods. The emulsion method gave the highest CPT encapsulation efficiency.

In 2010, Wang et al. [50] prepared folate-PEG coated cationic modified chitosan-cholesterol liposomes (FPLs) from octadecyl-quaternized lysine modified chitosan (OQLCS) and cholesterol. The calcein-loaded FPLs prepared by the gentle hydration method showed high encapsulation efficiency. The particles size of FPLs was about 160 nm with narrow distribution. The calcein-loaded FPLs gave increased uptake of the drug in MCF-7 cell.

In 2010, Tahara et al. [51] prepared siRNA-loaded chitosan (CS) -modified poly(D, L-lactide-co-glycolide) (PLGA) nanosphere by an emulsion solvent diffusion method. CS-modified PLGA nanosphere showed higher encapsulation efficiency than unmodified PLGA nanosphere and gave a positive zeta potential, while unmodified PLGA nanosphere were negatively charged. siRNA uptake studies in A549 human lung adenocarcinoma cell (A549 cell) increased with all the delivery systems.

1.11 Literature review of poly(vinyl alcohol)

In 2002, Luppi et al. [52] prepared nanocarriers from poly(vinyl acohol-co-vinyloleate), at a substitution degree of 4.8%. The obtained nanocarriers showed particles size in the range of 200-300 nm and demonstrated enhanced retinyl palmitate transcutaneous permeation.

In 2002, Orienti et al. [53] substituted poly(vinyl alcohol) with triethyleneglycolmonoethylether at different substitution degrees and obtained a suitable material for the formulation of a solid dispersion of progesterone. The drug-polymer solid mixtures were prepared by spray-drying at the following polymer-drug ratios: 2:1, 4:1, 6:1, 8:1 and 10:1. The particles analyzed by optical microscopy showed spherical shape with 0.5 to 3 μm diameter.

In 2003, Carchiara et al. [54] substituted poly(vinyl alcohol) with different alkyl chains (Iodododecane, Bromotetradecane) and crosslinked with bis-chloro-ethoxy-ethane. The polymer was used as β-carotene carrier. The physical mixtures were prepared by mixing β-carotene and polymer in a mortar until homogeneity. Comparing to pure β-carotene, the release of β-carotene-substituted polyvinyl alcohol mixtures presented faster β-carotene release in aqueous medium at pH 7.4.

In 2005, Orienti et al. [55] grafted oleyl amine onto poly(vinyl alcohol) at a substitution degree of 1.5% and prepared polymeric micelles from the grafted product. An entrapment of all-*trans* retinoic acid was then carried out by spray-dying method. The particle size was about 100-500 nm depending on polymer concentration used.

In 2008, Luadthong et al. [56] grafted cinnamic acid onto poly(vinyl acohol) at various substitution degree and prepared polymeric nanoparticles from the products by solvent displacement technique. Polymer with a higher degree of cinnamoyl substitution gave smaller particles.
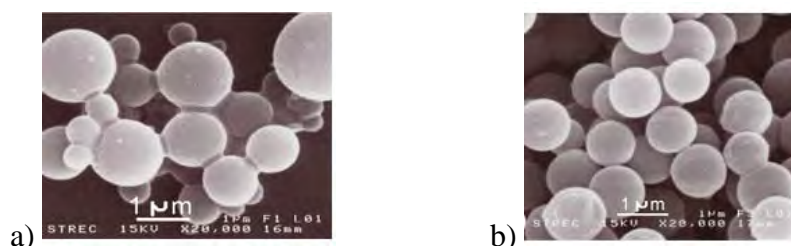
Figure1.10. SEM photograph of poly(vinyl alcohol-co-vinyl-cinnamate) with cinnamoyl substitution degree of 0.30 (a) and 0.44 (b)

In 2010, Margulis-Goshen et al. [57] prepared propylparaben-encapsulated poly(vinyl pyrrolidone) (PVP) nanoparticles by an oil-in-water emulsion solvent evaporation. It was found that more than 95 wt. % propylparaben was present after dispersion in water at PVP: propylparaben weight ratio of 7:3. The particles showed size average of less than 450 nm and the resulting dispersion was stable for months.

1.12 Literature review of vitamin A encapsulation

In 2004, Hwang et al. [24] encapsulated all-*trans* retinoic acid into phospholipid-based microemulsion. The process gave the encapsulation efficiency of higher than 99.9% and the ATRA loading of 32 %. Microemulsion formulation of all-trans retinoic acid improved the solubility and chemical stability of all-*trans* retinoic acid compared with all-*trans* retinoic acid in 1% Tween 80 and methanol solution (Fig.1.11) while maintained its pharmacokinetic profile and anti-cancer efficacy.
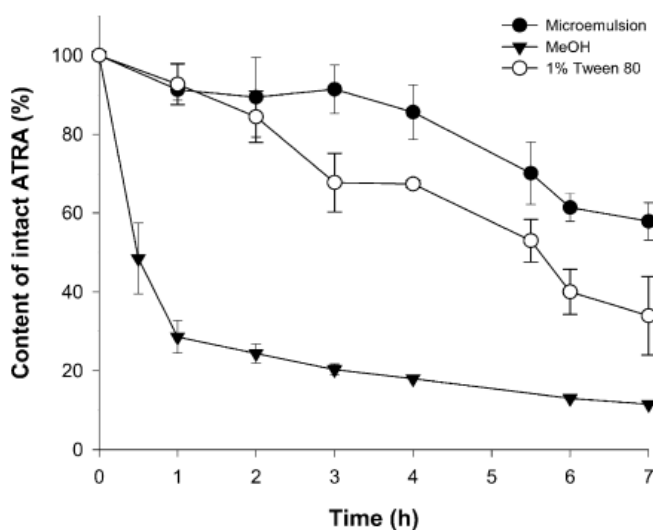
Figure1.11. Comparison of stability of All-*trans* retinoic acid in various preparations during incubation at room temperature under light exposure.

In 2006, Jee et al. [33] prepared all-*trans* retinol–loaded solid lipid nanoparticles (SLN) by hot melt homogenization method. The encapsulation efficiency was higher than 74% and drugs loading ranged from 2.17 to 2.94%. The particles size of all-*trans* retinol–loaded SLN ranged from 90 to 240 and the zeta potentials ranged from -27 to -37 mV, suggesting acceptable electrostatic stability of all-*trans* retinol–loaded SLN. The photostability at 12 h of all-*trans* retinol in SLN was higher than free retinol in methanolic solution.

In 2006, Kim et al. [4] prepared retinol-encapsulated chitosan nanoparticles by ultrasonication at an output power of 50W for 10 cycles of 2 s each on ice. Retinol-encapsulated chitosan nanoparticles has a spherical shape and its particle size was around 50-200 nm (Fig. 1.12). Particle size increased according to the increased drug content. The nanospheres gave the encapsulation efficiency higher than 60% with the highest retinol loading of 17.35 %
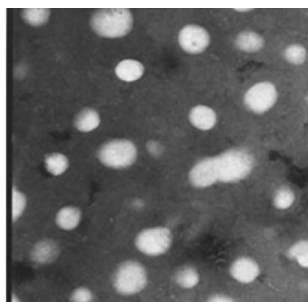
Figure1.12. TEM photograph of retinol-encapsulated chitosan nanoparticles

In 2007, Shah et al. [6] encapsulated tretinoin (TRE) into soild lipid nanoparticles (SLN) by emulsification-solvent diffusion (ESD) technique. SLN of TRE has a particle sizes around 300-500 nm, the encapsulation efficiency of 35.5% to 48.9% and the ATRA loading of 3.55 % to 4.89 %. Encapsulation of TRE in SLN resulted in a significant improvement in its photostability in comparison to TRE in methanolic solution.
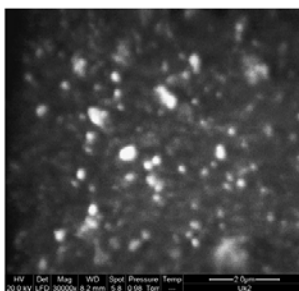
Figure1.13. SEM photograph of TRE-encapsulated soild lipid nanoparticles
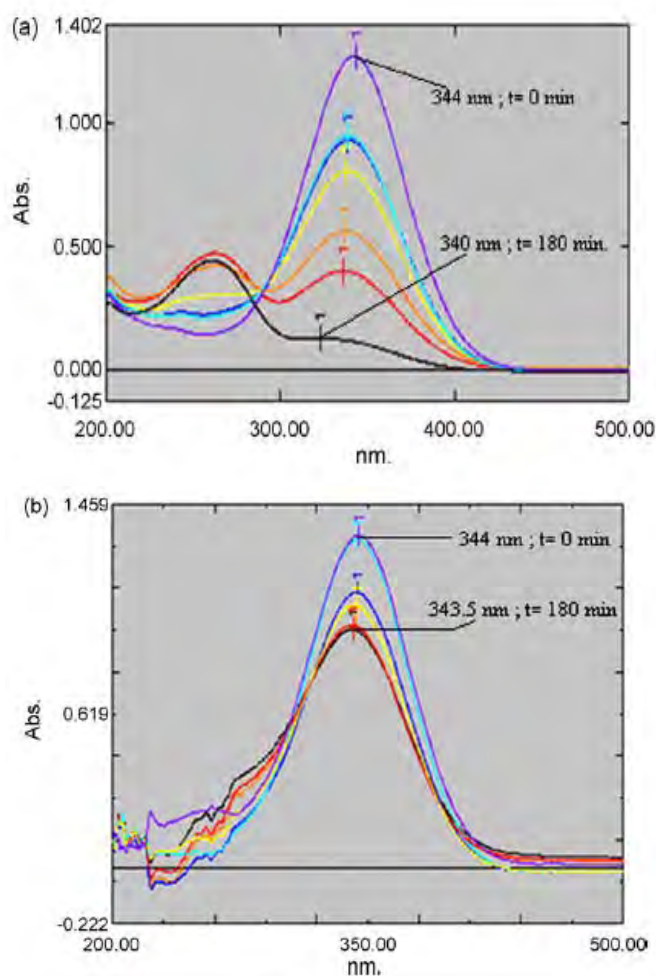
Figure1.14. Photodegradation of TRE after exposure to sunlight for different durations (a) methanolic solution, (b) SLN dispersion containing TRE.

In 2007, Liu et al. [1] prepared isotretinoin-loaded solid lipid nanoparticles. The isotretinoin-loaded SLN were formulated by hot homogenization method. The SLN formulations have high encapsulation efficiency ranging from 80% to 100% and drugs loading ranging from 19% to 24%. The isotretinoin-loaded SLN has low

average size of 30-50 nm. These particles showed high accumulation of isotretinoin in skins and possened a significant skin targeting effect.

In 2007, Redmond et al. [23] formulated all-*trans* retinoic acid nanodisks using phospholipid: all-trans retinoic acid ratio of 5.5:1. The all-trans retinoic acid nanodisks gave encapsulation efficiency of >85% and drugs loading of 1.25% to 1.78%. These nanodisks were in a nanoscale ranged of 8-20 nm.
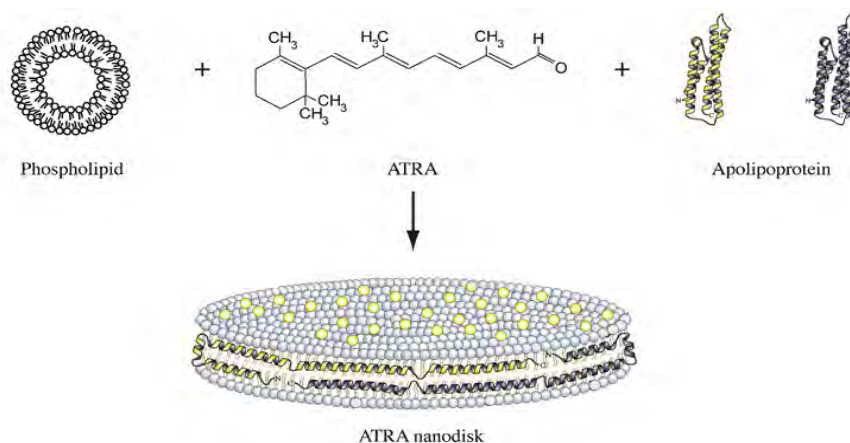
Figure1.15. All-*trans* retinoic acid nanodisks formulation scheme and structure model. All-*trans* retinoic acid nanodisks are comprised of a disk-shaped phospholipid bilayer in which all-trans retinoic acid molecules (yellow dots) are integrated.

In 2008, Ourique et al. [35] prepared tretinoin-loaded nanocapsules by interfacial deposition of performed poly-ε-caprolactone. The TRE-encapsulated poly-ε-caprolactone nanocapsules presented encapsulation efficiency of > 99.9% and drugs loading of 4.76%. These particles showed improved photostability of tretioin over free tretinoin in a methanolic solution.

In 2009, Errico et al. [58] encapsulated retinoic acid into poly (D, L-lactide-co-glycilide) (PLGA) and poly (3-hydroxybutyrate) (PHB) nanoparticles using the dialysis method. The particles size of retinoic acid-loaded PLGA and PHB ranged from 107±39 to 549±170 nm and 50±20 to 53±17 nm, respectively. The size of PHB nanoparticles prepared by dialysis method was quite singular when compared with other prepared techniques. The retinoic acid loading was 1.3% for retinoic acid-loaded PLGA and 1.04% for retinoic acid-loaded PHB.

1.13 Research goals

1. To find the suitable a polymer for ATRA nanoencapsulation.

2. To study chemical stability and photostability of the ATRA-loaded spheres.

3. To study skin penetration and release of the ATRA-loaded spheres.

CHAPTER II
EXPERIMENTAL

2.1. Materials and Chemicals

All-trans retinylacetate (ATRA) and ethylcellulose (EC) were purchased from Sigma-Aldrich (St. Louis, MO, USA). Poly(ethylene glycol)-phthaloylchitosan (PPLC) and poly(ethylene glycol)-4-methoxycinnamoylphthaloylchitosan (PCPLC) were prepared as previously described from chitosan [59]. Poly(vinyl alcohol-co-vinyl-cinnamate) with cinnamoyl substitution degree of 0.30 and 0.44 (PVA-C1 and PVA-C2) was prepared as previously described from poly (vinylalcohol) [60]. The dialysis bags used were made from regenerated cellulose tubular membrane (CelluSep T4, MWCO 12000-14000, 75 mm flat width, 17.9 ml cm^{-1} volume capacity, Membrane Filtration Products, Seguin, TX, USA).Centrifugal-filtering devices (MWCO 100,000, Amicon Ultra-15) were purchased from Millipore (Ireland). Centrifugation was carried out on an Allegra 64R et Avanti 30 (Beckman Coulter, Inc, USA). UV absorption spectra were acquired with a UV 2500 UV/vis spectrophotometer (Shimadzu Corporation, Kyoto, Japan) using a quartz cell with 1 cm path-length. Broad-band UVA spectrum (320-400 nm) was generated by an F24T12/BL/HO (PUVA) lamp and UVA irradiances was measured using UVA-400C power meter (National Biological Corporation, OH, USA). Confocal laser scanning microscopy (CLSM) was measured using Nikon Digital Eclipse C1si Confocal Microscope system (Tokyo, Japan). The CLSM equipped with BD Laser (405 nm), Ar Laser (488 nm), HeNe Laser (543 nm) (Melles Griot, USA). A Nikon TE2000-U microscope (Nikon, Tokyo, Japan) was used to visualize the structure and morphology of the nanoparticles. All confocal fluorescence pictures were taken with a Plan Apochromat VC 60X (60X objective: oil immersion, numeric aperture 1.40) and Plan Apochromat VC 100X (100X objective: oil immersion, numeric aperture 1.40). The software used for the Confocal Microscope system imaging was Nikon EZ-C1 (Nikon, Tokyo, Japan).

2.2. Encapsulation of ATRA into nanoparticles.

Five ATRA-encapsulated polymeric spheres were prepared by solvent displacement method using dialysis technique. For preparation of polymer solution, thirty milligrams of PPLC and PCPLC and three milligrams of PVA-C1 and PVA-C2

were dissolved in 10 ml of DMSO also thirty milligrams of EC was dissolved in 10 ml of acetone. After solubilization, ATRA was added into polymeric solution. Experiments were carried out at polymer: ATRA ratios of 3:3, 3:2 and 3:1. The clear solution was then placed in a dialysis bag (MWCO 12,400) with minimum void volume and dialyzed against 1 liter of Milli Q water. The dialysate water was changed repeatedly at 1, 2, 3 and 4 hours. After fifth hour, the resulting nanoparticles suspensions were subjected to the determination of encapsulation efficiency, ATRA loading, stability, *ex vivo* controlled release and characterized by scanning electron microscopy (SEM), transmission electron microscopy (TEM) and dynamic light scattering analyses (DLS).

2.3. Encapsulation efficiency and ATRA loading

To find the encapsulation efficiency, the suspension of ATRA-loading spheres was collected form the dialysis bag. ATRA-encapsulated polymeric nanoparticles suspension (1 ml) was filtering centrifuged (MWCO 100,000 (Amicon Ultra-15)) and the obtained solid was soaked in 5 ml ethanol for 1 hour at room temperature to ensure that the entire ATRA was dissolved. The suspension was then filtering centrifuged at 2,348 g for 10 minutes and the ethanol extract was collected then analyzed by UV/vis spectrophotometer as described above. The encapsulation efficiency (EE) and loading capacity were calculated using equation (1) and (2), respectively.

$$\% \text{ EE} = \frac{\text{Weight of encapsulated ATRA in the particles}}{\text{Weight of ATRA initially used}} \times 100 \qquad (1)$$

$$\% \text{ ATRA loading} = \frac{\text{Weight of encapsulated ATRA in the particles}}{\text{Weight of the ATRA-encapsulated particles}} \times 100 \qquad (2)$$

2.4. Differential scanning calorimetry

DSC was performed using a Netzsch DSC 204 Phoenix. Ten milligrams pf the dry samples were precisely weight into aluminum cups and sealed. A small hole was done at the top of the cup in order to allow the release of water. An empty cup was used as reference. The experiment consisted of two runs. The first one from -100 to 130 or

150°C and the second one from -100 to 350°C. The experiments were run at a scanning rate of 10 K/min.

2.5. Morphology and ζ potential of ATRA-encapsulated nanoparticles

The morphology of ATRA-encapsulated nanoparticles was determined with scanning electron microscope (SEM) and transmission electron microscope (TEM). Particle size distribution and the ζ potential of ATRA-encapsulated nanoparticles were determined using Zetasizer nano series (Malvern Instruments).

TEM photographs were acquired on a transmission electron microscope (JEM-2100, JEOL, Tokyo, Japan). A drop of nanoparticles suspension was placed on a carbon film coated on a copper grid and dried. Observation was performed at 100-120 kV.

SEM photographs were obtained using a scanning electron microscope (JEM-6400, JEOL, Tokyo, Japan). A drop of the nanoparticles suspension was placed on a glass slide and dried. The sample was coated with a gold layer under vacuum at 15 kV for 90 s. The coated sample was then mounted on an SEM stud for visualization. Analysis was carried out at 25 ± 2ºC.

An average particle size (z-average size) and a zeta potential (ζ) were measured by Zetasizer (Nano Series Model) (Malvern Instruments, Worcestershire, UK) equipped with a He-Ne laser beam at 632.8 nm (scattering angle of 173º) at 25 ± 2ºC. Each measurement was repeated three times and an average value was reported.

2.6. Stability of ATRA

2.6.1 Stability under light-proof condition. The chemical stability of the ATRA-encapsulated in the EC and in the PCPLC particles was examined by monitoring the concentration of non-degraded ATRA during incubation of the suspension at room temperature for 3 months. Briefly, 1 ml of the ATRA-encapsulated EC (or PCPLC) particle suspension was filtering centrifuged. The obtained solid was then soaked in 5 ml ethanol for 1 hour at room temperature to extract ATRA out into the solution. The suspension was then filtering centrifuged at 2,348 g for 10 min and the ethanol extract was collected for quantitative analysis by UV-absorption spectrophotometry with an aid of a calibration curve. The calibration

standard were prepared by dissolving 100 µg of ATRA in 1 ml ethanol and diluted with ethanol to obtain at 0, 1, 3, 5, 7, 10, 15 ppm ATRA solutions. The absorbance of the resulting solutions was scanned from 200 to 500 nm on a Shimadzu UV-2500, UV/vis double beam spectrophotometer (Shimadzu, Japan). Absorbance at the maximum absorption wavelength (325 nm) was used deviation form the normal peak shape was also examined and used as evidence for ATRA degradation. The linear range ($R^2 = 0.997$) was in the 1-15 µg/ml concentration range.

      2.6.2 Photostability of encapsulated ATRA. The photostability of encapsulated ATRA was determined in comparison to the free ATRA. Briefly, 2 ml of sample were exposed to UVA light (8.5 mW/ cm^2) for 0, 15, 30, 45, 60 and 90 min which corresponded to the light exposure of 0, 7.8, 15.4, 22.9, 30.7 and 45.9 J/cm^2, respectively. UV spectrum at each exposure was recorded. Free ATRA solutions of similar ATRA concentrations were freshly prepared in ethanol and the solutions were subjected to similar UVA exposure experiment. The suspension used in the experiment was prepared to give similar ATRA final concentration of 300 ppm. One milliliter of the ATRA-encapsulated EC and PCPLC particle suspension after UVA exposure were filtering centrifuged at 2,348 g for 10 min and the obtained solid was soaked in 5 ml ethanol for 1 h at room temperature to extract ATRA out into the solution. The suspension was then filtering centrifuged and the ethanol extract was collected for quantitative analysis by UV-absorption spectrophotometry compared with a calibration curve.
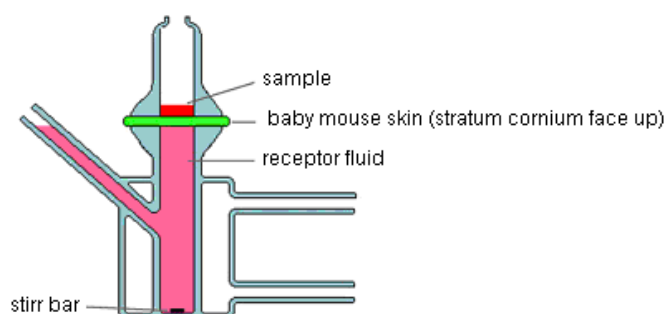
Figure2.1. Drawing of the Franz diffusion cell used in the ex vivo controlled release experiment.

2.7. *Ex vivo* controlled release test

2.7.1. Skin specimens. The skin specimens (Abdominal skin removed by a surgical procedure) of nine-day old baby mice (*M. musculus* Linn.) were purchased from National Laboratory Animal Centre (Nakhonpathom, Thailand). All animal experiments were performed under permission from the National Laboratory Animal Centre. The skin, comprised of epidermis and dermis layers, was kept at 4ºC and cut into approximately 2.0×2.0 cm^2 pieces prior to use. The full thickness of the baby mouse skins was approximately form 450 to 600 µm.

2.7.2. Diffusion cell experiments. *Ex vivo* permeation study of encapsulated ATRA was conducted with vertical Franz diffusion cells with a 13 ml capacity receptor compartment and 2.27 cm^2 diffusion area using the abdominal skin of baby mice (Fig. 2.1). The ATRA-encapsulated EC and ATRA-encapsulated PCPLC (concentration of ATRA = 333 ppm and concentration of polymer = 1000 ppm) were used and compared with unencapsulated ATRA. The experiment was initiated by 3 ml of encapsulated ATRA and unencapsulated ATRA into the upper compartment of the diffusion cell. The receptor medium consisted of isotonic phosphate buffered saline, pH 7.4 and 1% (v/v) Tween 20 to ensure the solubility of ATRA. This medium was maintained at room temperature and constantly stirred with a magnetic bar. The experiment was carried out, the medium (1 mL) as withdrawn at 1, 2, 4, 6, 18 and 24 h with the replacement of the same volume of fresh medium. Care was taken to avoid any air bubbles in the receptor fluid. The concentration of ATRA in each aliquot of withdrawn receptor fluid was determined by UV/vis spectrophotometer scanned from 200 to 500 nm. A calibration curve of ATRA in receptor fluid was constructed by measuring the absorbance of ATRA standard solution at 325 nm. Experiments were done at room temperature in 3 repetitions. Since the skins from different mice varied, the penetration of each sample was compared to the penetration of free ATRA (not encapsulated) using skin from the same mouse to normalize the results. The penetration of the nanoparticles was determined by analyzing the 24 h receptor medium. The ATRA released was calculated using equation (3).

$$\% \text{ ATRA release} = \frac{\text{Amount of ATRA initiated - remained ATRA upper compartment}}{\text{Amount of ATRA initiated}} \times 100 \qquad (3)$$

2.8. Confocal fluorescence Laser Scanning Microscopy (CLSM)

For verified the localization of ATRA-loaded PCPLC (concentration of ATRA = 333 ppm) in the mouse skin, confocal fluorescence laser scanning microscopy (CLSM) was used. The skin specimens of nine-day old baby mice (M. musculus Linn.) were purchased from National Laboratory Animal Centre (Nakhonpathom, Thailand) (see section 2.5.1). The ATRA-loaded PCPLC was dropped on the mouse skin (final coverage of PCPLC and ATRA were 50 and 16.67 μg/cm^2, respectively) and kept at 4 ℃ for 2 h. After that confocal fluorescence pictures were excited laser wavelength of 405 nm and taken with a Plan Apochromat VC 60X and 100 X using oil immersions, numeric aperture 1.40. The Confocal Microscope system imaging was performed by using Nikon EZ-C1 (Nikon, Tokyo, Japan) software.

CHAPTER III
RESULT AND DISCUSSION

In recent years, their have been much interest in the use of vitamin A and its derivative for the treatment of dermatological diseases such as acne and psoriasis. Unfortunately, some drawbacks such as poor water solubility, photostability and local irritating reactions strongly have limited the topical use of this vitamin. This work shows a solution to this problem through the nanoencapsulation of ATRA using five polymers, ethyl cellulose (EC), poly (ethylene glycol)-4-methoxycinnamoylphthaloyl chitosan (PCPLC), poly (vinylalcohol-co-vinyl-cinnamate) with cinnamoyl substitution degree of 0.30 and 0.44 (PVA-C1 and PVA-C2), poly (ethylene glycol)-phthaloylchitosan (PPLC). Study was performed at the ATRA: polymer weight ratios of 3:3, 2:3 and 1:3. Encapsulation of ATRA was carried out by performing the dialysis of 3% (w/v) PPLC or PCPLC solution (10 ml DMSO), 0.3% (w/v) PVA-C1 or PVA-C2 solution (10 ml DMSO) and 3% EC solution (10 ml acetone) in a presence of 10, 20 and 30 mg ATRA, against water.

To obtain loading, direct analysis of the particles were performed. The obtained particles were characterized by SEM, TEM and DLS (section 3.3). The obtained suspension of ATRA-encapsulated nanoparticles in water was centrifuged (10 min at 2,348 g) and soak in 5 ml ethanol for 1 h at room temperature to extract ATRA from the particles out into the solution. After 1 h incubation, the ethanol extract was centrifuged (10 min at 2,348 g) and the liquid was subjected to quantitative analysis of ATRA using UV/vis-spectrophotometry. The encapsulation efficiency and ATRA loading (section 3.1) could then be obtained. Then stability under light proof condition of the encapsulated ATRA was investigated (section 3.4). After that photostability of free ATRA and the selected encapsulated ATRA samples was compared (section 3.5). The *Ex vivo* permeation and release of encapsulated ATRA were conducted with vertical Franz diffusion cells (section 3.6). Localization of ATRA-loaded PCPLC in the mouse skin was carried out using confocal fluorescence laser scanning microscopy (CLSM) (section 3.7).

3.1. Encapsulation efficiency and ATRA loading

Here, five polymers; ethyl cellulose (EC), poly(ethylene glycol)-4-methoxycinnamoylphthaloylchitosan (PCPLC), poly(vinylalcohol-co-vinylcinnamate) with cinnamoyl substitution degree of 0.30 and 0.44 (PVA-C1 and PVA-C2), poly (ethylene glycol)-phthaloylchitosan (PPLC) were used for encapsulation of ATRA. Amongst the five polymers, only EC and PCPLC could effectively encapsulate ATRA (Table 3.1). Although PPLC, PVA-C1 and PVA-C2 could give stable aqueous suspension during the self-assembly in the present of ATRA, quantitative analysis of the three products showed no significant ATRA content. Therefore, it was conclude that these three polymers could not be used as carrier material for ATRA encapsulation. The results (Table 3.1) showed that the encapsulation efficiency of ATRA-encapsulated EC and PCPLC was more than 60%. As expected, ATRA loading increased according to the amount of ATRA used. Also, encapsulation efficiency decreased in proportion to the increase amount of ATRA used. The encapsulation efficiency and ATRA loading of ATRA-encapsulated EC were slightly higher than those of ATRA-encapsulated PCPLC. The reasons of these results probably lie on the particle size and the polymer's structure. The ATRA-encapsulated EC particles were bigger than ATRA-encapsulated PCPLC, therefore, the former should possessed a larger internal hydrophobic cargo space, resulting in higher loading of ATRA in the EC spheres. On the other hand, PCPLC spheres were smaller, thus, higher surface area. The more surface area required more polymers to form, therefore, the ratio between polymers to ATRA increased. This resulted in smaller loading volume. At the same time, PCPLC structure was more hydrophobic and complex since the polymer side chain were substituted with large cinnamoyl and phthaloyl groups, these should give better hydrophobic interaction at the interior of the spheres, leading to smaller particles with less ATRA loading. In other words, the PCPLC system possessed better hydrophobic interaction amongst themselves, thus, ATRA was less welcomed. As mentioned earlier that the PPLC, PVA-C1 and PVA-C2 could not encapsulated ATRA, the encapsulation of ATRA depends on compatibility between hydrophobic part of ATRA and polymer, thus, upon self-assembling, the hydrophobicity of the three polymers which would be at the interior of the spheres, was not in the range that could solubilize ATRA molecules. These

results indicated that ATRA was most effectively encapsulated into the EC and PCPLC at the polymer: ATRA ratio of 3: 1. Detection of ATRA indicated that the process was capable of not only incorporating ATRA into the nanospheres but also preserved the chemical integrity of this unstable compound.

Table 3.1. Encapsulation efficiency percentages (%EE) and ATRA loading of ATRA-encapsulated EC and PCPLC (% ATRA loading)

polymer	polymer: ATRA ratio	%EE	%ATRA loading
EC1	3:3	85.03 ± 4.3	45.44 ± 1.6
EC2	3:2	87.45 ± 2.5	36.82 ± 0.7
EC3	3:1	90.68 ± 1.9	23.21 ± 0.4
PCPLC1	3:3	61.01 ± 0.1	37.89 ± 0.03
PCPLC2	3:2	65.26 ± 3.1	30.31 ± 1.0
PCPLC3	3:1	80.03 ± 0.5	21.06 ± 0.1
PPLC 1	3:3	ND	ND
PPLC 2	3:2	ND	ND
PPLC 3	3:1	ND	ND
PVA-C1(1)	3:3	ND	ND
PVA-C1(2)	3:2	ND	ND
PVA-C1(3)	3:1	ND	ND
PVA-C2(1)	3:3	ND	ND
PVA-C2(2)	3:2	ND	ND
PVA-C2(3)	3:1	ND	ND

*ND: cannot detected, ATRA intact degraded

3.2. Differential scanning colorimetry

DSC analyses of the PCPLC nanoparticles, unencapsulated ATRA and ATRA-encapsulated PCPLC nanoparticles confirmed that the ATRA was in the solid solution state with the polymer. The thermograms of PCPLC nanoparticles and the ATRA-

encapsulated PCPLC nanoparticles (Fig. 3.2 and Fig. 3.3) showed initial broad endothermic peaks at 25-85°C which correlated with loss of water connected to hydrophilic groups of the nanoparticles. The endothermic peak of ATRA was 54.7°C which corresponded to the melting temperatures of ATRA while the endothermic peak of ATRA-encapsulated PCPLC was absent (Fig. 3.1). Thus, it could be concluded that ATRA-encapsulated PCPLC was in an amorphous or disordered-crystalline phase of a solid solution state.
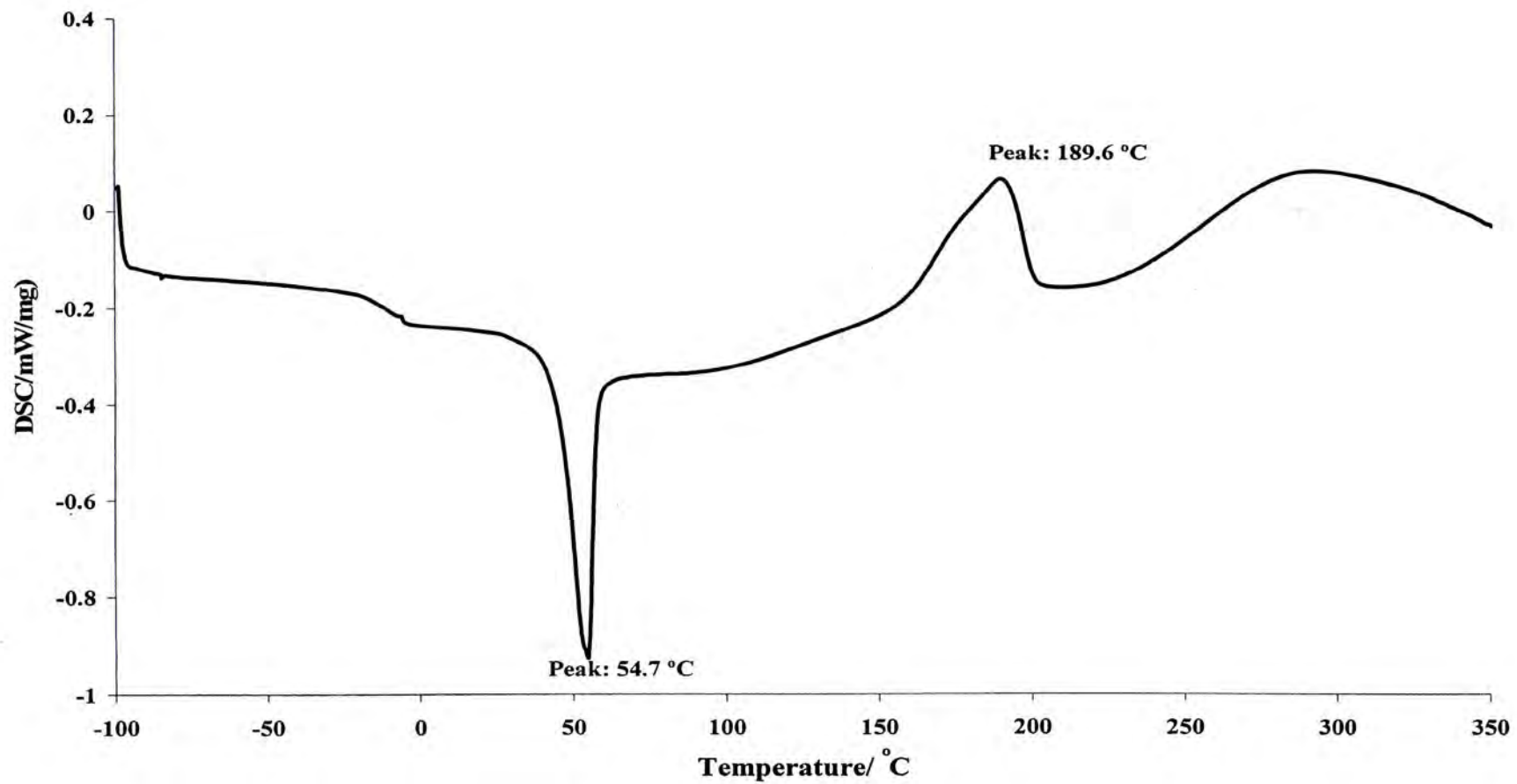
Figure 3.1 Differential scanning colorimetry curve of all-*trans* retinyl acetate
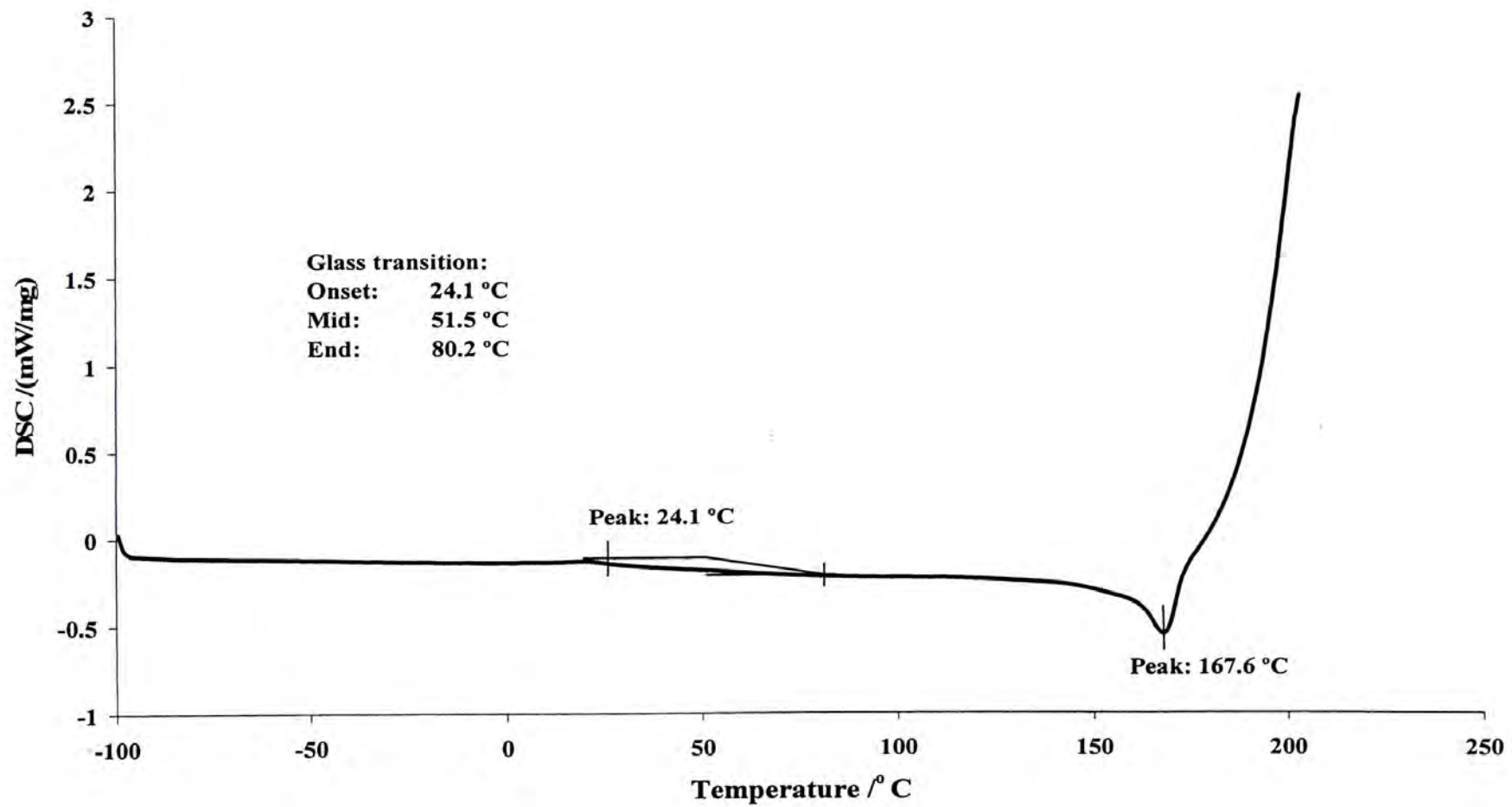
Figure 3.2 Differential scanning colorimetry curve of poly(ethylene glycol)-4-methoxycinnamoylphthaloylchitosan nanoparticle
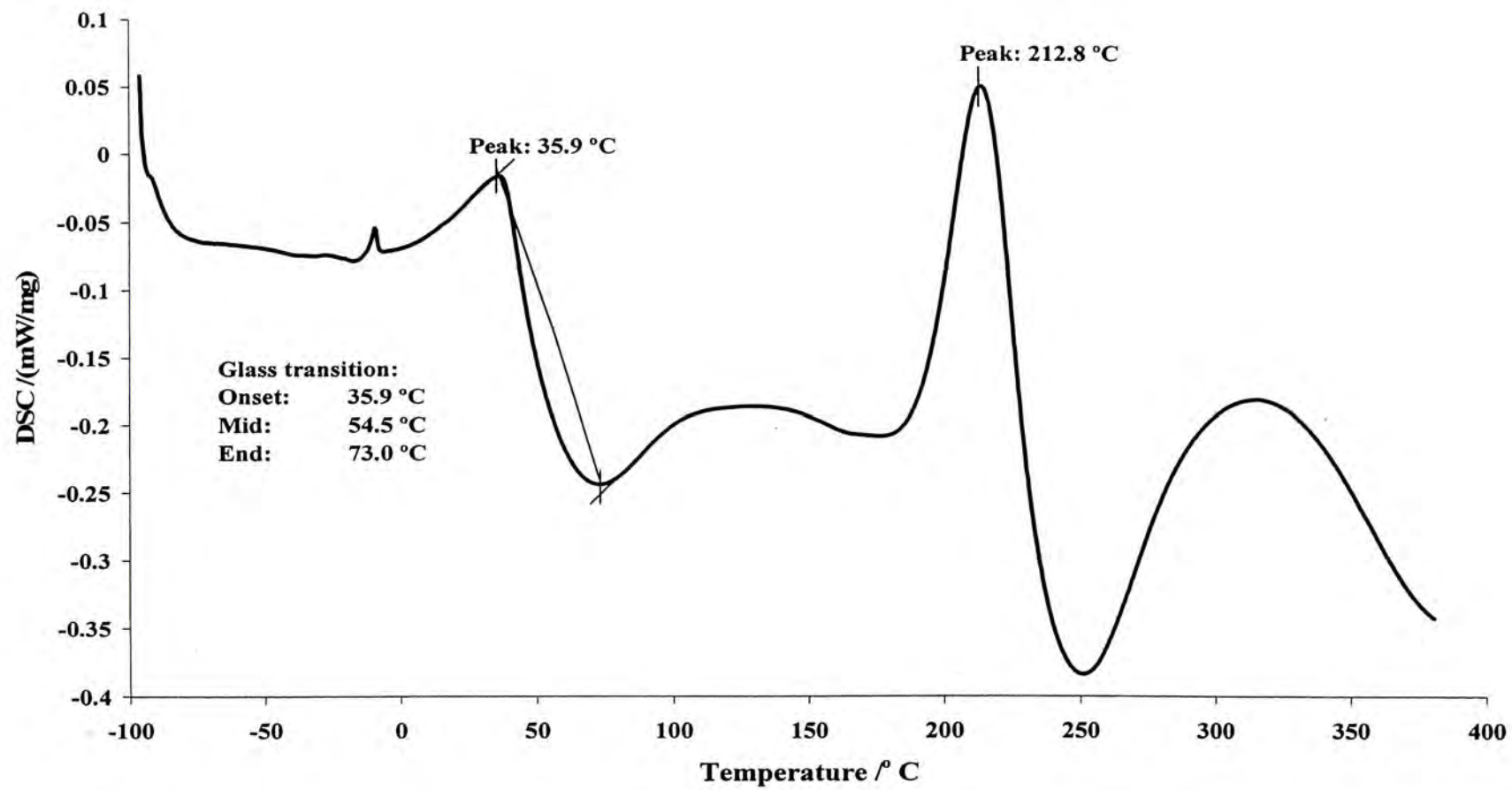
Figure 3.3 Differential scanning colorimetry curve of ATRA-encapsulated poly(ethylene glycol)-4-methoxycinnamoylphthaloylchitosan nanoparticle

3.3. Morphology, size distribution and ζ potential of ATRA-encapsulated nanoparticles

Morphology of ATRA-encapsulated nanoparticles was characterized with scanning electron microscope (SEM) and transmission electron microscope (TEM). The TEM photographs of ATRA-encapsulated EC and PCPLC nanoparticles and SEM photographs of five ATRA-encapsulated polymeric nanoparticles showed spherical shape with narrow distribution (Fig. 3.4 and Fig. 3.5). The particle size decreased in proportion to the decreased ATRA contents. The size distribution of the ATRA-loaded EC and PCPLC nanoparticles (Fig. 3.6 and Fig. 3.7) was measured by dynamic light scattering. The particle size and ζ potential are shown in Table 3.2. The particle size of ATRA-encapsulated nanoparticles by DLS was in nanometric range. Particles size obtained from DLS was bigger than particles size from SEM. The result concluded that the PCPLC spheres could swell in water medium. Whereas SEM characterization used dried sample, gave smaller particles size. Particle size and ζ potential increased according to the contents of ATRA as expected. The zeta potential, that is, surface charge, can greatly influence particle stability in suspension through the electric repulsion between particles. The ζ potential of ATRA-encapsulated EC nanoparticles has a little more negatively charged than ATRA-encapsulated PCPLC nanoparticles. Thus, the ATRA-encapsulated EC better dispersed in suspension than ATRA-encapsulated PCPLC did. The ζ potentials in Table 3.2 agreed well with the SEM photographs, the SEM photographs of ATRA-encapsulated PCPLC (Fig. 3.5. (d-f)) showed aggregated particles while those of encapsulated EC showed much less aggregated particles.
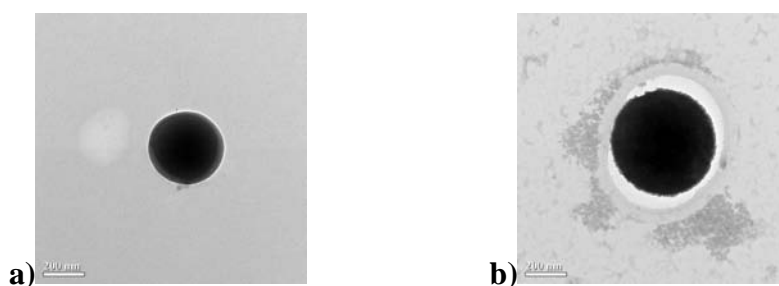
Figure3.4. TEM photograph of ATRA-encapsulated EC 3 (a) and ATRA-encapsulated PCPLC 3 (b)

Table3.2. Physicochemical characteristics of ATRA-encapsulated nanoparticles

polymer	ATRA: polymer ratio	Particle size distribution from SEM	Particle size distribution from DLS	PDI	ζ potential
EC1	3:3	705.3 ± 141.9	673.9 ± 9.2	0.306	-25.7 ± 0.1
EC2	2:3	602.7 ± 89.7	418.1 ± 2.3	0.237	-27.6 ± 0.2
EC3	1:3	330.4 ± 50.6	406.1 ± 4.1	0.213	-31.7 ± 0.3
PCPLC1	3:3	169.6 ± 43.7	519.9 ± 2.1	0.096	-10.9 ± 0.9
PCPLC2	2:3	121.5 ± 13.9	446.7 ± 5.9	0.056	-13.9 ± 1.3
PCPLC3	1:3	113.2 ± 27.1	226.9 ± 0.7	0.027	-22.7 ± 2.3
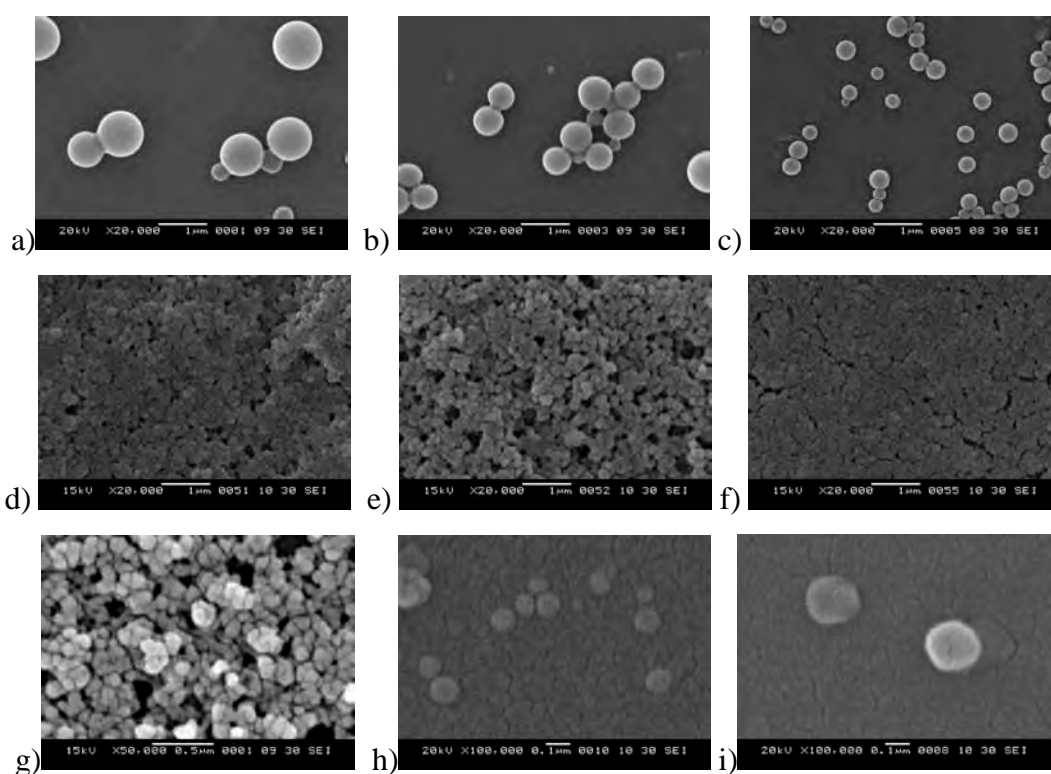
Figure3.5. SEM photograph of ATRA-encapsulated EC1 (a), ATRA-encapsulated EC2 (b), ATRA-encapsulated EC 3 (c), ATRA-encapsulated PCPLC1 (d), ATRA-encapsulated PCPLC2 (e), ATRA-encapsulated PCPLC3 (f), ATRA-encapsulated PPLC 3:1 ratio (g), ATRA-encapsulated PVA-C1 3:1 ratio (h) and ATRA-encapsulated PVA-C2 3:1 ratio (i).

a)

b)

c)
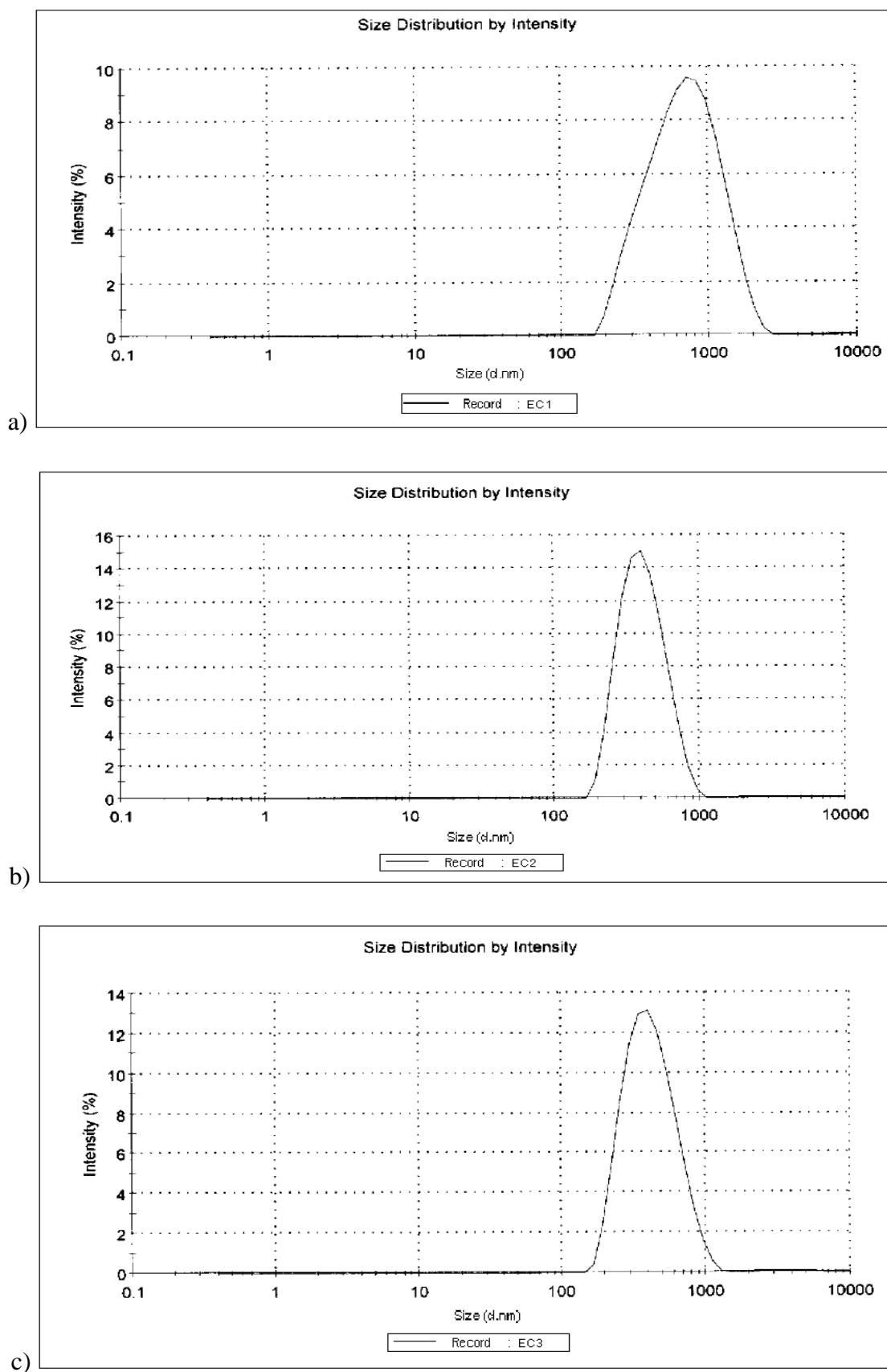
Figure 3.6 Size distribution of ATRA-encapsulated EC1 (a), EC2 (b) and EC3 (c)
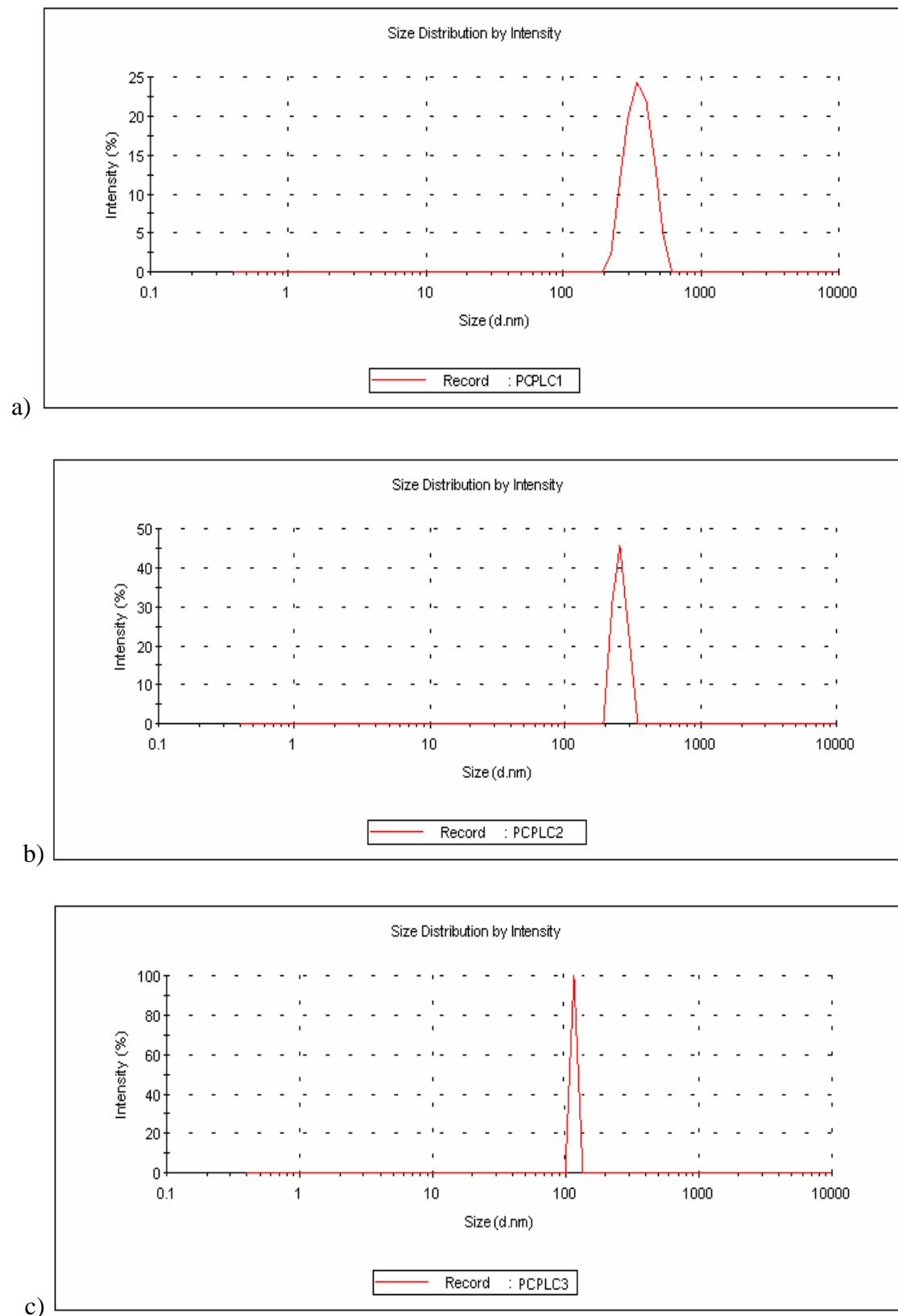
Figure 3.7 Size distribution of ATRA-encapsulated PCPLC1 (a), PCPLC (b) and PCPLC3 (c)

3.4. Stability of ATRA

The stability of the encapsulated ATRA compared with free ATRA under the light proofed condition during a period of 3 months was investigated. Here, the amount of ATRA was quantified through the UV absorption at 325 nm (λ_{max} of ATRA) with the aid of the calibration graph obtained from the very freshly prepared ATRA solution. The results indicated that after encapsulation, ATRA stability increased significantly (Fig. 3.8 and Fig. 3.9). Among the three ATRA-encapsulated PCPLC samples, particles with the least ATRA loading showed the most improvement of ATRA stability in water, i.e., ATRA-encapsulated PCPLC3 showed ~40% stability improvement in water after being kept as aqueous suspension for three months. At similar loading to PCPLC3, ATRA-encapsulated EC3 showed ~20% stability improvement after kept as aqueous suspension for only one month. As presented earlier that the PCPLC spheres were smaller than EC spheres, therefore, they possessed higher surface area. The high surface area of PCPLC spheres should allow more contact between reactive oxygen species (ROS) and PCPLC spheres, comparing to the contact of ROS with EC spheres which were bigger and thus possessed less surface area. However, the ATRA molecule encapsulated in the PCPLC spheres were more stable than those encapsulated in EC spheres. This implied that the PCPLC polymeric shell could more significantly retard the penetration of the ROS than the EC polymeric shell. As it has been reported previously that moisture (water) and oxygen could cause ATRA degradation [23, 24, 25]. It was likely that penetration of water and oxygen through PCPLC layer might be much harder than through EC. As a result, the ATRA molecules encapsulated in the PCPLC spheres were less degraded than those encapsulated in EC spheres. This speculation is also supported by the fact that EC structure is not as hydrophobic as the PCPLC structure. Considering the structure of EC, it can be seen clearly that the ethyl group is the only hydrophobic part. There was no well separated section between the hydrophobic ethyl groups and the hydrophilic unsubstituted sugar units, therefore, it was likely that upon self-assembling, EC polymer formed into a thin layer with hydrophobic part turned inside and hydrophilic part turned outside of the spheres. The ATRA molecules inside the spheres, were, then separated from the ROS in the medium by only this thin layer. It is likely that these ROS could penetrate into the spheres easily, causing fast degradation of ATRA. In contrast, PCPLC structure contains bulky hydrophobic groups (cinnamoyl and phthaloyl moieties) and enormous hydrophilic moieties (PEG). The well separation between PEG and the rest is very likely. Therefore, upon

self-assembling the thick hydrophobic shell should be formed through the cinnamoyl and phthaloyl groups while the bulky PEG should surround the sphere forming a hydrophilic layer. This structure effectively retarded the penetration of ROS species, thus the ATRA inside PCPLC spheres was more stable.
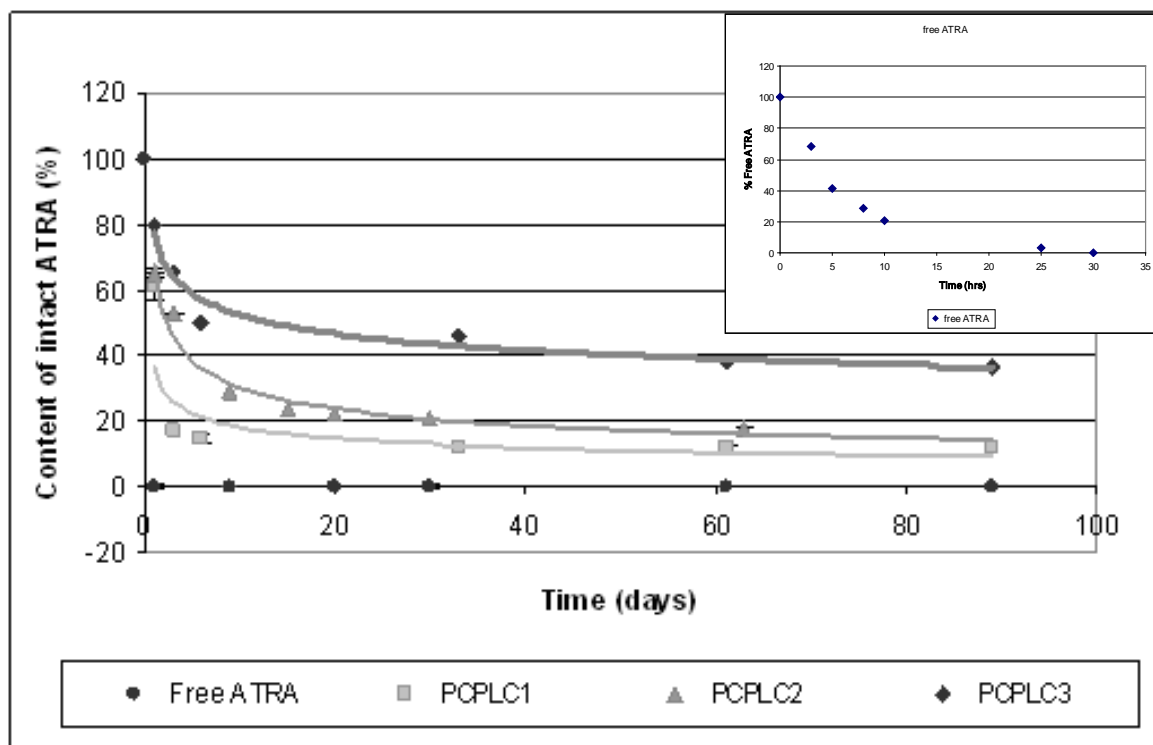
Figure3.8. Stability profile of three ATRA-encapsulated PCPLC compared with Free ATRA.
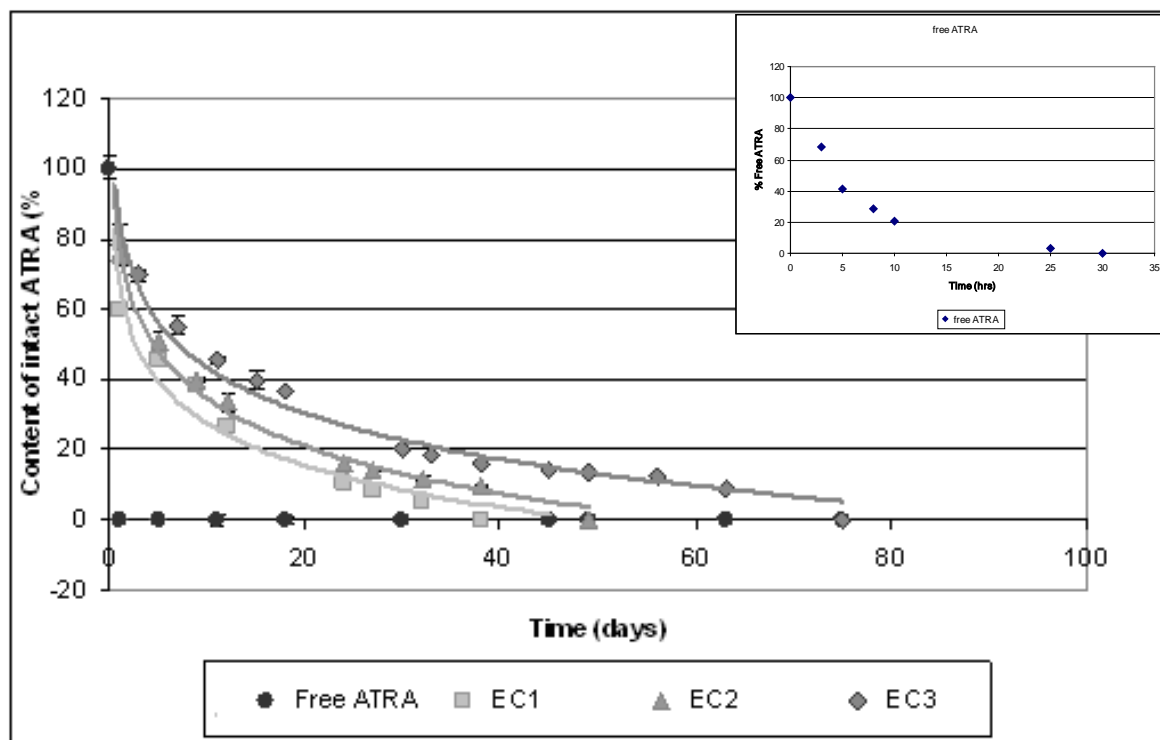
Figure3.9. Stability profile of three ATRA-encapsulated EC compared with Free ATRA.

3.5. Photostability of ATRA

As it has been known that ATRA degrades quickly with UVA radiation, investigation was carried out to see if encapsulation could lessen such photodegradation. From the encapsulation efficiency and the stability under the light proof result showed that ATRA-encapsulated EC3 and PCPLC3 gave the highest encapsulation efficiency of each polymer. Therefore, the photostability test chose two encapsulated ATRA (EC3 and PCPLC3) compared with free ATRA. The photostability test indicated that free ATRA and ATRA encapsulated in the EC spheres showed readily degradation after being exposed to UVA radiation, as witnessed by the decrease in absorption at 325 nm in its UV/vis absorption spectra (Fig. 3.10a and 3.10b). In contrast, significantly slower degradation was observed for the PCPLC3-encapsulated ATRA as witnessed by smaller decreases in the maximum absorption at 325 nm (Fig. 3.10c). Only small exposure of the UVA radiation caused a significant degradation of the unencapsulated ATRA as witnessed by a sharp decrease in the absorbance at 325 nm. It should be noted here that the experiments were conducted at similar final concentration of ATRA. To make sure that the increased photostability of the encapsulated ATRA was not the result of light shielding effect from the light scattering with the particles, free

ATRA solution added with unencapsulated PCPLC spheres were tested. The result also showed fast degradation (Figure. 3.10d). Comparing between EC and PCPLC carriers, it was obvious that the latter provided significantly more improvement in photostability for ATRA. For the PCPLC encapsulated ATRA, ~36 % of ATRA could still be detected after being exposed to 45.9 J of UVA radiations (Fig. 3.11). In contrast, complete degradation was observed when the free ATRA and the EC-encapsulated ATRA (EC3) were being exposed to similar radiation.

The above result is likely to be a result of UVA-absorption properties of PCPLC polymer itself [42]. While EC side chain was only ethyl group, the structure of PCPLC possess UV-absorptive groups, cinnamoyl and phthaloyl moieties, which could protect ATRA from UV radiation.

a)
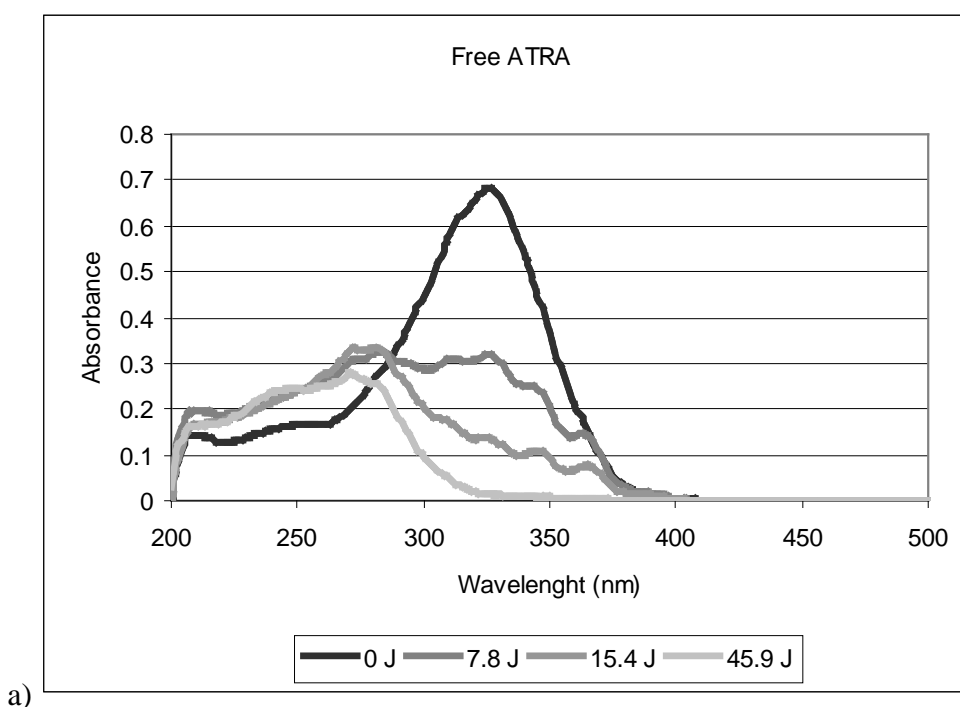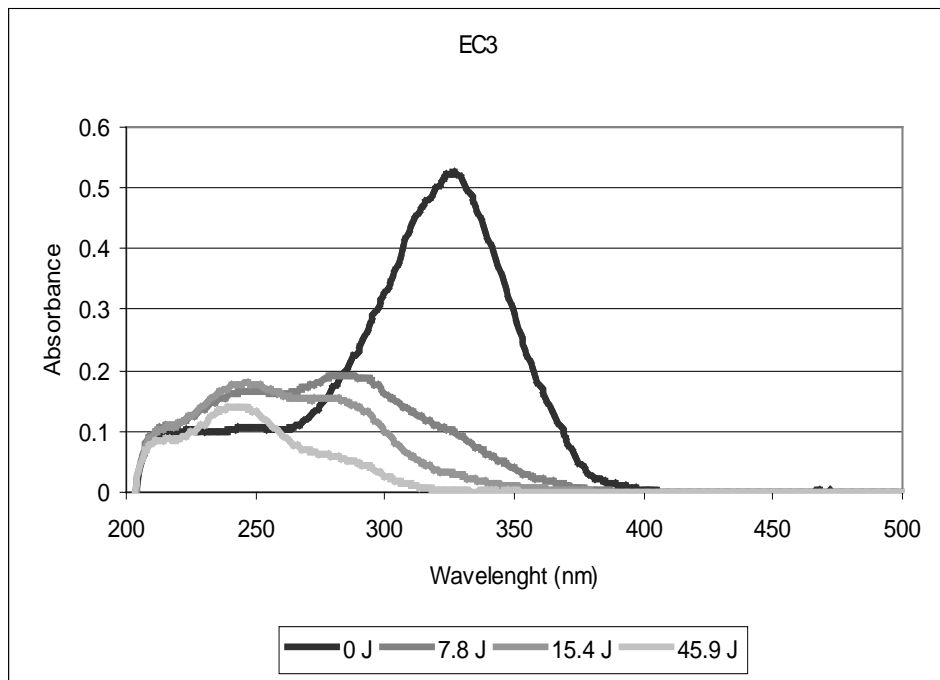
b)
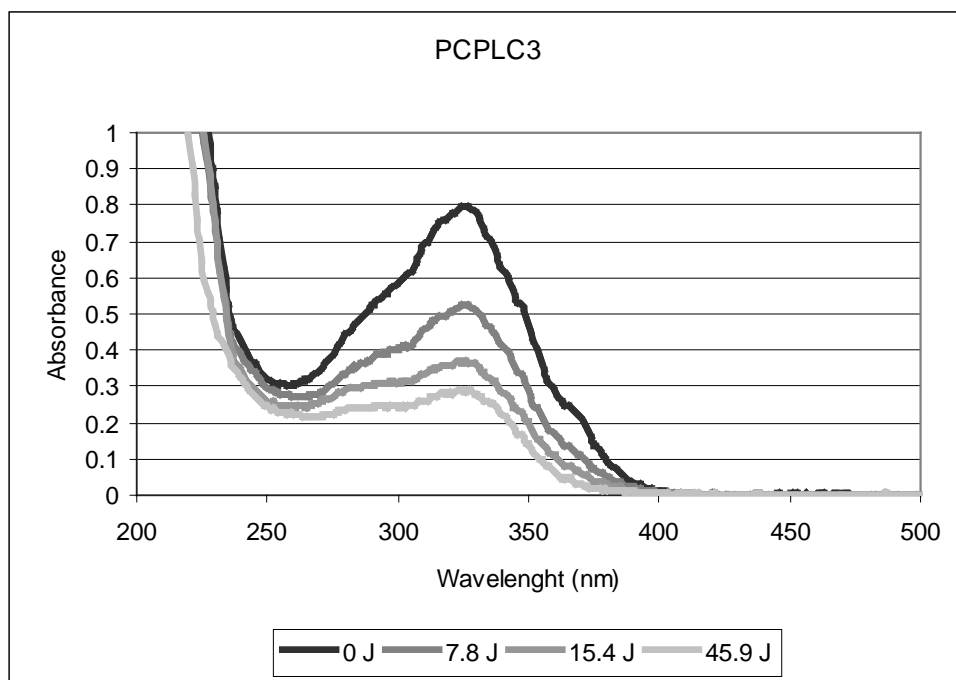
c)
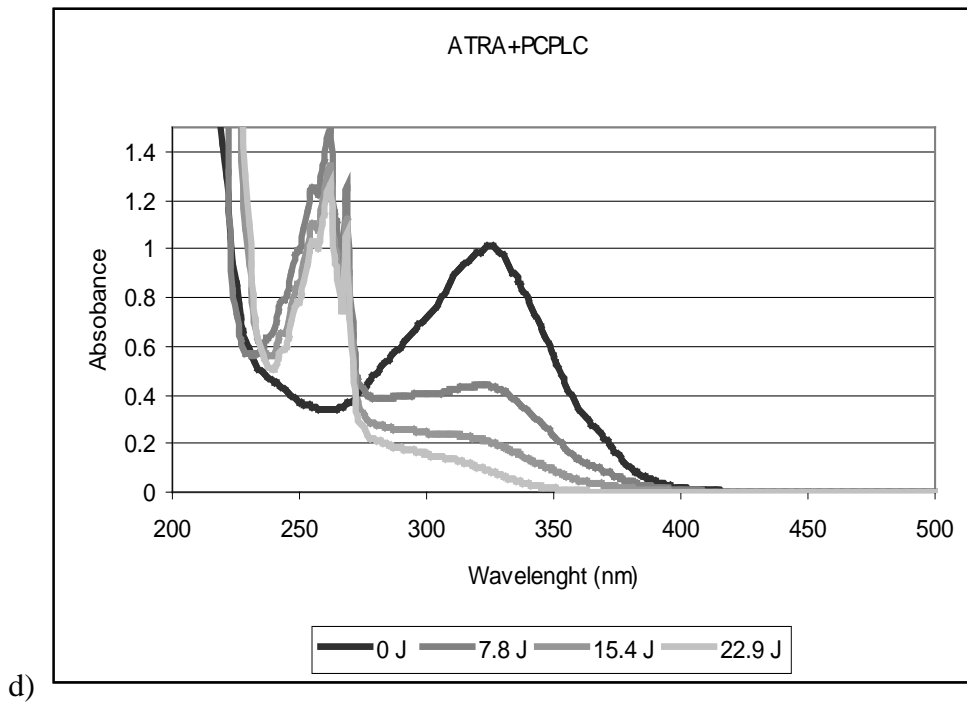
d)

Figure 3.10 Photodegradation of ATRA after various to UVA exposures: ethanolic solution of ATRA (a), ATRA-encapsulated EC (b), ATRA-encapsulated PCPLC (c) and free ATRA solution spiked with unencapsulated PCPLC spheres (d)
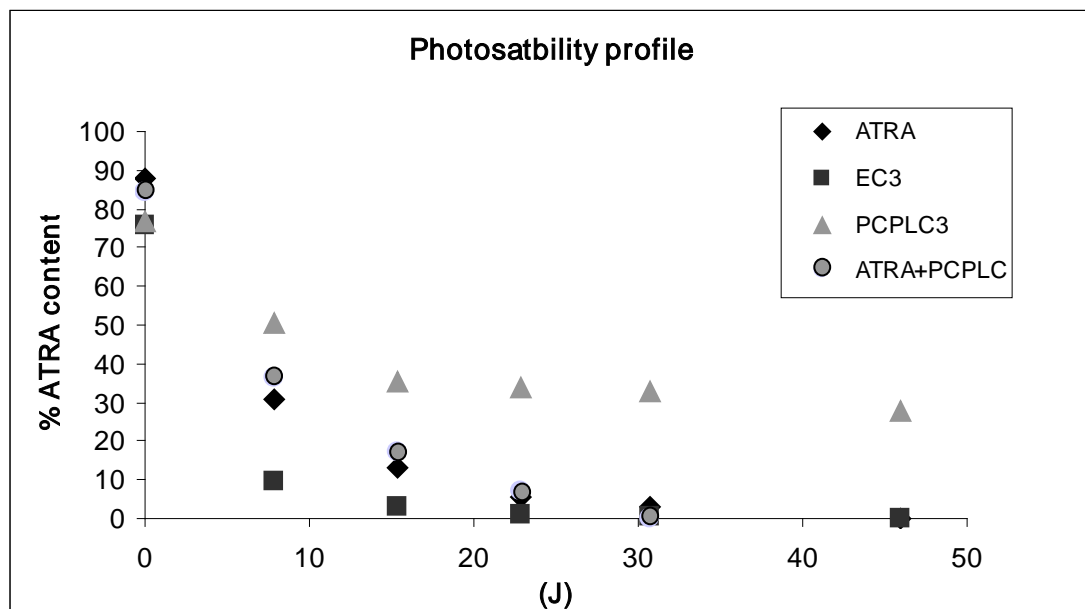
Figure3.11. Photostability profile of ATRA encapsulated in the EC and PCPLC particles compared with ATRA-unencapsulated.

3.6. Controlled release test

Transdermal penetration of all samples across baby mouse skin was performed with the Franz diffusion cell using baby mouse skin under sink condition [61]. The *ex vivo* controlled release tests were carried out by using unencapsulated ATRA, ATRA-encapsulated EC3 and ATRA-encapsulated PCPLC3 which were applied onto the mouse skin in the upper compartment of the Franz cell and the release of ATRA encapsulated nanoparticles were examined by UV/vis spectrometry. The receptor fluid (1 ml) was monitored at 1, 2, 4, 6, 18 and 24 h after application. Quantitives analysis of ATRA in the receptor fluid was carried out by UV absorption spectrophotometry using a calibration curve. The results indicated that after 24 h, neither ATRA nor nanospheres were detected in the receptor medium, thus, assuring that all samples could not transdermally cross into the receptor medium. As a result, all three particles could not transdermally through the skin then expect the ATRA was release in the skin. Quantitative analysis of ATRA indicated that 22.4±2.3%, 21.7±3.3% and 19.0±0.5% of ATRA from the free ATRA sample, ATRA-loaded EC and ATRA-loaded PCPLC samples were found in the skin layers, respectively.

3.7. Confocal Fluorescent laser scanning microscopy (CLSM)

To confirm the location of ATRA and PCPLC particles, confocal fluorescent laser scanning microscopy was used. The CLSM technique detected fluorescent signals of ATRA and PCPLC at various areas in the mouse skin. The obtained fluorescent signals from various areas were then resolved to fluorescent spectra of ATRA and PCPLC. Autofluorescence of the mouse skin could also be substracted out. All the unmixing was carried out using image algorithms and it was possible because the three spectra were significantly different (Fig 3.12). At the depth of ~40 µm from the surface, fluorescent signals of ATRA and PCPLC could be observed clearly around hair follicles (Fig 3.13a). This implied that the hair follicle was the major route of the ATRA-encapsulated PCPLC nanoparticles skin penetration (Fig 3.13a-c). At 1.5 µm deeper, the fluorescent signals of ATRA and PCPLC could still be observed, although at a little lower intensity than that at the~40 µm depth. Here, the fluorescent signal of PCPLC at the hair papilla was clearly more intense than that of ATRA (Fig 3.13d). This implied that some ATRA molecules had diffused out into the tissue around the hair follicles. At 3.5 µm deeper, the fluorescent signals of PCPLC decreased while the fluorescent signals of ATRA could be observed clearly. The ratios of the fluorescent

signals of ATRA to PCPLC increased along the depth of the tissue. This implied that ATRA was released from PCPLC particles and could better diffuse through the tissue while PCPLC particles were still around the hair follicles (Fig 3.13e). Therefore, it can be concluded that ATRA-encapsulated PCPLC nanoparticles could be transdermally penetrate through skin along the hair follicles and ATRA could be released from the particles. The released ATRA could diffuse into the surrounding tissue while PCPLC particles mostly remained in the hair follicles. These results obviously showed that ATRA-encapsulated PCPLC nanoparticles could penetrate through the dermis layer, meaning hat the compound was sent to the aimed target where it would be used to stimulate various biosynthetic pathways including collagen and elastin synthesis. It should be noted here that the released ATRA could not transdermally penetrate through the mouse skin over 600 µm since no ATRA could be detected in the receptor medium in the transdermal penetration experiment (section 3.6).
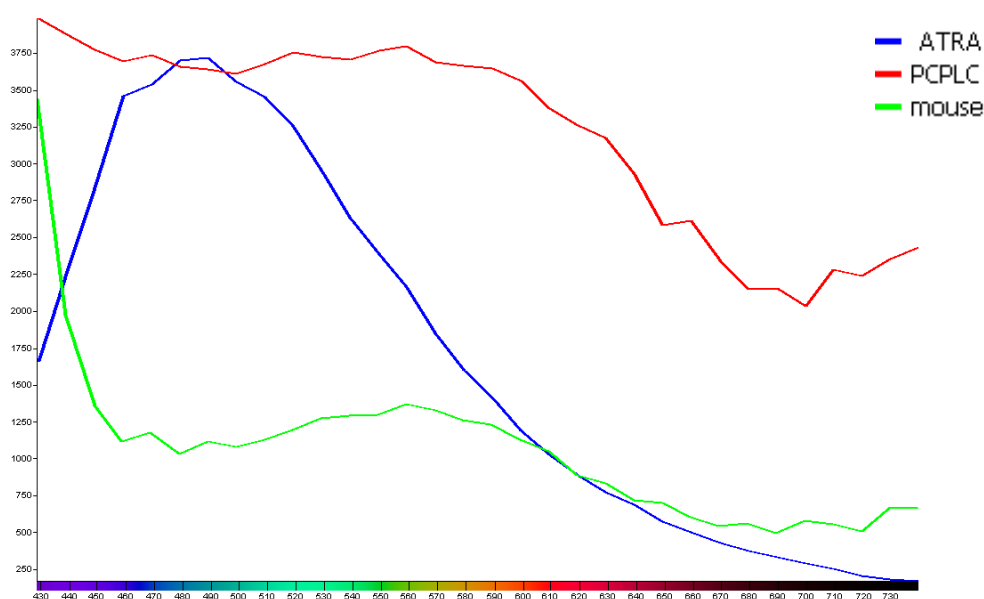
Figure3.12. The spectrum of three different fluorescent light: (blue) spectral of ATRA, (red) spectral of PCPLC and (green) spectral of mouse skin.

a)

At 40 µm (fluorescence)

b)

At 40 µm (three spectrum)

c)

At 40 µm (PCPLC-ATRA)

d)

At 41.5 µm (PCPLC-ATRA)

e)

At 45 µm (PCPLC-ATRA)
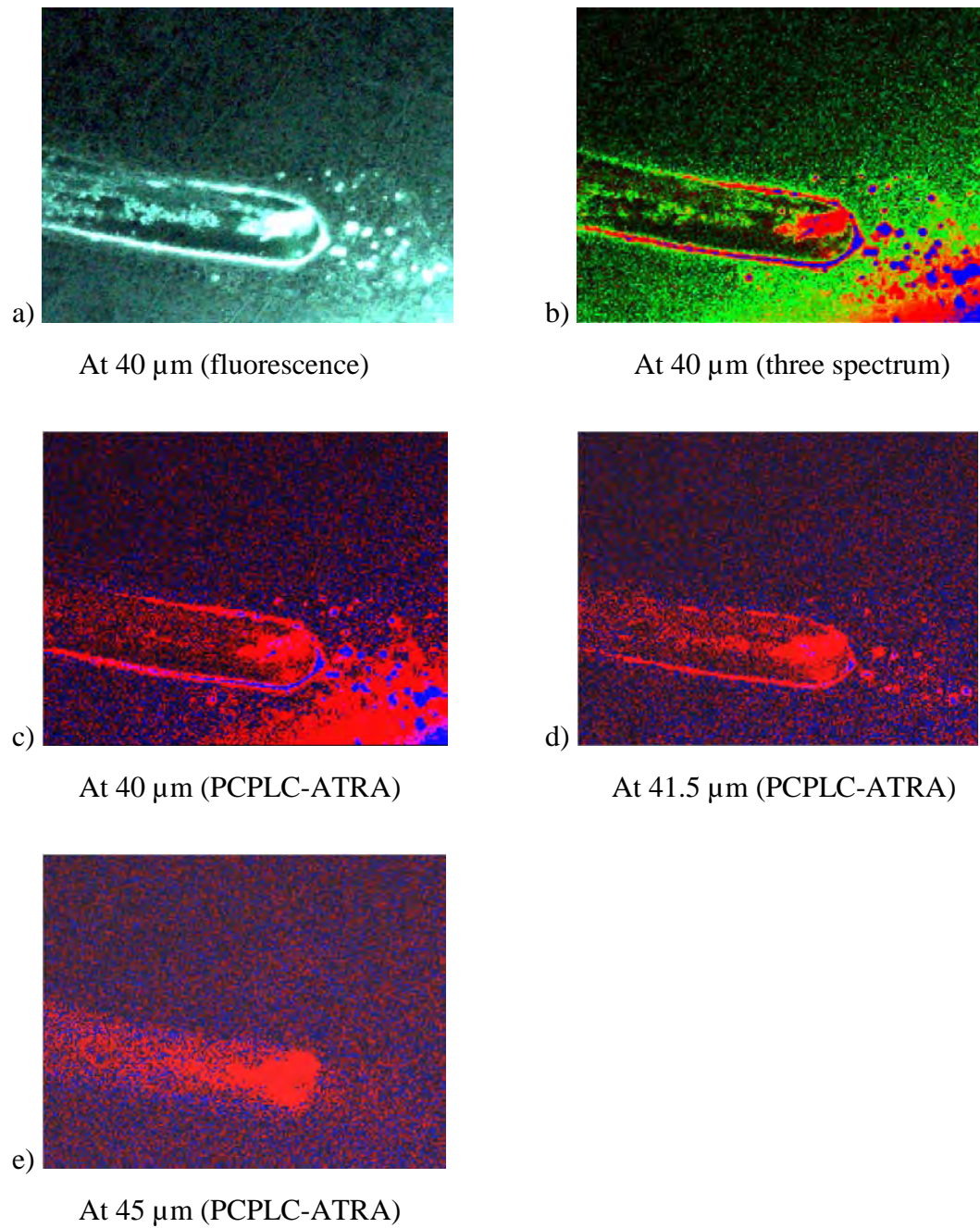
Figure3.13. The confocal laser scanning microscopy imaged. The subsurface depths of the displayed image are 40 µm, 41.5 µm and 45 µm: (a) fluorescence image at 40 µm, (b) confocal image of three spectrum at 40 µm, (c) confocal image of ATRA spectrum and PCPLC spectrum at 40 µm, (d) confocal image of ATRA spectrum and PCPLC spectrum at 41.5 µm, (e) confocal image of ATRA spectrum and PCPLC spectrum at 45 µm

CHAPTER IV
CONCLUSION

In this research, encapsulated ATRA with five polymer include ethyl cellulose (EC), poly(ethylene glycol)-phthaloylchitosan (PPLC), poly(ethylene glycol)-4-methoxycinnamoylphthaloylchitosan (PCPLC), Poly(vinylalcohol-co-vinyl-cinnamate) with cinnamoyl substitution degree of 0.30 and 0.44 (PVA-C1 and PVA-C2) to find the suitable polymer for encapsulation. The encapsulation efficiency into PCPLC gave 80.03 ± 0.5 % at 21.06 ± 0.1 % (w/w) loading and the particles were spherical with the diameter of 113.2 ± 27.1 nm. The encapsulation of ATRA showed the stability and photostability of ATRA could be significantly improved through encapsulation into the PCPLC particles while the encapsulation into EC spheres gave small improvement in ATRA stability and showed no improvement in ATRA photostability. To confirm the location of the released ATRA and the particles applied the ATRA-loaded PCPLC particle suspension onto the 9-day-old-baby mouse abdominal skin showed that approximately 19.0 % of the materials were retained in the skin layers and no transdermal penetration of the ATRA could be detected up to 24 h post application. Fluorescent images of the skin applied with ATRA loaded PCPLC, indicated that the PCPLC accumulated at the hair follicles while the ATRA could be released out in the skin.

REFFERENCES

[1]   Liu, J., Hu, W., Chen, H.B., Ni, Q., Xu, H.B. and Yang, X.L. Isotretinoin-loaded solid lipid nanoparticles with skin targeting for topical delivery. International Journal of Pharmaceutics, 328(2007): 191- 195.

[2]   Serri, R. and Iorizzo, M. Cosmeceuticals: focus on topical retinoids in photoaging. *Clinics in Dermatology,* 26(2008): 633-635.

[3]   Lupo, M.P. Antioxidants and vitamins in cosmetics. *Clinics in Dermatology,* 19(2001): 467-473.

[4]   Kim, D.G., Jeong, Y.I., Choi, C., Roh, S.H., Kang, S.K., Jang, M.K. and Nah, J.W. Retinol-encapsulated low molecular water-soluble chitosan nanoparticles. *International Journal of Pharmaceutics,* 319(2006): 130-138.

[5]   Schäfer-Korting, M., Korting, H.C. and Ponce-Pöschl, E. Liposomal tretinoin for uncomplicated acne vulgaris. *Journal of Molecular Medicine,* 72(1994): 1086-1091.

[6]   Shah, K.A., Date, A.A., Joshi, M.D. and Patravale, V.B. Solid lipid nanoparticles (SLN) of tretinoin: potential in topical delivery. *International Journal of Pharmaceutics* 345(2007): 163-171.

[7]   Patel, V.B., Misra, A. and Marfatia, Y.S. Topical liposomal gel of tretinoin for the treatment of acne: research and clinical implications. *Pharmaceutical Development and Technology,* 5(2000): 455-464.

[8]   Ioele, G., Cione, E., Risoli, A., Genchi, G. and Ragno, G. Accelerated photostability study of tretinoin and isotretinoin in liposome formulations. *International Journal of Pharmaceutics* 293(2005): 251-260.

[9]   Boswell, C.B. Skincare science: update on topical retinoids. *Aesthetic Surgery Journal,* 26(2006): 233-239.

[10]   Fu, P.P., Xia, Q., Boudreau, M.D., Howard, P.C., Tolleson, W.H. and Wamer, W.G. Physiological role of retinyl palmitate in the skin. *Vitamins & Hormones,* 75(2007): 223-256.

[11]   Duell, E.A., Kang, S. and Voorhees, J.J. Unoccluded retinol penetrates human skin in vivo more effectively than unoccluded retinyl palmitate or

retinoic acid. *Journal of Investigative Dermatology,* 109(1997): 301-305.

[12] Randolph, R.K. and Simon, M. Characterization of retinol metabolism in cultured human epidermal keratinocytes. *The Journal of Biological Chemistry,* 268(1993): 9198-9205.

[13] Lavker, R.M. and Leyden, J.J. Lamellar inclusions in follicular horny cells: a new aspect of abnormal keratinization. *Journal of Ultrastructure Research,* 69(1979): 362-370.

[14] Lovell, C.R., Smolenski, K.A., Duance, V.C., Light, N.D., Young, S. and Dyson, M. Type I and III collagen content and fibre distribution in normal human skin during ageing. *British Journal of Dermatology,* 117(1987): 419-428.

[15] Oikarinen, A. Aging of the skin connective tissue: how to measure the biochemical and mechanical properties of aging dermis. *Photodermatology, Photoimmunology and Photomedicine,* 10(1994): 47-52.

[16] Fisher, G.J., Wang, Z.Q., Datta, S.C., Varani, J., Kang, S. and Voorhees, J.J. Pathophysiology of premature skin aging induced by ultraviolet light. *New England Journal of Medicine,* 337(1997): 1419-1428.

[17] Kang, S., Fisher, G.J. and Voorhees, J.J. Photoaging and topical tretinoin: therapy, pathogenesis, and prevention. *Archives of Dermatology,* 133(1997): 1280-1284.

[18] Fisher, G.J., Kang, S., Varani, J., Bata-Csorgo, Z., Wan, Y., Datta, S. and Voorhees, J.J. Mechanisms of photoaging and chronological skin aging. *Archives of Dermatology,* 138(2002): 1462-1470.

[19] Helfrich, Y.R., Sachs, D.L. and Voorhees, J.J. Overview of skin aging and photoaging. *Dermatology Nursing,* 20(2008): 177-183.

[20] Koivukangas, V., Kallioinen, M., Autio-Harmainen, H. and Oikarinen, A. UV irradiation induces the expression of gelatinases in human skin in vivo. *Acta Dermato-Venereologica,* 74(1994): 279-282.

[21] Thomas, M.J., Brown, M.G. and Lovell, G.A. UV radiation measurement in a study of elderly subjects. *Photodermatology journal,* 4(1987): 141-143.

[22] Cheng, W. and Petris, S.D. Vitamin A Complex. *Skin Inc.,* 10(1998): 82-88.

[23]   Redmond, K.A., Nguyen, T.-S. and Ryan, R.O. All-trans-retinoic acid nanodisks. *International Journal of Pharmaceutics,* 339(2007): 246-250.

[24]   Hwang, S.R., Lim, S.-J., Park, J.-S. and Kim, C.-K. Phospholipid-based microemulsion formulation of all-trans-retinoic acid for parenteral administration. *International Journal of Pharmaceutics,* 276(2004): 175-183.

[25]   Failloux, N., Baron, M.H., Abdul-Malak, N. and Perrier, E. Contribution of encapsulation on the biodisponibility of retinol. *International Journal of Cosmetic Science,* 26(2004): 71-77.

[26]   Isoe, S., Hyeon, S.B., Katsumura, S. and Sakan, T. Photo-oxygenation of carotenoids. II. The absolute configuration of loliolide and dihydroactinidiolide. *Tetrahedron Letters,* 13(1972): 2517-2520.

[27]   Crank, G. and Pardijanto, M.S. Photo-oxidations and photosensitized oxidations of vitamin A and its palmitate ester. *Journal of Photochemistry and Photobiology, A: Chemistry,* 85(1995): 93-100.

[28]   Reddy, A.M. and Rao, V.J. Ionic Photodissociation of Polyenes via a Highly Polarized Singlet Excited State. *The Journal of Organic Chemistry,* 57(1992): 6727-6731.

[29]   Diaz, C., Vargas, E. and Gatjens-Boniche, O. Cytotoxic effect induced by retinoic acid loaded into galactosyl-sphingosine containing liposomes on human hepatoma cell lines. *International Journal of Pharmaceutics,* 325(2006): 108-115.

[30]   Sinico, C., Manconi, M., Peppi, M., Lai, F., Valenti, D. and Fadda, A.M. Liposomes as carriers for dermal delivery of tretinoin: in vitro evaluation of drug permeation and vesicle-skin interaction. *Journal of Controlled Release,* 103(2005): 123-136.

[31]   Manconi, M., Sinico, C., Valenti, D., Lai, F. and Fadda, A.M. Niosomes as carriers for tretinoin III. A study into the in vitro cutaneous delivery of vesicle-incorporated tretinoin. *International Journal of Pharmaceutics,* 311(2006): 11-19.

[32]   Lim, S.J. and Kim, C.K. Formulation parameters determining the physicochemical characteristics of solid lipid nanoparticles loaded with

all-trans retinoic acid. *International Journal of Pharmaceutics,* 243(2002): 135-146.

[33] Jee, J.-P., Lim, S.-J., Park, J.-S. and Kim, C.-K. Stabilization of all-trans retinol by loading lipophilic antioxidants in solid lipid nanoparticles. *European Journal of Pharmaceutics and Biopharmaceutics,* 63(2006): 134-139.

[34] Hwang, Y.J., Oh, C. and Oh, S.G. Controlled release of retinol from silica particles prepared in O/W/O emulsion: the effects of surfactants and polymers. *Journal of Controlled Release,* 106(2005): 339-349.

[35] Ourique, A.F., Pohlmann, A.R., Guterres, S.S. and Beck, R.C. Tretinoin-loaded nanocapsules: Preparation, physicochemical characterization, and photostability study. *International Journal of Pharmaceutics,* 352(2008): 1-4.

[36] Opanasopit, P., Ngawhirunpat, T., Chaidedgumjorn, A., Rojanarata, T., Apirakaramwong, A., Phongying, S., Choochottiros, C. and Chirachanchai, S. Incorporation of camptothecin into N-phthaloyl chitosan-g-mPEG self-assembly micellar system. *European Journal of Pharmaceutics and Biopharmaceutics,* 64(2006): 269-276.

[37] Opanasopit, P., Ngawhirunpat, T., Rojanarata, T., Choochottiros, C. and Chirachanchai, S. N-phthaloylchitosan-g-mPEG design for all-trans retinoic acid-loaded polymeric micelles. *European Journal of Pharmaceutical Sciences,* 30(2007): 424-431.

[38] Chen, H., Yang, W., Chen, H., Liu, L., Gao, F., Yang, X., Jiang, Q., Zhang, Q. and Wang, Y. Surface modification of Mitoxantrone-loaded PLGA nanospheres with chitosan. *Colloids and Surfaces B: Biointerfaces,* 73(2009): 212-218.

[39] Rekhi, G.S. and Jambhekar, S.S. Ethylcellulose- A Polymer Review. *Drug Development and Industrial Pharmacy,* 21(1995): 61-77.

[40] Joshi, H.N. and Wilson, T.D. Calorimetric studies of dissolution of hydroxypropyl methylcellulose E5 (HPMC E5) in water. *Journal of Pharmaceutical Sciences,* 82(1993): 1033-1038.

[41] Agrawal, A.M., Manek, R.V., Kolling, W.M. and Neau, S.H. Studies on the Interaction of Water with Ethylcellulose: Effect of Polymer Particle

Size *American Association of Pharmaceutical Scientists' electronic journals,* 4(2003): 1-11.

[42] Anumansirikul, N., Wittayasuporn, M., Klinubol, P., Tachaprutinun, A. and Wanichwecharungruang, S.P. UV-screening chitosan nanocontainers: Increasing the photostability of encapsulated materials and controlled release. *Nanotechnology,* 19(2008): 1-9.

[43] Santhi, K., Venkatesh, D.N., Dhanaraj, S.A., Sangeetha, S. and Suresh, B. Development and in-vitro Evaluation of a Topical Drug Delivery System Containing Betamethazone Loaded Ethyl Cellulose Nanospheres. *Tropical Journal of Pharmaceutical Research,* 4(2005): 495-500.

[44] Choy, Y.B., Choi, H. and Kim, K. Uniform ethyl cellulose microspheres of controlled sizes and polymer viscosities and their drug-release profiles. *Journal of Applied Polymer Science,* 112(2008): 850-857.

[45] Ravikumara, N.R., Madhusudhan, B., Nagaraj, T.S., Hiremat, S.R., & Raina, G. 2009. Preparation and evaluation of nimesulide-loaded ethylcellulose and methylcellulose nanoparticles and microparticles for oral delivery. *Journal of Biomaterials Applications,* 24(1), 47-64.

[46] Valot, P., Baba, M., Nedelec, J.M. and Sintes-Zydowicz, N. Effects of process parameters on the properties of biocompatible ibuprofen-loaded microcapsules. *International Journal of Pharmaceutics,* 369(2009): 53-63.

[47] Sansukcharearnpon, A., Wanichwecharungruang, S., Leepipatpaiboon, N., Kerdcharoen, T. and Arayachukeat, S. High loading fragrance encapsulation based on a polymer-blend: Preparation and release behavior. *International Journal of Pharmaceutics,* 391(2010): 267-273.

[48] Yuan, X.b., Li, H. and Yuan, Y.b. Preparation of cholesterol-modified chitosan self-aggregated nanoparticles for delivery of drugs to ocular surface. *Carbohydrate Polymers,* 65(2006): 337-345.

[49] Ngawhirunpat, T., Wonglertnirant, N., Opanasopit, P., Ruktanonchai, U., Yoksan, R., Wasanasuk, K. and Chirachanchai, S. Incorporation methods for cholic acid chitosan-g-mPEG self-assembly micellar

system containing camptothecin. *Colloids and Surfaces B: Biointerfaces,* 74(2009): 253-259.

[50]   Wang, H., Zhao, P., Liang, X., Gong, X., Song, T., Niu, R. and Chang, J. Folate-PEG coated cationic modified chitosan - Cholesterol liposomes for tumor-targeted drug delivery. *Biomaterials,* 31(2010): 4129-4138.

[51]   Tahara, K., Yamamoto, H., Hirashima, N. and Kawashima, Y. Chitosan-modified poly (D, L-lactide-co-glycolide) nanospheres for improving siRNA delivery and gene-silencing effects. *European Journal of Pharmaceutics and Biopharmaceutics,* 74(2010): 421-426.

[52]   Luppi, B., Orienti, I., Bigucci, F., Cerchiara, T., Zuccari, G., Fazzi, S. and Zecchi, V. Poly (vinylalcohol-co-vinyloleate) for the preparation of micelles enhancing retinyl palmitate transcutaneous permeation. *Drug Delivery,* 9(2002): 147-152.

[53]   Orienti, I., Bigucci, F., Luppi, B., Cerchiara, T., Zuccari, G., Giunchedi, P. and Zecchi, V. Polyvinylalcohol substituted with triethyleneglycol monoethylether as a new material for preparation of solid dispersions of hydrophobic drugs. *European Journal of Pharmaceutics and Biopharmaceutics,* 54(2002): 229-233.

[54]   Cerchiara, T., Luppi, B., Bigucci, F., Orienti, I. and Zecchi, V. Substituted polyvinylalcohol as a drug carrier for beta-carotene. *European Journal of Pharmaceutics and Biopharmaceutics,* 56(2003): 401-405.

[55]   Zuccari, G., Carosio, R., Fini, A., Montaldo, P.G. and Orienti, I. Modified polyvinylalcohol for encapsulation of all-trans-retinoic acid in polymeric micelles. *Journal of Controlled Release,* 103(2005): 369-380.

[56]   Luadthong, C., Tachaprutinun, A. and Wanichwecharungruang, S.P. Synthesis and characterization of micro/nanoparticles of poly (vinylalcohol-co-vinylcinnamate) derivatives. *European Polymer Journal,* 44(2008): 1285-1295.

[57]   Margulis-Goshen, K., Netivi, H.D., Major, D.T., Gradzielski, M., Raviv, U. and Magdassi, S. Formation of organic nanoparticles from volatile microemulsions. *Journal of Colloid and Interface Science,* 342(2010): 283-292.

[58] Errico, C., Gazzarri, M. and Chiellini, F. A Novel Method for the Preparation of Retinoic Acid-Loaded Nanoparticles. *International Journal of Molecular Sciences,* 10(2009): 2336-2347.

[59] Nattaporn Anumansirikul. *Entrapment of unstable active compounds by chitosan nanocapsules.* Master's Thesis, Graduate School, Chulalongkorn University, 2006.

[60] Chuleeporn Luadthong. *Nanoparticles from cinnamate derivatives of poly (vinyl alcohol).* Master's Thesis, Graduate School, Chulalongkorn University, 2007.

[61] Klinubol, P., Asawanonda, P. and Wanichwecharungruang, S.P. Transdermal penetration of UV filters. *Skin Pharmacology and Physiology,* 21(2008): 23-29.

APPENDIX

APPENDIX

1. % encapsulation efficiency of all-*trans* retinyl acetate loaded into polymeric nanoparticles and % ATRA loading

Calibration curve of all-trans retinyl acetate at 325 nm
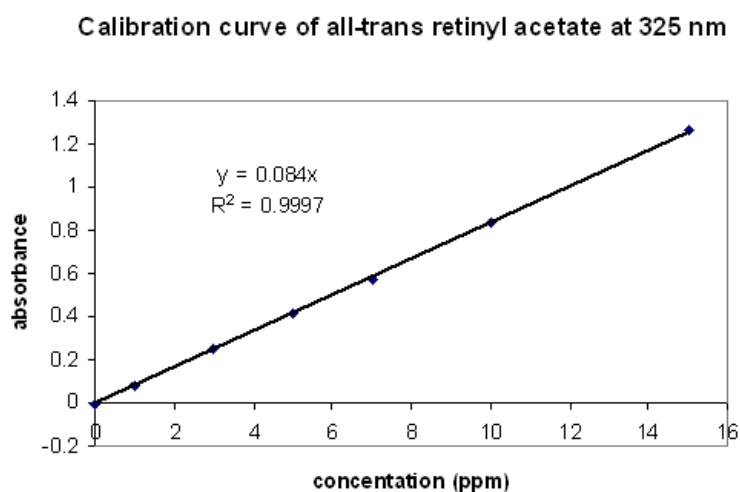
Figure A.1 Calibration curve of all-trans retinyl acetate at 325 nm in ethanol solution.

From the equation of calibration curve

$$Y = 0.084X, R^2 = 0.9997$$

$$\varepsilon_{stable\ 325} = 27594$$

Concentration (ppm)	1	3	5	7	10	15
Absorbance	0.084	0.252	0.42	0.588	0.84	1.2685

From $A = \varepsilon bc$ (1)

A = absorbance

$\varepsilon_{stable\ 325}$ = molar absorptivity (27594)

b = path length (1 cm)

c = concentration (mol/L)

1. ATRA-encapsulated EC nanoparticles

1.1) ATRA: EC ratio of 3:3 (EC1)

1.1.1) first replicate (EC1); ATRA: EC ratio of 3:3

The amount of ATRA-encapsulated EC at the inside of particles was calculated by equation (1)

$$1.008 = (27594)\ (1)\ c$$

$$c = 3.65 \times 10^{-5} \text{ M}$$

Dilution factor = 60, molecular weight = 328.5 and total volume = 35 ml

$$= 3.65 \times 10^{-5} \times 60 \times 328.5 \times 35$$

Weight of ATRA loaded into particle = 25.2 mg

Weight of ATRA and EC initially used were 30 mg and 30 mg

% encapsulation efficiency (%EE) and % ATRA loading were calculated by

$$\% \text{ EE} = \frac{\text{Weight of encapsulated ATRA in the particles}}{\text{Weight of ATRA initially used}} \times 100 \quad (2)$$

% EE = (25.2 x 100)/30

    = 84.00 %

$$\% \text{ ATRA loading} = \frac{\text{Weight of encapsulated ATRA in the particles}}{\text{Weight of the ATRA-encapsulated particles}} \times 100 \quad (3)$$

% ATRA loading = (25.2 x 100)/ 55.2

    = 44.16 %

1.1.2) second replicate (EC1); ATRA: EC ratio of 3:3

The amount of ATRA-encapsulated EC at the inside of particles was calculated by equation (1)

$$0.754 = (27594) (1) c$$

$$c = 2.73 \times 10^{-5} \text{ M}$$

Dilution factor = 120, molecular weight = 328.5 and total volume = 25 ml

$$= 2.73 \times 10^{-5} \times 120 \times 328.5 \times 25$$

Weight of ATRA loaded into particle = 26.9286 mg

Weight of ATRA and EC initially used were 30 mg and 30 mg

%EE and % ATRA loading were calculated by equations (2) and (3), respectively;

    % EE = (26.93 x 100)/30

       = 89.76 %

    % ATRA loading = (26.93 x 100)/ 56.93

       = 47.30 %

1.1.3) third replicate (EC1); ATRA: EC ratio of 3:3

The amount of ATRA-encapsulated EC at the inside of particles was calculated by equation (1)

$$0.881 = (27594) (1) c$$

$$c = 3.35 \times 10^{-5} M$$

Dilution factor = 60, molecular weight = 328.5 and total volume = 37 ml

$$= 3.35 \times 10^{-5} \times 60 \times 328.5 \times 37$$

Weight of ATRA loaded into particle = 24.3964 mg

Weight of ATRA and EC initially used were 30 mg and 30 mg

%EE and % ATRA loading were calculated by equations (2) and (3), respectively;

% EE = (24.39 x 100)/30

= 81.32 %

% ATRA loading = (24.39 x 100)/ 54.39

= 44.85 %

	1	2	3
A	1.008	0.754	0.881
c	3.65×10^{-5}	2.73×10^{-5}	3.35×10^{-5}
x DF	0.002192	0.003279	0.002007
x Mw (328.5)	0.72	1.08	0.66
x mL	25.2	26.93	24.39
% EE	84.00	89.76	81.32
% ATRA loading	44.16	47.30	44.85

Therefore, %EE and % ATRA loading of ATRA-encapsulated EC1 nanoparticles were 85.03 ± 4.3 % and 45.44 ± 1.6 %, respectively.

1.2) ATRA: EC ratio of 2:3 (EC2)

1.2.1) first replicate (EC2); ATRA: EC ratio of 2:3

The amount of ATRA-encapsulated EC at the inside of particles was calculated by equation (1)

$$0.969 = (27594) (1) c$$

$$c = 3.52 \times 10^{-5} M$$

Dilution factor = 60, molecular weight = 328.5 and total volume = 26 ml

$$= 3.52 \times 10^{-5} \times 60 \times 328.5 \times 26$$

Weight of ATRA loaded into particle = 18.0605 mg

Weight of ATRA and EC initially used were 20 mg and 30 mg

%EE and % ATRA loading were calculated by equations (2) and (3), respectively;

% EE = (18.06 x 100)/20

= 90.30 %

% ATRA loading = (18.06 x 100)/ 48.06

= 37.58 %

1.2.2) second replicate (EC2); ATRA: EC ratio of 2:3

The amount of ATRA-encapsulated EC at the inside of particles was calculated by equation (1)

$$0.961 = (27594) (1) c$$

$$c = 3.49 \times 10^{-5} \text{ M}$$

Dilution factor = 60, molecular weight = 328.5 and total volume = 25 ml

$$= 3.49 \times 10^{-5} \times 60 \times 328.5 \times 25$$

Weight of ATRA loaded into particle = 17.2225 mg

Weight of ATRA and EC initially used were 20 mg and 30 mg

%EE and % ATRA loading were calculated by equations (2) and (3), respectively;

% EE = (17.22 x 100)/20

= 86.11%

% ATRA loading = (17.22 x 100)/ 47.22

= 36.47 %

1.2.3) third replicate (EC2); ATRA: EC ratio of 2:3

The amount of ATRA-encapsulated EC at the inside of particles was calculated by equation (1)

$$0.922 = (27594) (1) c$$

$$c = 3.35 \times 10^{-5} \text{ M}$$

Dilution factor = 60, molecular weight = 328.5 and total volume = 26 ml

$$= 3.35 \times 10^{-5} \times 60 \times 328.5 \times 26$$

Weight of ATRA loaded into particle = 17.1845 mg

Weight of ATRA and EC initially used were 20 mg and 30 mg

%EE and % ATRA loading were calculated by equations (2) and (3), respectively;

% EE = (17.18 x 100)/20

= 85.92 %

% ATRA loading = (17.18 x 100)/ 47.18

= 36.42 %

	1	2	3
A	0.969	0.961	0.922
c	3.52×10^{-5}	3.49×10^{-5}	3.35×10^{-5}
x DF	0.002115	0.002097	0.002012
x Mw (328.5)	0.694635	0.688900	0.660943
x mL	18.0605	17.2225	17.1845
% EE	90.30	86.11	85.92
% ATRA loading	37.58	36.47	36.42

Therefore, %EE and % ATRA loading of ATRA-encapsulated EC2 nanoparticles were 87.45 ± 2.5 % and 36.82 ± 0.7 %, respectively.

1.3) ATRA: EC ratio of 1:3 (EC3)

1.3.1) first replicate (EC3); ATRA: EC ratio of 1:3

The amount of ATRA-encapsulated EC at the inside of particles was calculated by equation (1)

0.601 = (27594) (1) c

c = 2.19×10^{-5} M

Dilution factor = 60, molecular weight = 328.5 and total volume = 21 ml

= 2.19×10^{-5} x 60 x 328.5 x 21

Weight of ATRA loaded into particle = 9.0475 mg

Weight of ATRA and EC initially used were 10 mg and 30 mg

%EE and % ATRA loading were calculated by equations (2) and (3), respectively;

% EE = (9.05 x 100)/10

　　　= 90.47 %

% ATRA loading = (9.05 x 100)/ 39.05

　　　　= 23.17 %

1.3.2) first replicate (EC3); ATRA: EC ratio of 1:3

The amount of ATRA-encapsulated EC at the inside of particles was calculated by equation (1)

$$0.681 = (27594) (1) c$$

$$c = 2.48 \times 10^{-5} M$$

Dilution factor = 60, molecular weight = 328.5 and total volume = 19 ml

$$= 2.48 \times 10^{-5} \times 60 \times 328.5 \times 19$$

Weight of ATRA loaded into particle = 9.2754 mg

Weight of ATRA and EC initially used were 10 mg and 30 mg

% EE and % ATRA loading were calculated by equations (2) and (3), respectively;

% EE = (9.28 x 100)/10

　　　= 92.75 %

% ATRA loading = (9.28 x 100)/ 39.28

　　　　= 23.61 %

1.3.3) first replicate (EC3); ATRA: EC ratio of 1:3

The amount of ATRA-encapsulated EC at the inside of particles was calculated by equation (1)

$$0.59 = (27594) (1) c$$

$$c = 2.15 \times 10^{-5} M$$

Dilution factor = 60, molecular weight = 328.5 and total volume = 21 ml

$$= 2.15 \times 10^{-5} \times 60 \times 328.5 \times 21$$

Weight of ATRA loaded into particle = 8.8819 mg

Weight of ATRA and EC initially used were 10 mg and 30 mg

% EE and % ATRA loading were calculated by equations (2) and (3), respectively;

% EE = (8.88 x 100)/10

　　　= 88.82 %

% ATRA loading = (8.88 x 100)/ 38.88

= 22.84 %

	1	2	3
A	0.601	0.681	0.59
c	2.19×10^{-5}	2.48×10^{-5}	2.15×10^{-5}
x DF	0.001312	0.001486	0.001288
x Mw (328.5)	0.430831	0.488180	0.422946
x mL	9.0475	9.2754	8.8819
% EE	90.47	92.75	88.82
% ATRA loading	23.17	23.61	22.84

Therefore, %EE and % ATRA loading of ATRA-encapsulated EC3 nanoparticles were 90.68 ± 1.9 % and 23.21 ± 0.4 %, respectively.

2. ATRA-encapsulated PCPLC nanoparticles

2.1) ATRA: PCPLC ratio of 3:3 (PCPLC1)

2.1.1) first replicate (PCPLC1); ATRA: PCPLC ratio of 3:3

The amount of ATRA-encapsulated PCPLC at the inside of particles was calculated by equation (1)

$$1.025 = (27594) (1) c$$

$$c = 3.71 \times 10^{-5} \text{ M}$$

Dilution factor = 50, molecular weight = 328.5 and total volume = 30 ml

$$= 3.71 \times 10^{-5} \times 50 \times 328.5 \times 30$$

Weight of ATRA loaded into particle = 18.3036 mg

Weight of ATRA and EC initially used were 30 mg and 30 mg

% EE and % ATRA loading were calculated by equations (2) and (3), respectively;

% EE = (18.30 x 100)/30

= 61.01 %

% ATRA loading = (18.30 x 100)/ 48.30

= 37.89 %

2.1.2) first replicate (PCPLC1); ATRA: PCPLC ratio of 3:3

The amount of ATRA-encapsulated PCPLC at the inside of particles was calculated by equation (1)

$$1.024 = (27594) (1) c$$

$$c = 3.71 \times 10^{-5} \text{ M}$$

Dilution factor = 50, molecular weight = 328.5 and total volume = 30 ml

$$= 3.71 \times 10^{-5} \times 50 \times 328.5 \times 30$$

Weight of ATRA loaded into particle = 18.2857 mg

Weight of ATRA and EC initially used were 30 mg and 30 mg

% EE and % ATRA loading were calculated by equations (2) and (3), respectively;

% EE = (18.29 x 100)/30

= 60.95 %

% ATRA loading = (18.30 x 100)/ 48.30

= 37.87 %

2.1.3) first replicate (PCPLC1); ATRA: PCPLC ratio of 3:3

The amount of ATRA-encapsulated PCPLC at the inside of particles was calculated by equation (1)

$$1.026 = (27594) (1) c$$

$$c = 3.72 \times 10^{-5} \text{ M}$$

Dilution factor = 50, molecular weight = 328.5 and total volume = 30 ml

$$= 3.72 \times 10^{-5} \times 50 \times 328.5 \times 30$$

Weight of ATRA loaded into particle = 18.3214 mg

Weight of ATRA and EC initially used were 30 mg and 30 mg

% EE and % ATRA loading were calculated by equations (2) and (3), respectively;

% EE = (18.32 x 100)/30

= 61.07 %

% ATRA loading = (18.30 x 100)/ 48.30

= 37.92 %

	1	2	3
A	1.025	1.024	1.026
c	3.71×10^{-5}	3.71×10^{-5}	3.72×10^{-5}
x DF	0.001857	0.001855	0.001859
x Mw (328.5)	0.610119	0.609524	0.610714
x mL	18.3036	18.2857	18.3214
% EE	61.01	60.95	61.07
% ATRA loading	37.89	37.87	37.92

Therefore, %EE and % ATRA loading of ATRA-encapsulated PCPLC1 nanoparticles were 61.01 ± 0.1 % and 37.89 ± 0.03 %, respectively.

2.2) ATRA: PCPLC ratio of 2:3 (PCPLC2)

2.2.1) first replicate (PCPLC2); ATRA: PCPLC ratio of 2:3

The amount of ATRA-encapsulated PCPLC at the inside of particles was calculated by equation (1)

$$0.274 = (27594) (1) c$$
$$c = 9.92 \times 10^{-6} \text{ M}$$

Dilution factor = 150, molecular weight = 328.5 and total volume = 27 ml

$$= 9.92 \times 10^{-6} \times 150 \times 328.5 \times 27$$

Weight of ATRA loaded into particle = 13.1946 mg

Weight of ATRA and EC initially used were 20 mg and 30 mg

% EE and % ATRA loading were calculated by equations (2) and (3), respectively;

% EE = (13.19 x 100)/20

    = 65.97 %

% ATRA loading = (13.19 x 100)/ 43.19

    = 30.55 %

2.2.2) second replicate (PCPLC2); ATRA: PCPLC ratio of 2:3

The amount of ATRA-encapsulated PCPLC at the inside of particles was calculated by equation (1)

$$0.301 = (27594) (1) c$$

$$c = 1.09 \times 10^{-5} \text{ M}$$

Dilution factor = 150, molecular weight = 328.5 and total volume = 23 ml

$$= 1.09 \times 10^{-5} \times 150 \times 328.5 \times 23$$

Weight of ATRA loaded into particle = 12.3762 mg

Weight of ATRA and EC initially used were 20 mg and 30 mg

% EE and % ATRA loading were calculated by equations (2) and (3), respectively;

% EE = (12.38 x 100)/20

= 61.88 %

% ATRA loading = (13.19 x 100)/ 41.19

= 29.21 %

2.2.3) third replicate (PCPLC2); ATRA: PCPLC ratio of 2:3

The amount of ATRA-encapsulated PCPLC at the inside of particles was calculated by equation (1)

$$0.380 = (27594) \, (1) \, c$$

$$c = 1.38 \times 10^{-5} \text{ M}$$

Dilution factor = 150, molecular weight = 328.5 and total volume = 20 ml

$$= 1.38 \times 10^{-5} \times 150 \times 328.5 \times 20$$

Weight of ATRA loaded into particle = 13.5833 mg

Weight of ATRA and EC initially used were 20 mg and 30 mg

% EE and % ATRA loading were calculated by equations (2) and (3), respectively;

% EE = (13.58 x 100)/20

= 67.92 %

% ATRA loading = (13.58 x 100)/ 43.58

= 31.17 %

	1	2	3
A	0.274	0.301	0.380
c	9.92×10^{-6}	1.09×10^{-5}	1.38×10^{-5}
x DF	0.001488	0.001638	0.002067
x Mw (328.5)	0.48869	0.538095	0.679167
x mL	13.1946	12.3762	13.5833
% EE	65.97	61.88	67.92
% ATRA loading	30.55	29.21	31.17

Therefore, %EE and % ATRA loading of ATRA-encapsulated PCPLC2 nanoparticles were 65.26 ± 3.1 % and 30.31 ± 1.0 %, respectively.

2.3) ATRA: PCPLC ratio of 1:3 (PCPLC3)

2.3.1) first replicate (PCPLC3); ATRA: PCPLC ratio of 1:3

The amount of ATRA-encapsulated PCPLC at the inside of particles was calculated by equation (1)

$$0.4485 = (27594)(1) c$$
$$c = 1.63 \times 10^{-5} \text{ M}$$

Dilution factor = 50, molecular weight = 328.5 and total volume = 30 ml

$$= 1.63 \times 10^{-5} \times 50 \times 328.5 \times 30$$

Weight of ATRA loaded into particle = 8.0089 mg

Weight of ATRA and EC initially used were 10 mg and 30 mg

% EE and % ATRA loading were calculated by equations (2) and (3), respectively;

% EE = (8.01 x 100)/10
= 80.09 %

% ATRA loading = (8.01 x 100)/ 38.01
= 21.07 %

2.3.2) second replicate (PCPLC3); ATRA: PCPLC ratio of 1:3

The amount of ATRA-encapsulated PCPLC at the inside of particles was calculated by equation (1)

$$0.445 = (27594)(1) c$$
$$c = 1.61 \times 10^{-5} \text{ M}$$

Dilution factor = 50, molecular weight = 328.5 and total volume = 30 ml

$$= 1.61 \times 10^{-5} \times 50 \times 328.5 \times 30$$

Weight of ATRA loaded into particle = 7.9464 mg

Weight of ATRA and EC initially used were 10 mg and 30 mg

% EE and % ATRA loading were calculated by equations (2) and (3), respectively;

% EE = (7.95 x 100)/10

$$= 79.46 \%$$

% ATRA loading = (7.95 x 100)/ 37.95

$$= 20.94 \%$$

2.3.3) third replicate (PCPLC3); ATRA: PCPLC ratio of 1:3

The amount of ATRA-encapsulated PCPLC at the inside of particles was calculated by equation (1)

$$0.451 = (27594) (1) c$$

$$c = 1.63 \times 10^{-5} \text{ M}$$

Dilution factor = 50, molecular weight = 328.5 and total volume = 30 ml

$$= 1.63 \times 10^{-5} \times 50 \times 328.5 \times 30$$

Weight of ATRA loaded into particle = 8.0536 mg

Weight of ATRA and EC initially used were 10 mg and 30 mg

% EE and % ATRA loading were calculated by equations (2) and (3), respectively;

% EE = (8.05 x 100)/10

$$= 80.54 \%$$

% ATRA loading = (8.05 x 100)/ 38.05

$$= 21.16 \%$$

	1	2	3
A	0.4485	0.445	0.451
c	1.63×10^{-5}	1.61×10^{-5}	1.63×10^{-5}
x DF	0.000813	0.000806	0.000817
x Mw (328.5)	0.266964	0.264881	0.268452
x mL	8.0089	7.9464	8.0536
% EE	80.09	79.46	80.54
% ATRA loading	21.07	20.94	21.16

Therefore, %EE and % ATRA loading of ATRA-encapsulated PCPLC3 nanoparticles were 80.03 ± 0.5 % and 21.06 ± 0.1 %, respectively.

2. Stability of ATRA under the light proof condition during the period of 3 months

Figure A.2 Calibration curve of all-trans retinyl acetate at 290 nm in ethanol solution

From the equation of calibration curve

$$Y = 0.0383X, R^2 = 0.9989$$

$$\varepsilon_{stable290} = 12581.55$$

Concentration (ppm)	1	3	5	7	10	15
Absorbance	0.03	0.111	0.187	0.2615	0.3825	0.5815
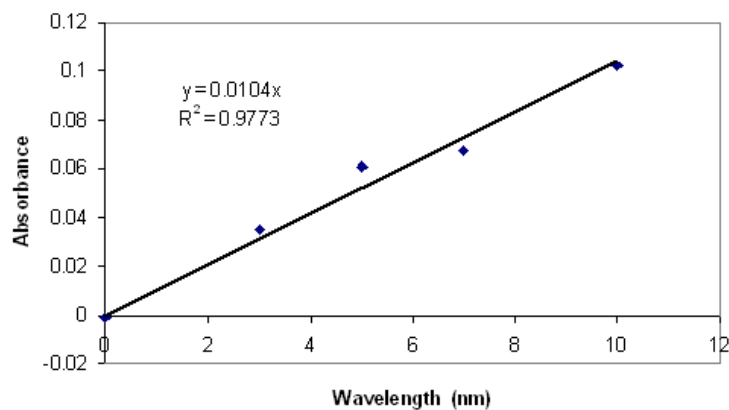
Figure A.3 Calibration curve of degraded all-trans retinyl acetate at 325 nm in ethanol solution

From the equation of calibration curve

$$Y= 0.0104X, R^2= 0.9773$$

$$\varepsilon_{deg325}= 3416.4$$

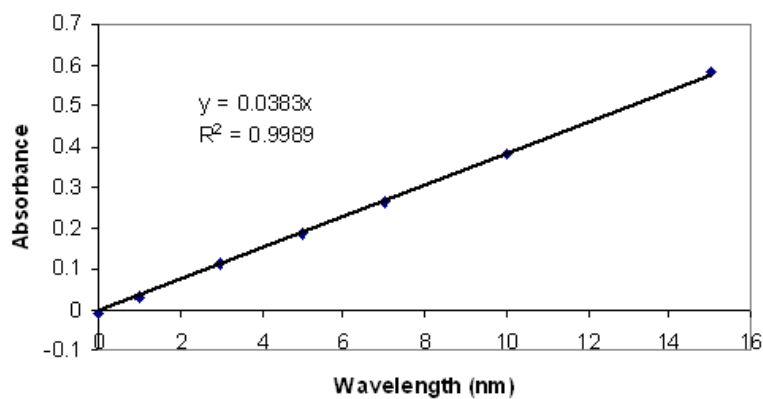| Concentration (ppm)	0	3	5	7	10
Absorbance	-0.00123	0.035306	0.061047	0.067168	0.102241
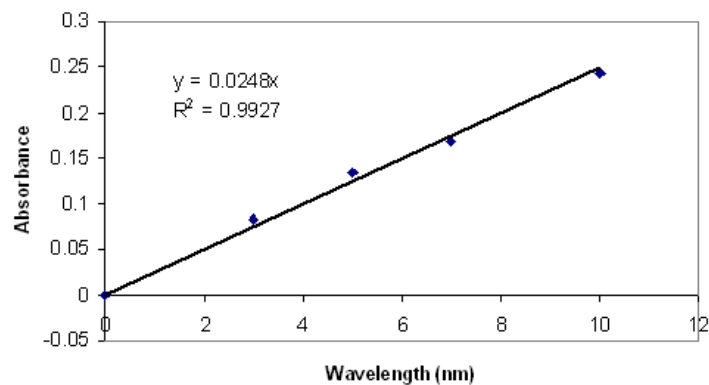
Figure A.4 Calibration curve of degraded all-trans retinyl acetate at 290 nm in ethanol solution

From the equation of calibration curve

$$Y= 0.0248X, R^2= 0.9927$$

$$\varepsilon_{deg290}= 8146.8$$

Concentration (ppm)	0	3	5	7	10
Absorbance	-0.000864029	0.083467	0.135098	0.168513	0.244178

For separated % ATRA content of ATRA-encapsulated from 2 peak overlap were calculated by equation

$$A= \varepsilon_1 C_1 + \varepsilon_2 C_2$$

$$A_d= 8146.8 C_d + 12581.55 C_s \qquad (1)$$

$$A_s= 3416.4 C_d + 27594 C_s \qquad (2)$$

A_d = Absorbance of degraded ATRA

A_s = Absorbance of stable ATRA

C_d = Concentration of degraded ATRA

C_s = Concentration of stable ATRA

Equation (2) was multiply 2.384615 and minus equation (1)

$$(2.384615)A_s - A_d = 53219.53 C_s \qquad (4)$$

Fig. A.5 Stability profile of ATRA-encapsulated EC1 under the light proof condition

2.1.) ATRA-encapsulated EC1 nanoparticles

2.1.1.) Storage at 1 day

The amount of ATRA-encapsulated EC1 at the inside of particles was calculated by equation (1)

$$1.1423 = (27594)(1)c$$

$$c = 4.14 \times 10^{-5} \text{ M}$$

Dilution factor = 60, molecular weight = 328.5 and total volume = 22 ml

$$= 4.14 \times 10^{-5} \times 60 \times 328.5 \times 22$$

Weight of remained ATRA in the particles = 17.9509 mg

Weight of ATRA and EC initially used were 30 mg

Content of % intact ATRA were calculated by

$$\% \text{ ATRA content} = \frac{\text{Weight of remained ATRA in the particles}}{\text{Weight of ATRA initially used}} \times 100 \qquad (5)$$

$$\% \text{ ATRA content} = (17.95 \times 100)/30$$

$$= 59.84 \%$$

2.1.2.) Storage at 24 days

The amount of ATRA-encapsulated EC1 at the inside of particles was calculated by equation (4)

$$(2.384615)A_s - A_d = (53219.53) C_s \qquad (4)$$

$$(2.384615)(0.689) - 0.843667 = (53219.53) C_s$$

$$C_s = 1.50 \times 10^{-5} \text{ M}$$

Dilution factor = 30, molecular weight = 328.5 and total volume = 22 ml

$$= 1.50 \times 10^{-5} \times 30 \times 328.5 \times 22$$

Weight of remained ATRA in the particles = 3.2564 mg

Weight of ATRA and EC initially used were 30 mg

Content of % intact ATRA were calculated by equation (5)

$$\% \text{ ATRA content} = (3.26 \times 100)/30$$
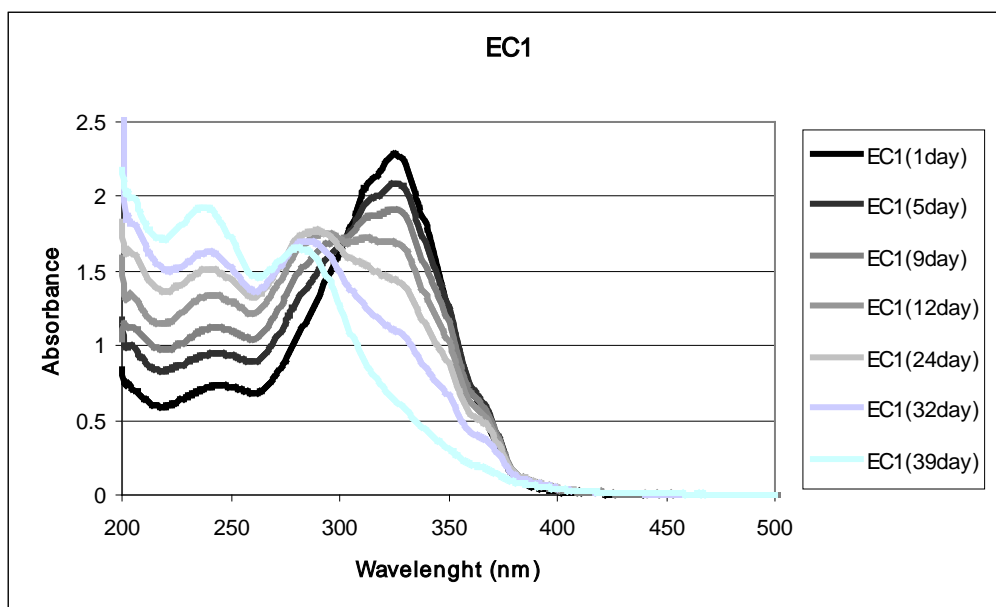
$$= 10.85 \%$$

Fig. A.6 Stability profile of ATRA-encapsulated EC2 under the light proof condition

2.2.) ATRA-encapsulated EC2 nanoparticles

2.2.1.) Storage at 1 day

The amount of ATRA-encapsulated EC2 at the inside of particles was calculated by equation (1)

$$0.921667 = (27594) (1) c$$
$$c = 3.34 \times 10^{-5} \text{ M}$$

Dilution factor = 60, molecular weight = 328.5 and total volume = 23 ml

$$= 3.34 \times 10^{-5} \times 60 \times 328.5 \times 23$$

Weight of remained ATRA in the particles = 15.1417 mg

Weight of ATRA and EC initially used were 20 mg

Content of % intact ATRA were calculated by equation (5)

$$\% \text{ ATRA content} = (15.14 \times 100)/20$$

$$= 75.71 \%$$

2.2.2.) Storage at 24 days

The amount of ATRA-encapsulated EC2 at the inside of particles was calculated by equation (4)

$$(2.384615)(0.553) - 0.559333 = (53219.53) Cs$$

$$Cs = 1.43 \times 10^{-5} \text{ M}$$

Dilution factor = 30, molecular weight = 328.5 and total volume = 23 ml

$$= 1.43 \times 10^{-5} \times 30 \times 328.5 \times 23$$

Weight of remained ATRA in the particles= 3.2347 mg

Weight of ATRA and EC initially used were 20 mg

Content of % intact ATRA were calculated by equation (5)

$$\% \text{ ATRA content} = (3.23 \times 100)/20$$
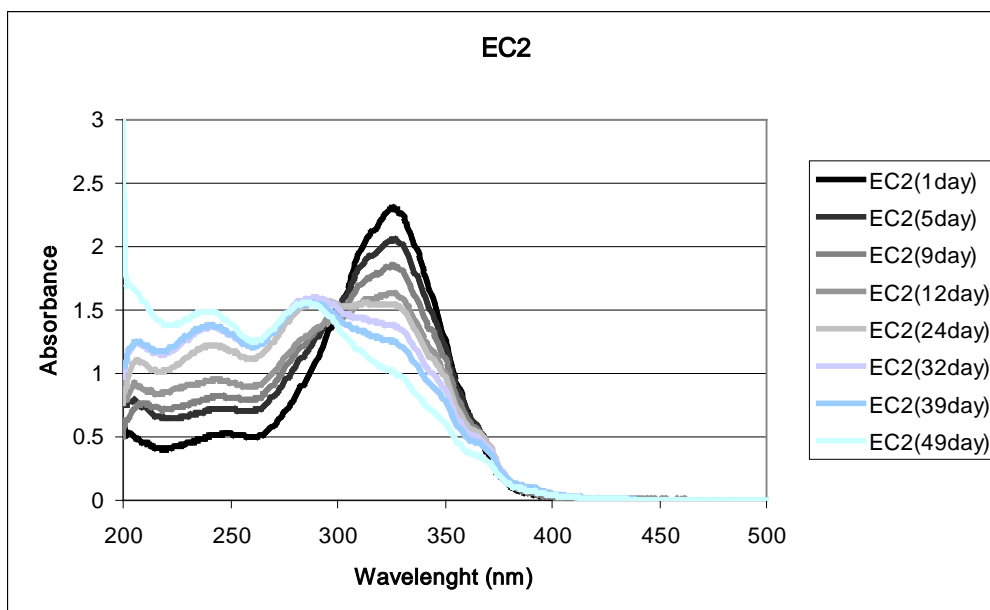
$$= 16.17 \%$$

Fig. A.7 Stability profile of ATRA-encapsulated EC3 under the light proof condition

2.3.) ATRA-encapsulated EC3 nanoparticles

2.3.1.) Storage at 1 day

The amount of ATRA-encapsulated EC3 at the inside of particles was calculated by equation (1)

$$0.590667 = (27594) (1) c$$
$$c = 2.14 \times 10^{-5} \text{ M}$$

Dilution factor = 60, molecular weight = 328.5 and total volume = 19 ml

$$= 2.14 \times 10^{-5} \times 60 \times 328.5 \times 19$$

Weight of remained ATRA in the particles = 7.8052 mg

Weight of ATRA and EC initially used were 10 mg

Content of % intact ATRA were calculated by equation (5)

$$\% \text{ ATRA content} = (7.81 \times 100)/10$$

$$= 78.05 \%$$

2.3.2.) Storage at 30 days

The amount of ATRA-encapsulated EC3 at the inside of particles was calculated by equation (4)

$$(2.384615)(0.4033) - 0.3793 = (53219.53) \ C_s$$
$$C_s = 1.09 \times 10^{-5} \ M$$

Dilution factor = 30, molecular weight = 328.5 and total volume = 19 ml

$$= 1.09 \times 10^{-5} \times 10 \times 328.5 \times 19$$

Weight of remained ATRA in the particles = 1.9954 mg

Weight of ATRA and EC initially used were 10 mg

Content of % intact ATRA were calculated by equation (5)

$$\% \ ATRA \ content = (1.995 \times 100)/10$$
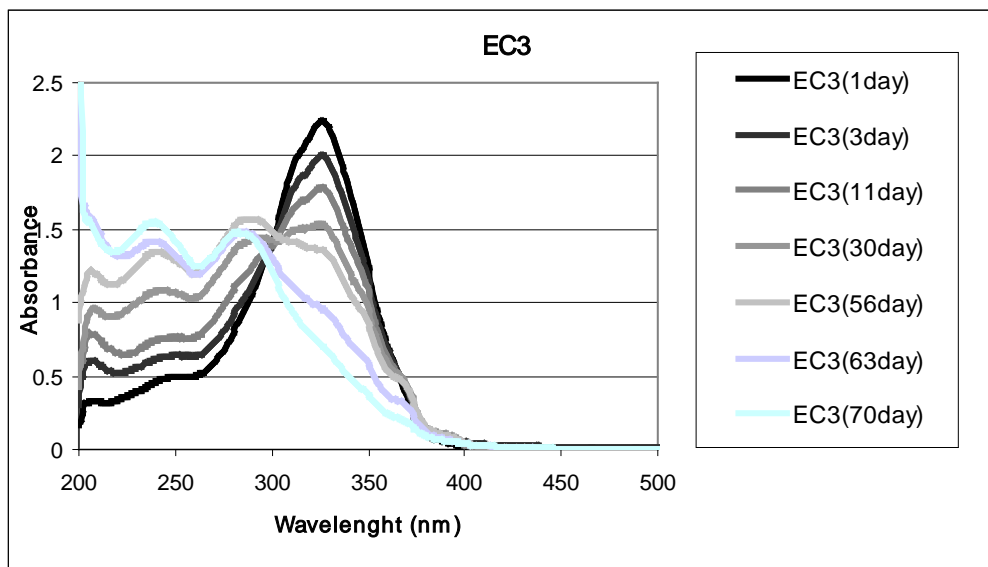
$$= 19.95 \ \%$$

Fig. A.8 Stability profile of ATRA-encapsulated PCPLC1 under the light proof condition

2.4.) ATRA-encapsulated PCPLC1 nanoparticles

2.4.1.) Storage at 1 day

The amount of ATRA-encapsulated PCPLC1 at the inside of particles was calculated by equation (1)

$$1.025 = (27594) \ (1) \ c$$

$$c = 3.71 \times 10^{-5} \ M$$

Dilution factor = 50, molecular weight = 328.5 and total volume = 30 ml

$$= 3.71 \times 10^{-5} \times 50 \times 328.5 \times 30$$

Weight of remained ATRA in the particles = 18.3036 mg

Weight of ATRA and EC initially used were 30 mg

Content of % intact ATRA were calculated by equation (5)

% ATRA content = (18.30 x 100)/30

= 61.01 %

2.4.2.) Storage at 33 days

The amount of ATRA-encapsulated EC3 at the inside of particles was calculated by equation (4)

$$(2.384615)(0.5273) - 0.4763 = (53219.53) \, Cs$$
$$Cs = 1.47 \times 10^{-5} \, M$$

Dilution factor = 25, molecular weight = 328.5 and total volume = 30 ml

$$= 1.47 \times 10^{-5} \times 25 \times 328.5 \times 30$$

Weight of remained ATRA in the particles= 3.6163 mg

Weight of ATRA and EC initially used were 30 mg

Content of % intact ATRA were calculated by equation (5)

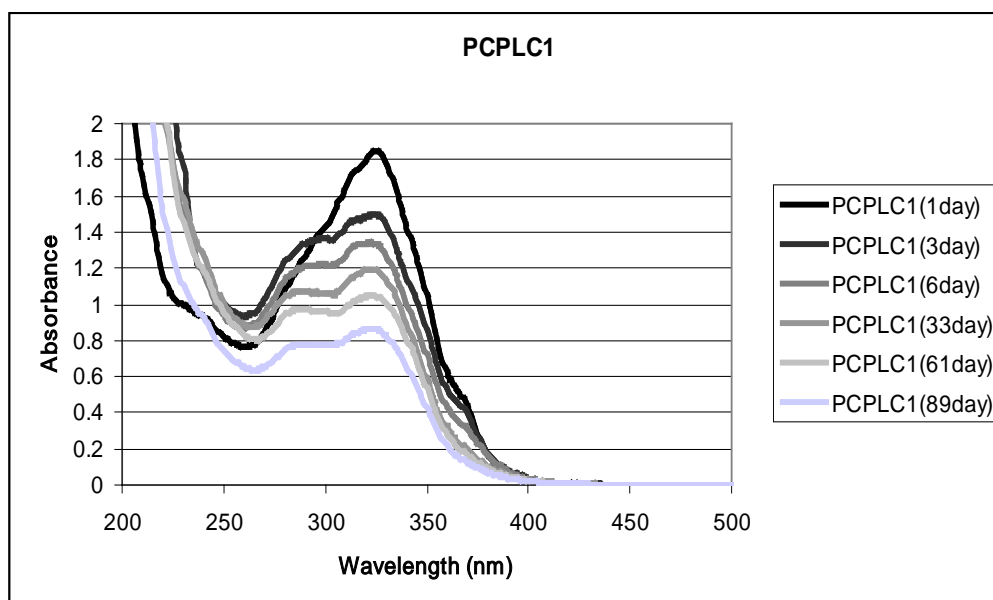% ATRA content = (3.6163 x 100)/30

= 12.05 %

Fig. A.9 Stability profile of ATRA-encapsulated PCPLC2 under the light proof condition

2.5.) ATRA-encapsulated PCPLC2 nanoparticles

2.5.1.) Storage at 1 day

The amount of ATRA-encapsulated PCPLC2 at the inside of particles was calculated by equation (1)

$$1.3683 = (27594) (1) c$$

$$c = 4.96 \times 10^{-5} \text{ M}$$

Dilution factor = 30, molecular weight = 328.5 and total volume = 27 ml

$$= 4.96 \times 10^{-5} \times 30 \times 328.5 \times 27$$

Weight of remained ATRA in the particles = 13.1946 mg

Weight of ATRA and EC initially used were 20 mg

Content of % intact ATRA were calculated by equation (5)

$$\% \text{ ATRA content} = (13.19 \times 100)/20$$

$$= 65.97 \%$$

2.4.2.) Storage at 20 days

The amount of ATRA-encapsulated EC3 at the inside of particles was calculated by equation (4)

$$(2.384615)(0.6127) - 0.5277 = (53219.53) Cs$$
$$Cs = 1.75 \times 10^{-5} \text{ M}$$

Dilution factor = 30, molecular weight = 328.5 and total volume = 27 ml

$$= 1.75 \times 10^{-5} \times 30 \times 328.5 \times 27$$

Weight of remained ATRA in the particles= 4.6663 mg

Weight of ATRA and EC initially used were 20 mg

Content of % intact ATRA were calculated by equation (5)

$$\% \text{ ATRA content} = (4.6663 \times 100)/20$$
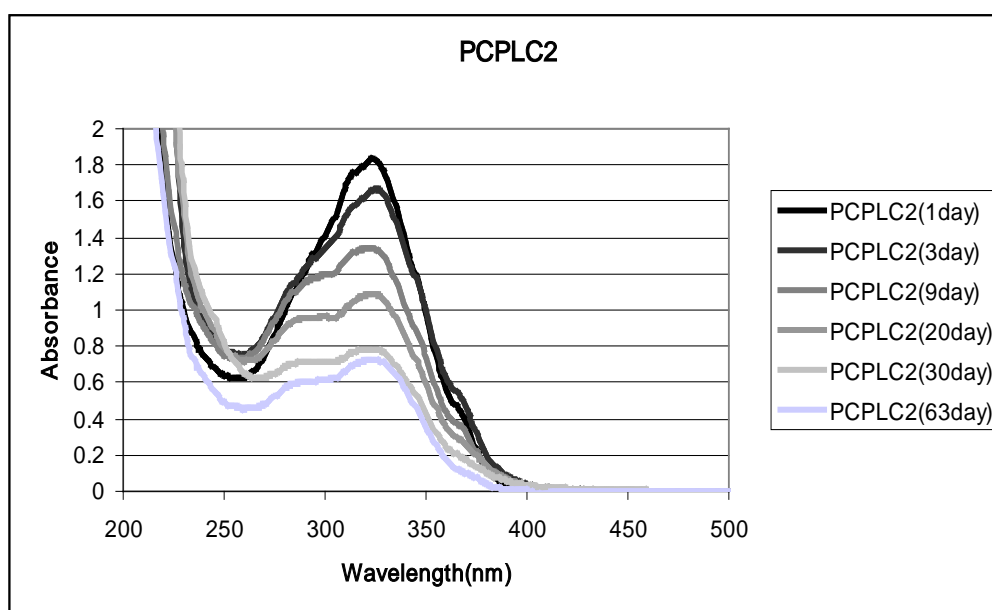
$$= 23.33 \%$$
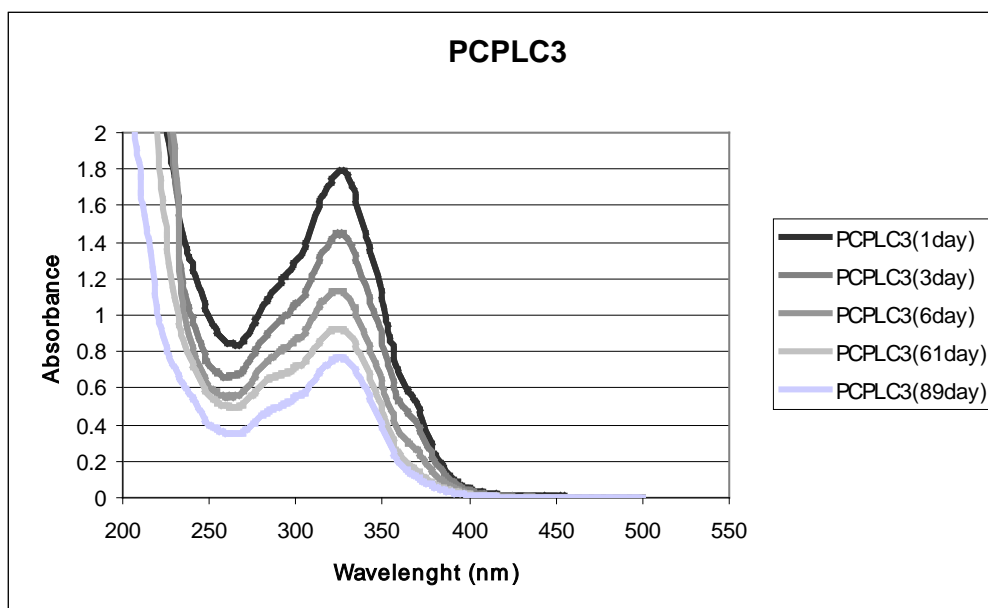
Fig. A.10 Stability profile of ATRA-encapsulated PCPLC3 under the light proof condition

2.6.) ATRA-encapsulated PCPLC3 nanoparticles

2.6.1.) Storage at 1 day

The amount of ATRA-encapsulated PCPLC3 at the inside of particles was calculated by equation (1)

$$0.897 = (27594) (1) c$$

$$c = 3.25 \times 10^{-5} \text{ M}$$

Dilution factor = 25, molecular weight = 328.5 and total volume = 30 ml

$$= 3.25 \times 10^{-5} \times 25 \times 328.5 \times 30$$

Weight of remained ATRA in the particles = 8.0089 mg

Weight of ATRA and EC initially used were 10 mg

Content of % intact ATRA were calculated by equation (5)

$$\% \text{ ATRA content} = (8.01 \times 100)/20$$

$$= 80.10 \%$$

2.6.2.) Storage at 33 days

The amount of ATRA-encapsulated EC3 at the inside of particles was calculated by equation (4)

$$(2.384615)(0.5273) - 0.4763 = (53219.53) C_s$$

$$C_s = 1.47 \times 10^{-5} \text{ M}$$

Dilution factor = 25, molecular weight = 328.5 and total volume = 30 ml

$$= 1.47 \times 10^{-5} \times 25 \times 328.5 \times 30$$

Weight of remained ATRA in the particles= 3.6163 mg

Weight of ATRA and EC initially used were 10 mg

Content of % intact ATRA were calculated by equation (5)

$$\% \text{ ATRA content} = (3.6163 \times 100)/10$$

$$= 12.05 \%$$

3. Photostability

The photostability of encapsulated ATRA was determined in comparison to the free ATRA. The sample were exposed to UVA light (8.5 mW/ cm^2) for 0, 15, 30, 45, 60 and 90 min which corresponded to the light exposure to 0, 7.8, 15.4, 22.9, 30.7 and 45.9 J/cm^2, respectively. The % ATRA content was calculated by equation (1)

3.1. Unencapsulated ATRA

3.1.1. Unencapsulated ATRA was exposed to 0 J/cm^2

The ATRA content of unencapsulated ATRA was calculated by equation (1)

$$0.6825 = (27594) (1) c$$

$$c = 2.47 \times 10^{-5} \text{ M}$$

Dilution factor = 40, molecular weight = 328.5 and total volume = 27 ml

$$= 2.47 \times 10^{-5} \times 40 \times 328.5 \times 27$$

The ATRA content of unencapsulated ATRA = 8.775 mg

Weight of ATRA initially used was 10 mg

% ATRA content was calculated by

$$\% \text{ ATRA content} = \frac{\text{Weight of ATRA content}}{\text{Weight of ATRA initially used}} \times 100 \qquad (5)$$

$$\% \text{ ATRA content} = (8.775 \times 100)/10$$

$$= 87.75 \%$$

3.1.2. Unencapsulated ATRA was exposed to 7.8 J/cm^2

The ATRA content of unencapsulated ATRA was calculated by equation (1)

$$0.3193 = (27594) (1) c$$

$$c = 1.16 \times 10^{-5} \text{ M}$$

Dilution factor = 30, molecular weight = 328.5 and total volume = 27 ml

$$= 1.16 \times 10^{-5} \times 30 \times 328.5 \times 27$$

The ATRA content of unencapsulated ATRA = 3.0793 mg

Weight of ATRA initially used was 10 mg

% ATRA content was calculated by equation (5)

% ATRA content = (3.0793 x 100)/10

$$= 30.79 \%$$

3.1.3. Unencapsulated ATRA was exposed to 15.4 J/cm^2

The ATRA content of unencapsulated ATRA was calculated by equation (1)

$$0.1363 = (27594) \, (1) \, c$$

$$c = 4.94 \times 10^{-6} \, M$$

Dilution factor = 30, molecular weight = 328.5 and total volume = 27 ml

$$= 4.94 \times 10^{-6} \times 30 \times 328.5 \times 27$$

The ATRA content of unencapsulated ATRA = 1.3146 mg

Weight of ATRA initially used was 10 mg

% ATRA content was calculated by equation (5)

% ATRA content = (1.3146 x 100)/10

$$= 13.14 \%$$

3.1.4. Unencapsulated ATRA was exposed to 22.9 J/cm^2

The ATRA content of unencapsulated ATRA was calculated by equation (1)

$$0.057 = (27594) \, (1) \, c$$

$$c = 2.07 \times 10^{-6} \, M$$

Dilution factor = 30, molecular weight = 328.5 and total volume = 27 ml

$$= 2.07 \times 10^{-6} \times 30 \times 328.5 \times 27$$

The ATRA content of unencapsulated ATRA = 0.5496 mg

Weight of ATRA initially used was 10 mg

% ATRA content was calculated by equation (5)

% ATRA content = (0.5496 x 100)/10

$$= 5.49 \%$$

3.1.5. Unencapsulated ATRA was exposed to 30.7 J/cm^2

The ATRA content of unencapsulated ATRA was calculated by equation (1)

$$0.029 = (27594) \, (1) \, c$$

$$c = 1.05 \times 10^{-6} \text{ M}$$

Dilution factor = 30, molecular weight = 328.5 and total volume = 27 ml

$$= 1.05 \times 10^{-6} \times 30 \times 328.5 \times 27$$

The ATRA content of unencapsulated ATRA = 0.2796 mg

Weight of ATRA initially used was 10 mg

% ATRA content was calculated by equation (5)

% ATRA content = (0.2796 x 100)/10

$$= 2.79 \text{ \%}$$

3.1.6. Unencapsulated ATRA was exposed to 45.9 J/cm^2

The ATRA content of unencapsulated ATRA was calculated by equation (1)

$$0.0153 = (27594) (1) c$$
$$c = 5.56 \times 10^{-7} \text{ M}$$

Dilution factor = 30, molecular weight = 328.5 and total volume = 27 ml

$$= 5.56 \times 10^{-7} \times 30 \times 328.5 \times 27$$

The ATRA content of unencapsulated ATRA = 0.1479 mg

Weight of ATRA initially used was 10 mg

% ATRA content was calculated by equation (5)

% ATRA content = (0.1479 x 100)/10

$$= 1.48 \text{ \%}$$

3.2. The ATRA-encapsulated EC3

3.1.1. ATRA-encapsulated EC3 was exposed to 0 J/cm^2

The ATRA content of ATRA-encapsulated EC3 was calculated by equation (1)

$$0.524 = (27594) (1) c$$

$$c = 1.90 \times 10^{-5} \text{ M}$$

Dilution factor = 45, molecular weight = 328.5 and total volume = 27 ml

$$= 1.90 \times 10^{-5} \times 45 \times 328.5 \times 27$$

The ATRA content of unencapsulated ATRA = 7.5793 mg

Weight of ATRA initially used was 10 mg

% ATRA content was calculated by equation (1)

% ATRA content = (7.5793 x 100)/10

$$= 75.79 \text{ \%}$$

3.1.2. ATRA-encapsulated EC3 was exposed to 7.8 J/cm^2

The ATRA content of ATRA-encapsulated EC3 was calculated by equation (1)

$$0.1020 = (27594) (1) c$$

$$c = 3.7 \times 10^{-6} \text{ M}$$

Dilution factor = 30, molecular weight = 328.5 and total volume = 27 ml

$$= 3.7 \times 10^{-6} \times 30 \times 328.5 \times 27$$

The ATRA content of unencapsulated ATRA = 0.9836 mg

Weight of ATRA initially used was 10 mg

% ATRA content was calculated by equation (5)

% ATRA content = (0.9836 x 100)/10

$$= 9.84 \%$$

3.1.3. ATRA-encapsulated EC3 was exposed to 15.4 J/cm^2

The ATRA content of ATRA-encapsulated EC3 was calculated by equation (1)

$$0.0317 = (27594) (1) c$$

$$c = 1.15 \times 10^{-6} \text{ M}$$

Dilution factor = 30, molecular weight = 328.5 and total volume = 27 ml

$$= 1.15 \times 10^{-6} \times 30 \times 328.5 \times 27$$

The ATRA content of unencapsulated ATRA = 0.3054 mg

Weight of ATRA initially used was 10 mg

% ATRA content was calculated by equation (5)

% ATRA content = (0.3054 x 100)/10

$$= 3.05 \%$$

3.1.4. ATRA-encapsulated EC3 was exposed to 22.9 J/cm^2

The ATRA content of ATRA-encapsulated EC3 was calculated by equation (1)

$$0.01 = (27594) (1) c$$

$$c = 3.62 \times 10^{-7} \text{ M}$$

Dilution factor = 30, molecular weight = 328.5 and total volume = 27 ml

$$= 3.62 \times 10^{-7} \times 30 \times 328.5 \times 27$$

The ATRA content of unencapsulated ATRA = 0.0964 mg

Weight of ATRA initially used was 10 mg

% ATRA content was calculated by equation (5)

% ATRA content = (0.0964 x 100)/10

$$= 0.96 \%$$

3.1.5. ATRA-encapsulated EC3 was exposed to 30.7 J/cm^2

The ATRA content of ATRA-encapsulated EC3 was calculated by equation (1)

$$0.0063 = (27594) (1) c$$

$$c = 2.3 \times 10^{-7} M$$

Dilution factor = 30, molecular weight = 328.5 and total volume = 27 ml

$$= 2.3 \times 10^{-7} \times 30 \times 328.5 \times 27$$

The ATRA content of unencapsulated ATRA = 0.0610 mg

Weight of ATRA initially used was 10 mg

% ATRA content was calculated by equation (5)

% ATRA content = (0.0610 x 100)/10

$$= 0.61 \%$$

3.1.6. ATRA-encapsulated EC3 was exposed to 45.9 J/cm^2

The ATRA content of ATRA-encapsulated EC3 was calculated by equation (1)

$$0.0033 = (27594) (1) c$$
$$c = 1.21 \times 10^{-7} M$$

Dilution factor = 30, molecular weight = 328.5 and total volume = 27 ml

$$= 1.21 \times 10^{-7} \times 30 \times 328.5 \times 27$$

The ATRA content of unencapsulated ATRA = 0.0321 mg

Weight of ATRA initially used was 10 mg

% ATRA content was calculated by equation (5)

% ATRA content = (0.0321 x 100)/10

$$= 0.32 \%$$

3.3. The ATRA-encapsulated PCPLC3

3.1.1. ATRA-encapsulated PCPLC3 was exposed to 0 J/cm^2

The ATRA content of ATRA-encapsulated PCPLC3 was calculated by equation (1)

$$0.7983 = (27594) (1) c$$

$$c = 2.89 \times 10^{-5} M$$

Dilution factor = 30, molecular weight = 328.5 and total volume = 27 ml

$$= 2.89 \times 10^{-5} \times 30 \times 328.5 \times 27$$

The ATRA content of unencapsulated ATRA = 7.6982 mg

Weight of ATRA initially used was 10 mg

% ATRA content was calculated by equation (1)

% ATRA content = (7.6982 x 100)/10

= 76.98 %

3.1.2. ATRA-encapsulated PCPLC3 was exposed to 7.8 J/cm^2

The ATRA content of ATRA-encapsulated PCPLC3 was calculated by equation (1)

0.5233 = (27594) (1) c

c = 1.9 x 10^{-5} M

Dilution factor = 30, molecular weight = 328.5 and total volume = 27 ml

= 1.9 x 10^{-5} x 30 x 328.5 x 27

The ATRA content of unencapsulated ATRA = 5.0464 mg

Weight of ATRA initially used was 10 mg

% ATRA content was calculated by equation (5)

% ATRA content = (5.0464 x 100)/10

= 50.46 %

3.1.3. ATRA-encapsulated PCPLC3 was exposed to 15.4 J/cm^2

The ATRA content of ATRA-encapsulated PCPLC3 was calculated by equation (1)

0.365 = (27594) (1) c

c = 1.32 x 10^{-5} M

Dilution factor = 30, molecular weight = 328.5 and total volume = 27 ml

= 1.32 x 10^{-5} x 30 x 328.5 x 27

The ATRA content of unencapsulated ATRA = 3.5196 mg

Weight of ATRA initially used was 10 mg

% ATRA content was calculated by equation (5)

% ATRA content = (3.5196 x 100)/10

= 35.19 %

3.1.4. ATRA-encapsulated PCPLC3 was exposed to 22.9 J/cm^2

The ATRA content of ATRA-encapsulated PCPLC3 was calculated by equation (1)

0.35 = (27594) (1) c

c = 1.27 x 10^{-5} M

Dilution factor = 30, molecular weight = 328.5 and total volume = 27 ml

= 1.27 x 10^{-5} x 30 x 328.5 x 27

The ATRA content of unencapsulated ATRA = 3.375 mg

Weight of ATRA initially used was 10 mg

% ATRA content was calculated by equation (5)

% ATRA content = (3.375 x 100)/10

= 33.75 %

3.1.5. ATRA-encapsulated PCPLC3 was exposed to 30.7 J/cm^2

The ATRA content of ATRA-encapsulated PCPLC3 was calculated by equation (1)

$$0.34 = (27594) (1) c$$

$$c = 1.23 \times 10^{-5} \text{ M}$$

Dilution factor = 30, molecular weight = 328.5 and total volume = 27 ml

$$= 1.23 \times 10^{-5} \times 30 \times 328.5 \times 27$$

The ATRA content of unencapsulated ATRA = 3.2785 mg

Weight of ATRA initially used was 10 mg

% ATRA content was calculated by equation (5)

% ATRA content = (3.2785 x 100)/10

= 32.79 %

3.1.6. ATRA-encapsulated PCPLC3 was exposed to 45.9 J/cm^2

The ATRA content of ATRA-encapsulated PCPLC3 was calculated by equation (1)

$$0.29 = (27594) (1) c$$
$$c = 1.05 \times 10^{-5} \text{ M}$$

Dilution factor = 30, molecular weight = 328.5 and total volume = 27 ml

$$= 1.05 \times 10^{-5} \times 30 \times 328.5 \times 27$$

The ATRA content of unencapsulated ATRA = 2.7964 mg

Weight of ATRA initially used was 10 mg

% ATRA content was calculated by equation (5)

% ATRA content = (2.7964 x 100)/10

= 27.96 %

3.4. The free ATRA in PCPLC nanoparticles dispersion

3.1.1. The free ATRA in PCPLC nanoparticles dispersion was exposed to 0 J/cm^2

The ATRA content of free ATRA in PCPLC nanoparticles dispersion was calculated by equation (1)

$$1.0094 = (27594) (1) c$$

$$c = 3.66 \times 10^{-5} \text{ M}$$

Dilution factor = 35, molecular weight = 328.5 and total volume = 20 ml

$$= 3.66 \times 10^{-5} \times 35 \times 328.5 \times 20$$

The ATRA content of unencapsulated ATRA = 8.4116 mg

Weight of ATRA initially used was 10 mg

% ATRA content was calculated by equation (1)

% ATRA content = (8.4116 x 100)/10

$$= 84.12 \%$$

3.1.2. The free ATRA in PCPLC nanoparticles dispersion was exposed to 7.8 J/cm^2

The ATRA content of free ATRA in PCPLC nanoparticles dispersion was calculated by equation (1)

$$0.437 = (27594) \ (1) \ c$$

$$c = 1.58 \times 10^{-5} \ M$$

Dilution factor = 35, molecular weight = 328.5 and total volume = 20 ml

$$= 1.58 \times 10^{-5} \times 35 \times 328.5 \times 20$$

The ATRA content of unencapsulated ATRA = 3.6416 mg

Weight of ATRA initially used was 10 mg

% ATRA content was calculated by equation (5)

% ATRA content = (3.6416 x 100)/10

$$= 36.42 \%$$

3.1.3. The free ATRA in PCPLC nanoparticles dispersion was exposed to 15.4 J/cm^2

The ATRA content of free ATRA in PCPLC nanoparticles dispersion was calculated by equation (1)

$$0.2065 = (27594) \ (1) \ c$$

$$c = 7.48 \times 10^{-6} \ M$$

Dilution factor = 30, molecular weight = 328.5 and total volume = 20 ml

$$= 7.48 \times 10^{-6} \times 30 \times 328.5 \times 20$$

The ATRA content of unencapsulated ATRA = 1.7206 mg

Weight of ATRA initially used was 10 mg

% ATRA content was calculated by equation (5)

% ATRA content = (1.7206 x 100)/10

$$= 17.21 \%$$

3.1.4. The free ATRA in PCPLC nanoparticles dispersion was exposed to 22.9 J/cm^2

The ATRA content of free ATRA in PCPLC nanoparticles dispersion was calculated by equation (1)

$$0.0862 = (27594) (1) c$$

$$c = 3.12 \times 10^{-6} \text{ M}$$

Dilution factor = 30, molecular weight = 328.5 and total volume = 27 ml

$$= 3.12 \times 10^{-6} \times 30 \times 328.5 \times 27$$

The ATRA content of unencapsulated ATRA = 0.7183 mg

Weight of ATRA initially used was 10 mg

% ATRA content was calculated by equation (5)

% ATRA content = (0.7183 x 100)/10

$$= 7.18 \%$$

4. Controlled release

To investigate the release of ATRA encapsulated within the particles after the particles were applied on to the skin, the ex vivo controlled release experiments were carried out by applying free ATRA, ATRA-encapsulated EC and ATRA-encapsulated PCPLC onto the skin in the upper compartment of the Franz cell.

4.1. Unencapsulated ATRA

4.1.1. First replicate

After 24 h, the unencapsulated ATRA (free ATRA) was 2.8 ml onto the skin in the upper compartment of the Franz cell.

The amount of unencapsulated ATRA in upper compartment of the Franz cell was calculated by equation (2)

$$0.5852 = (27594) (1) c$$

$$c = 2.12 \times 10^{-5} \text{ M}$$

Dilution factor = 60, molecular weight = 328.5 and total volume = 2.8 ml

$$= 2.12 \times 10^{-5} \times 60 \times 328.5 \times 2.8$$

Weight of ATRA in upper compartment of the Franz cell = 1.1704 mg

Weight of ATRA initially used were 1.5 mg

Weight of ATRA diffused into the mouse skin was 1.5-1.1704= 0.3296 mg

The ATRA released was calculated using equation

% ATRA release =

$$\frac{\text{Amount of ATRA initiated - remained ATRA upper compartment}}{\text{Amount of ATRA initiated}} \times 100 \quad (6)$$

% ATRA release = (0.3296 x 100)/ 1.5

= 21.97 %

4.1.2. Second replicate

After 24 h, the unencapsulated ATRA (free ATRA) was 2.6 ml onto the skin in the upper compartment of the Franz cell.

The amount of unencapsulated ATRA in upper compartment of the Franz cell was calculated by equation (2)

0. 6426 = (27594) (1) c

$c = 2.33 \times 10^{-5}$ M

Dilution factor = 60, molecular weight = 328.5 and total volume = 2.6 ml

$= 2.33 \times 10^{-5} \times 60 \times 328.5 \times 2.6$

Weight of ATRA in upper compartment of the Franz cell = 1.1934 mg

Weight of ATRA initially used were 1.5 mg

Weight of ATRA diffused into the mouse skin was 1.5-1.1934= 0.3065 mg

% ATRA release was calculated by equation (5)

% ATRA release = (0.3065 x 100)/ 1.5

= 20.44 %

4.1.3. Third replicate

After 24 h, the unencapsulated ATRA (free ATRA) was 2.6 ml onto the skin in the upper compartment of the Franz cell.

The amount of unencapsulated ATRA in upper compartment of the Franz cell was calculated by equation (2)

0. 6065 = (27594) (1) c

$c = 2.2 \times 10^{-5}$ M

Dilution factor = 60, molecular weight = 328.5 and total volume = 2.6 ml

$= 2.2 \times 10^{-5} \times 60 \times 328.5 \times 2.6$

Weight of ATRA in upper compartment of the Franz cell = 1.1264 mg

Weight of ATRA initially used were 1.5 mg

Weight of ATRA diffused into the mouse skin was 1.5-1.1264= 0.3735 mg

% ATRA release was calculated by equation (5)

$$\% \text{ ATRA release} = (0.3735 \times 100)/\ 1.5$$
$$= 20.44\ \%$$

	1	2	3
A	0.5852	0.6426	0.6065
c	2.12×10^{-5}	2.33×10^{-5}	2.2×10^{-5}
x DF x Mw (328.5)	0.4180	0.4590	0.4332
x mL	1.1704	1.1934	1.1264
ATRA release	0.3296	0.3065	0.3735
% ATRA release	21.97	20.44	24.90

Therefore, % ATRA release of unencapsulated ATRA into the mouse skin was 22.44± 2.3%

4.2. ATRA-encapsulated EC3

4.2.1. First replicate

After 24 h, the ATRA-encapsulated EC3 was 2.9 ml onto the skin in the upper compartment of the Franz cell.

The amount of unencapsulated ATRA in upper compartment of the Franz cell was calculated by equation (2)

$$0.3748 = (27594)\ (1)\ c$$
$$c = 1.36 \times 10^{-5}\ \text{M}$$

Dilution factor = 60, molecular weight = 328.5 and total volume = 2.9 ml

$$= 1.36 \times 10^{-5} \times 60 \times 328.5 \times 2.9$$

Weight of ATRA in upper compartment of the Franz cell = 0.7764 mg

Weight of ATRA initially used were 1.04 mg

Weight of ATRA diffused into the mouse skin was 1.04-0.7764= 0.2650 mg

The ATRA released was calculated by equation (5)

$$\% \text{ ATRA release} = (0.2650 \times 100)/\ 1.04$$
$$= 25.45\ \%$$

4.2.2. Second replicate

After 24 h, the ATRA-encapsulated EC3 was 2.4 ml onto the skin in the upper compartment of the Franz cell.

The amount of unencapsulated ATRA in upper compartment of the Franz cell was calculated by equation (2)

$$0.4913 = (27594) (1) c$$

$$c = 1.78 \times 10^{-5} \text{ M}$$

Dilution factor = 60, molecular weight = 328.5 and total volume = 2.4 ml

$$= 1.78 \times 10^{-5} \times 60 \times 328.5 \times 2.4$$

Weight of ATRA in upper compartment of the Franz cell = 0.8422 mg

Weight of ATRA initially used were 1.04 mg

Weight of ATRA diffused into the mouse skin was 1.04- 0.8422= 0.1993 mg

The ATRA released was calculated by equation (5)

% ATRA release = (0.1993x 100)/ 1.04

$$= 19.13 \text{ \%}$$

4.2.3. Third replicate

After 24 h, the ATRA-encapsulated EC3 was 2.6 ml onto the skin in the upper compartment of the Franz cell.

The amount of unencapsulated ATRA in upper compartment of the Franz cell was calculated by equation (2)

$$0.4459 = (27594) (1) c$$

$$c = 1.62 \times 10^{-5} \text{ M}$$

Dilution factor = 60, molecular weight = 328.5 and total volume = 2.6 ml

$$= 1.62 \times 10^{-5} \times 60 \times 328.5 \times 2.6$$

Weight of ATRA in upper compartment of the Franz cell = 0. 8281 mg

Weight of ATRA initially used were 1.04 mg

Weight of ATRA diffused into the mouse skin was 1.04- 0.8281= 0.2133 mg

The ATRA released was calculated by equation (5)

% ATRA release = (0.2133x 100)/ 1.04

$$= 20.49 \text{ \%}$$

	1	2	3
A	0.3748	0.4913	0.4459
c	1.36×10^{-5}	1.78×10^{-5}	1.62×10^{-5}

x DF x Mw (328.5)	0.2677	0.3509	0.3185
x mL	0.7764	0.8422	0.8281
ATRA release	0.2650	0.1993	0.2133
% ATRA release	25.45	19.13	20.49

Therefore, % ATRA release of ATRA-encapsulated EC3 into the mouse skin was 21.67± 3.3%

4.3. ATRA-encapsulated PCPLC3

4.2.1. First replicate

After 24 h, the ATRA-encapsulated PCPLC3 was 2.8 ml onto the skin in the upper compartment of the Franz cell.

The amount of unencapsulated ATRA in upper compartment of the Franz cell was calculated by equation (2)

$$0.1426 = (27594) (1) c$$
$$c = 5.14 \times 10^{-5} \text{ M}$$

Dilution factor = 60, molecular weight = 328.5 and total volume = 2.8 ml

$$= 5.14 \times 10^{-5} \times 60 \times 328.5 \times 2.8$$

Weight of ATRA in upper compartment of the Franz cell = 0.7128 mg

Weight of ATRA initially used were 0.8857 mg

Weight of ATRA diffused into the mouse skin was 0.8857-0.7128= 0.1729 mg

The ATRA released was calculated by equation (5)

% ATRA release = (0.1729x 100)/ 0.8857

= 19.52 %

4.2.2. Second replicate

After 24 h, the ATRA-encapsulated PCPLC3 was 2.8 ml onto the skin in the upper compartment of the Franz cell.

The amount of unencapsulated ATRA in upper compartment of the Franz cell was calculated by equation (2)

$$0.1445 = (27594) (1) c$$
$$c = 5.27 \times 10^{-5} \text{ M}$$

Dilution factor = 60, molecular weight = 328.5 and total volume = 2.8 ml

$$= 5.27 \times 10^{-5} \times 60 \times 328.5 \times 2.8$$

Weight of ATRA in upper compartment of the Franz cell = 0.7224 mg

Weight of ATRA initially used were 0.8857 mg

Weight of ATRA diffused into the mouse skin was 0.8857-0.7224= 0.1634 mg

The ATRA released was calculated by equation (5)

% ATRA release = (0.1634x 100)/ 0.8857

= 18.44 %

4.2.2. Third replicate

After 24 h, the ATRA-encapsulated PCPLC3 was 2.8 ml onto the skin in the upper compartment of the Franz cell.

The amount of unencapsulated ATRA in upper compartment of the Franz cell was calculated by equation (2)

$$0.1435 = (27594) (1) c$$

$$c = 5.2 \times 10^{-5} M$$

Dilution factor = 60, molecular weight = 328.5 and total volume = 2.8 ml

$$= 5.2 \times 10^{-5} \times 60 \times 328.5 \times 2.8$$

Weight of ATRA in upper compartment of the Franz cell = 0.7176 mg

Weight of ATRA initially used were 0.8857 mg

Weight of ATRA diffused into the mouse skin was 0.8857-0.7176= 0.1681 mg

The ATRA released was calculated by equation (5)

% ATRA release = (0.1681x 100)/ 0.8857

= 18.98 %

	1	2	3
A	0.1426	0.1445	0.1435
c	5.14×10^{-6}	5.27×10^{-6}	5.2×10^{-6}
x DF x Mw (328.5)	0.2546	0.2579	0.2563
x mL	0.7128	0.7224	0.7176
ATRA release	0.1729	0.1634	0.1681
% ATRA release	19.52	18.44	18.98

Therefore, % ATRA release of ATRA-encapsulated EC3 into the mouse skin was 18.98± 0.5%

VITA

Ms. Sunatda Arayachukeat was born on July 22, 1986 in Bankok. She received a Bachelor's Degree of Science in Medical Technology from Chulalongkorn University in 2007. After that, she started her graduate study a Master's degree in the Program of Petrochemistry and Polymer Science, Faculty of Science, Chulalongkorn University. During she had presented "Nanoencapsulation of all-*trans* retinyl acetate" in the 3rd Asian Conference on Colloid & Interface Science (ACCIS 2009 KOREA) and "Improving Stability of all-*trans* retinyl acetate" in 6th International Symposium on Advance Material in Asia-Pacific Rim (6th ISAMAP) by poster presentation. The latter got the scholarships from National Center of Excellence, for Petrochemicals, and Advanced Material (NCE-PPAM) and the Graduate School, Chulalongkorn University.

My address is 1046/103, Moo1, Soi. Prachau-tid 41, Prachau-tid Road, Bangmod, Tungkru, Bangkok, 10140, Tel. 083-9214461.